DESIGN, MANUFACTURE AND TEST OF A BEARINGLESS ROTOR HUB FOR THE 24% SCALE MODEL OF THE ROOIVALK ATTACK HELICOPTER

By

J. Steyn

Pectora roborant cultus recti

Thesis presented in partial fulfilment
of the requirements for the degree of
Masters of Engineering at the
University of Stellenbosch

Study leader: Mr. K. van der Westhuizen

November 2000

Stellenbosch University http://scholar.sun.ac.za/

DECLARATION

I, the undersigned, hereby declare that the work contained in this thesis is my own original work and that I have not previously in its entirety or in part submitted it at any university for a degree.

Signature:

Date:

Stellenbosch University http://scholar.sun.ac.za/

SUMMARY

This document contains the work done on the bearingless rotor hub for the 24% scale model of the Rooivalk Attack Helicopter situated at the CSIR in Pretoria. This work forms part of the MSc Ing degree of Johannes Steyn.

This work was deemed necessary because of a movement away from the fully articulated rotor to one of hingeless and more recently bearingless rotors.

The main emphasis of this thesis is to be a technology demonstrator more than the design of a fully working bearingless rotor hub. With this in mind the final design in this report is not an optimal one, but the procedures and methodology in getting to a design are laid out in this document.

To verify the design, tests were identified and created. The procedures for these tests are also included in this document. For the fatigue test a test bench had to be designed and built. This document also includes the design of this test bench.

Stellenbosch University http://scholar.sun.ac.za/

OPSOMMING

Die dokument lewer verslag van die aktiwiteite vir die ontwerp van 'n laerlose rotor van die 24% skaal model van die Rooivalk Helikopter, geleë by die WNNR in Pretoria. Die werk gedoen vorm deel van die MSc Ing graad van Johannes Steyn.

Dié werk is nodig geag omdat daar 'n tendens is om weg te beweeg van die volledig geartikuleerde rotor na die van 'n skanierlose en meer huidig 'n laerlose rotor.

Die hoof klem van die tesis is om as tegnologie demonstrator op te tree, eerder as die daarstel van 'n werkende laerlose rotor. Na aanleiding van bogenoemde stelling kan die finale ontwerp nie as optimaal beskou word nie. Die prosedures en metodiek wat gevolg is om die ontwerp te kry word uitgelê in die dokument.

Om die ontwerp te verifieer is toetse geïdentifiseer. Die prosedures vir elk van die toetse word ook in die dokument ingesluit. Vir die uitputtingstoetse moes 'n spesiale toetsbank ontwerp en gebou word. Die ontwerp van hierdie toetsbank is ook in die dokument.

Stellenbosch University http://scholar.sun.ac.za/

DEDICATION

This thesis is dedicated to Adri Brown, the love of my life, my parents, Johannes en Yvonne Steyn and my sister, Anjé Steyn.

Stellenbosch University http://scholar.sun.ac.za/

ACKNOWLEDGEMENTS

Mr. Kobus van der Westhuizen for his guidance at the end of my thesis period. He was thrown in at the deep end and came out swimming.

Prof. N.J. Theron for his guidance throughout the first part of my Masters degree. I wish him al the best in his new appointment.

Mr. Ferdi Zietsman for all the assistance he gave throughout the entire period of my Masters degree. If it were not for him the manufacturing of the test bench and especially the flexbeam mould would not have been completed at all.

Mr. E. Terblanche and Mr. J.F. du Toit for their help in the testing phase. Now I know how to make a displacement sensor.

The CSIR for information on the blade profile of the 24% scale model of the Rooivalk Attack Helicopter, as well as the aerodynamic load conditions acting on the blade.

ARMSCOR for the design specifications of the 24% scale model and for the financial support needed through the entire period. And for their patience while the thesis was being completed.

I also want to thank everybody that helped me in the completion of this thesis. I didn't mention you here because there are so many of you, not because I forgot you.

Stellenbosch University http://scholar.sun.ac.za/

TABLE OF CONTENTS

Stellenbosch University http://scholar.sun.ac.za/

Stellenbosch University http://scholar.sun.ac.za/

Stellenbosch University http://scholar.sun.ac.za/

UNIVERSITEITSBIBLIOTEEK U.S.

Stellenbosch University http://scholar.sun.ac.za/

LIST OF TABLES

Stellenbosch University http://scholar.sun.ac.za/

LIST OF FIGURES

Stellenbosch University http://scholar.sun.ac.za/

Stellenbosch University http://scholar.sun.ac.za/

NOMENCLATURE

ACRONYMS AND ABREVIATIONS

CROSEC	Part of the DYMORE Program for Calculating Cross-Section Properties
CSIR	Council for Scientific and Industrial Research
DYMORE	Program for Calculating Static (e.g. Deflections and Stresses) and Dynamic (e.g. Natural Frequencies and Time Response) Behaviour of High Aspect Ratio Rotors. Developed by a Research Group at the Rensselaer Polytechnic Institute
FEA	Finite Element Analysis
FEM	Finite Element Methods
FEMANA	Part of the DYMORE Program for Doing the FEM Analyses
FEMAP	Finite Element Modelling Application
FLEXBEAM	Bearingless Rotor Hub
FOS	Factor of Safety
PREFEM	Part of the DYMORE Program for Initialising the FEM Model
PSTFEM	Part of the DYMORE Program for Doing the Post Processing

Stellenbosch University http://scholar.sun.ac.za/

SYMBOLS

E	Modulus of Elasticity, GN/m^2
G	Shear Modulus of Elasticity, GN/m^2
ε	Normal Strain
γ	Shear Strain
σ	Normal Stress, MPa
τ	Shear Stress, MPa

SUBSCRIPTS

F	Denotes the Fibre in a Lamina
L	In the Direction of the Fibre
M	Denotes the Resin/Matrix of the Lamina
T	In the Direction Perpendicular to the Fibre
U	Maximum Allowable Stress

Stellenbosch University http://scholar.sun.ac.za/

CHAPTER 1: INTRODUCTION

A movement away from the fully articulated rotor towards the hingeless and later the bearingless rotor began almost 30 or so years ago. In the early days and still today there are a lot of companies doing feasibility and upgrade studies on these types of rotors for their various helicopters [1].

It was in regard of this that the CSIR contacted the University of Stellenbosch to do an upgrade study and conceptual design of a bearingless rotor hub for the Rooivalk Attack Helicopter. At that stage they wanted to know whether or not it could be manufactured locally. A study to determine this was done by Prof. N.J. Theron [2] from beginning of 1996 until middle 1998.

His study focussed only on the dynamic characteristics of the bearingless rotor and specifically the flexbeam to see whether a replacement was possible. Thus the strength of the system was not looked at. He did conclude that the torsional stiffness of the flexbeam would most probably be too high for field operations. The author joined him in that study at the beginning of 1998, investigating specifically the strength.

That study showed that replacing the rotor with a bearingless system would be possible, but that more work needed to be done on it. Unfortunately, because of financial constraints on the CSIR, future work on the full scale was suspended. Due to the outcome of that report and the potential it could have for the Rooivalk, the CSIR showed interest in a bearingless rotor hub development study for the 24% scale model [15] of the Rooivalk Attack Helicopter that they have at their facility in Pretoria. The main focus then switched from the full scale to the scale model.

This thesis contains the work that was done on the development of the bearingless rotor for the scale model. From the onset the main objective of this thesis was not to obtain an optimal design for the rotor, but to find a

Stellenbosch University http://scholar.sun.ac.za/

design methodology to a design and so make possible future work on this topic faster.

Because the focus shifted towards the 24% scale model, the bearingless rotor that is mentioned in this document is not a scaled version of the full-scale rotor of the Rooivalk Attack helicopter, but a design done specifically for the 24% scale model. The procedures laid out in this document are not just for the scale model, but are general procedures for designing a bearingless system; this means that it can be applied to any scale.

Stellenbosch University http://scholar.sun.ac.za/

CHAPTER 2: OVERVIEW OF ROTORS

2.1 General

Before any work can be done on the rotor system of a helicopter it is necessary to have a basic understanding of how helicopters and specifically the rotor system works. The various types of rotors and their advantages and disadvantages are also discussed.

2.2 Principles of Flight and Operation

Unlike fixed-wing aircraft, the helicopter's main airfoil is the rotating blade assembly, the rotor, mounted atop its fuselage on a hinged shaft connected with the vehicle's engine and flight controls. In comparison to airplanes, the tail of a helicopter is somewhat elongated and the rudder smaller. The tail is fitted with a small antitorque rotor, the tail rotor. The landing gear sometimes consists of a pair of skids rather than wheel assemblies.

The fact that the helicopter obtains its lifting power by means of a rotating airfoil greatly complicates the factors affecting its flight, for not only does the rotor turns, but it also moves up and down in a flapping motion and is affected by the horizontal or vertical movement of the helicopter itself.

The relative wind is the direction of the wind in relation to the airfoil. In an airplane, the flight path of the wing is fixed in relation to its forward flight; in a helicopter, the flight path of the rotor advances forward (to the helicopter's nose) and then rearward (to the helicopter's tail) in the process of its circular movement. Relative wind is always considered to be in parallel and opposite direction to the flight path. In considering helicopter flight, the relative wind can be affected by the rotation of the blades, the horizontal movement of the helicopter, the flapping of the rotor blades, and wind speed and direction. In flight, the relative wind is a combination of the rotation of the rotor blade and the movement of the helicopter.

Stellenbosch University http://scholar.sun.ac.za/

Like a propeller, the rotor has a pitch angle, which is the angle between the horizontal plane of rotation of the rotor disc and the chord line of the airfoil. The pilot uses the collective and cyclic pitch control to vary this pitch angle. In a fixed-wing aircraft, the angle of attack (the angle of the wing in relation to the relative wind) is important in determining lift. The same is true in a helicopter, where the angle of attack is the angle at which the relative wind meets the chord line of the rotor blade.

Angle of attack and pitch angle are two distinct conditions. Varying the pitch angle of a rotor blade changes its angle of attack and hence its lift. A higher pitch angle (up to the point of stall) will increase lift; a lower pitch angle will decrease it. Individual blades of a rotor have their pitch angles adjusted individually.

Rotor speed also controls lift: the higher the revolutions per minute (rpm), the higher the lift. However, the pilot will generally attempt to maintain a constant rotor rpm and will change the lift force by varying the angle of attack.

As with fixed-wing aircraft, air density (the result of air temperature, humidity and pressure) affects helicopter performance. The higher the density, the more lift will be generated; the lower the density, the less lift will be generated. Just as in fixed-wing aircraft, a change in lift also results in a change in drag. When enlarging the angle of pitch and thus the angle of attack increases lift, drag will increase and slow down the rotor rpm. Additional power will then be required to sustain a desired rpm. Thus, while a helicopter is affected like a conventional aircraft by the forces of lift, thrust, weight and drag, its mode of flight induces additional effects.

In a helicopter, the total lift and thrust forces generated by the rotor are exerted perpendicular to its plane of rotation. When a helicopter hovers in a windless condition, the plane of rotation of the rotor (the tip-path plane) is parallel to the ground, and the sum of the weight and drag forces are exactly balanced by the sum of the thrust and lift forces. In vertical flight, the components of weight and drag are combined in a single vector that is

Stellenbosch University http://scholar.sun.ac.za/

directed straight down; the components of lift and thrust are combined in a single vector that is directed straight up. To achieve forward flight in a helicopter, the plane of rotation of the rotor is tipped forward. (It should be understood that the helicopter's rotor mast does not tip but rather the individual rotor blades within the plane of rotation have their pitch angle varied.) For sideward flight, the plane of the rotation of the rotor is tilted in the direction desired. For rearward flight, the plane of the rotation of the rotor is tilted rearward.

Because the rotor is powered, there is an equal and opposite torque reaction, which tends to rotate the fuselage in a direction opposite to the rotor. This torque is offset by the tail rotor (antitorque rotor) located at the end of the fuselage. The pilot controls the thrust of the tail rotor by means of foot pedals, neutralizing torque as required.

There are other forces acting upon a helicopter not found in a conventional aircraft. These include the gyroscopic precession effect of the rotor: that is, the dissymmetry of lift created by the forward movement of the helicopter, resulting in the advancing blade having more lift and the retreating blade less. This occurs because the advancing blade has a combined speed of the blade velocity and the speed of the helicopter in forward flight, while the retreating blade has the difference between the blade velocity and the speed of the helicopter. This difference in speed causes a difference in lift: the advancing blade is moving faster and hence is generating more lift. If uncontrolled, this would result in the helicopter rolling. However, the difference in lift is compensated for by the blade flapping and by cyclic feathering (changing the angle of pitch). Because the blades are attached to a rotor hub by horizontal flapping hinges, which permit their movement in a vertical plane, the advancing blade flaps up, decreasing its angle of attack, while the retreating blade flaps down, increasing its angle of attack. This combination of effects equalizes the lift. (Blades also are attached to the hub by a vertical hinge, which permits each blade to move back and forth in the plane of rotation. The vertical hinge dampens out vibration and absorbs the effect of acceleration or

Stellenbosch University http://scholar.sun.ac.za/

deceleration.) In addition, in forward flight, the position of the cyclic pitch control causes a similar effect, contributing to the equalization of lift.

Other forces acting upon helicopters include coning, the downward bending effect on blades caused by centrifugal force; Coriolis effect, the acceleration or deceleration of the blades caused by the flapping movement bringing them closer to (acceleration) or farther away from (deceleration) the axis of rotation; and drift, the tendency of the tail rotor thrust to move the helicopter in hover [30, 31, 32].

2.3 Types of Rotors

Basically there are three types of rotors:

1) The fully articulated rotor
2) The hingeless rotor
3) The bearingless rotor

These three types of rotors are illustrated in Figure 2-1.

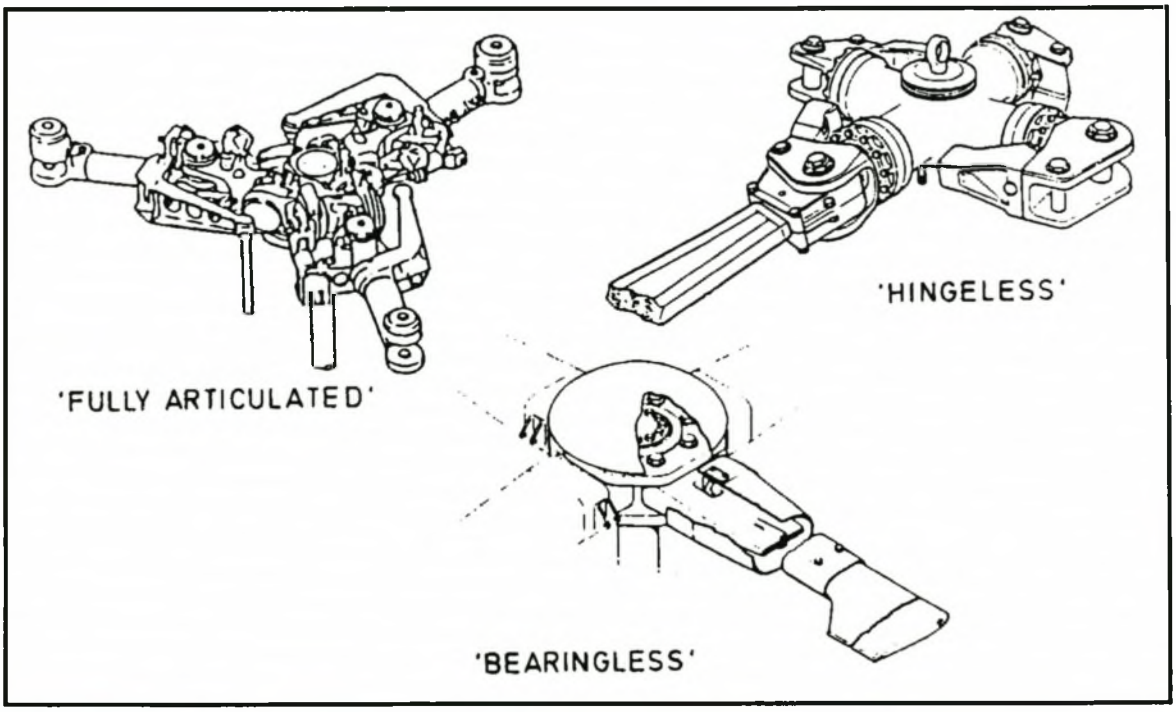

Figure 2-1: Different types of rotors

Stellenbosch University http://scholar.sun.ac.za/

2.3.1 Fully articulated

In this type of rotor the three rotational movements, i.e. flap, lead-lag and pitch, are carried by three sets of bearings in the hub and moments are not transferred to the rest of the helicopter structure. The blade is free to hinge around these bearings. Originally bearings were used because it was the only way that rotational movement could be taken up by the system due to material limitations especially fatigue life [30].

2.3.2 Hingeless

In the years following the fully articulated rotor, advances in material science made it possible to replace the flap and lead-lag bearings with elastomeric bearings. This was largely due to the advances in the field of composite materials. In this design the pitch bearing is however left to take up the pitch control.

2.3.3 Bearingless

In a bearingless rotor hub all three bearings are removed and replaced with an equivalent structure to absorb the rotational movements of the blade. This structure usually takes on the form of a beam that stretches between the drive axis of the helicopter and the blades. The properties of this beam must be so that not only the necessary dynamic performance of the helicopter, but also a satisfactory fatigue life can still be achieved and maintained.

The bearingless rotor hub is usually constructed of some sort of composite materials. There are three main reasons for this.

1. The strength to weight ratio of composites is very high, making it very suitable for the aviation industry.

2. Because of the unique property of composites that it is laid up into separate layers, it can be "tweaked' to give the desired stiffness in the

Stellenbosch University http://scholar.sun.ac.za/

directions wanted, to ensure dynamic stability and correct "bearing" performance.

3. Composite materials have a better fatigue life than metals, when the right lay-ups are applied.

2.4 Advantages of Hingeless and Bearingless Rotors

The biggest disadvantage of the fully articulated rotor is its bulkiness and that means that aerodynamically it has a lot of drag. The bulkiness is a direct result of the three sets of bearings that needs to be housed in the rotor. In comparison to these bearings that the fully articulated rotor needs, the bearingless rotor has a structure that is much smaller, due to the fact that the bearings has now been removed, and thus an aerodynamically much cleaner design is obtained. If the design is aerodynamically much cleaner than there is less drag on the system and thus more power available.

Also when designing with composite materials it results in a design with considerable reduction in weight and a much smaller number of parts [10]. The second fact, namely the reduced number of parts plays a very important role especially when looking at issues such as maintenance and/or replacement of the parts. Smaller number of part means fewer parts that can fail and thus less maintenance. Also because there are now no moving parts, the necessity for lubricants is eliminated, again less maintenance.

Another advantage of the hingeless and specifically the bearingless rotor hub systems are that of stiffness. Because these systems are stiffer than the fully articulated hub, higher control moments can be applied to the system and that leads to greater responsiveness and gives better manoeuvrability of the helicopter, which could prove vital in a military application. [30]

Stellenbosch University http://scholar.sun.ac.za/

CHAPTER 3: ORIGINAL FULLY ARTICULATED ROTOR

3.1 Overview

The original fully articulated rotor is part of the 24% scale model at the facilities of the CSIR in Pretoria. The model is used for scale testing of the Rooivalk Attack helicopter. It is for this model that the bearingless rotor had to be designed. The layout of the scale model is given in Figure 3-1

3.2 Rotor Layout

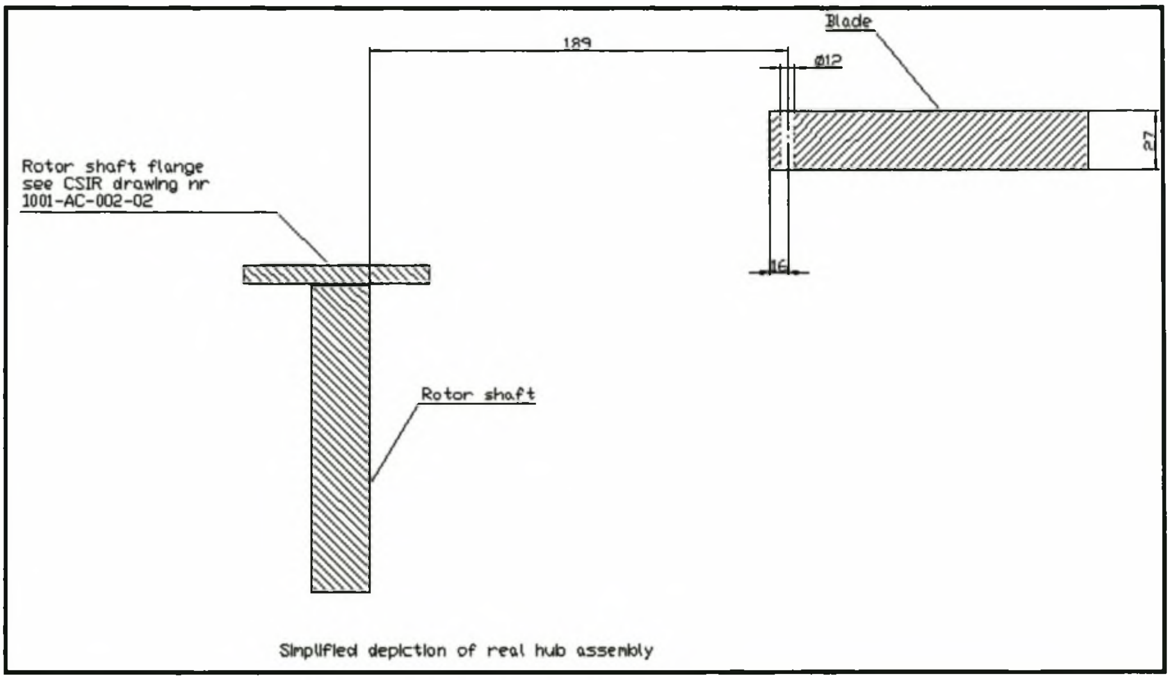

Figure 3-1: Layout of 24% scale model rotor system

3.3 Forces and Constraints

The constraints on this model are situated at two points, firstly at the base where the rotor hub joins up with the drive shaft and secondly at the intersection of the rotor hub and the blade. On the scale model these occur at respective distances of about 50 mm and 189 mm. The three bearings are located between these distances.

Stellenbosch University http://scholar.sun.ac.za/

Another constraint is the limit on the pitch rotation of 20 degrees.

The forces acting on the structure were taken from those supplied by the CSIR and can be found in Appendix B.

3.4 Computer Simulation on Dymore

The fully articulated model was constructed with information and technical drawings given by the CSIR [24]. It was necessary to construct a DYMORE [19, 20] computer model of the fully articulated rotor, because the new bearingless rotor had to be compared with the fully articulated model in as far as the dynamic characteristics were concerned. For this reason the fully articulated model's Southwell plot was needed.

The DYMORE model consisted of

1) 27 triads
2) 96 nodes
3) 6 beam elements
4) 3 revolute joints, to model the three bearings
5) 14 cross-sections. These cross-sections included are those of the blade. For calculating the blade cross-sections information supplied by the CSIR was used, see Appendix A.

A quasi-static analysis was done to determine the natural frequencies of the system for the Southwell plot. It consisted of 121 time steps taking the rotor speed from 0% to 120%.

No other analysis was done on the fully articulated model, because only the Southwell plots was needed for comparison. The Southwell plot is given in Figure 3-2.

Stellenbosch University http://scholar.sun.ac.za/

3.5 Southwell Plot

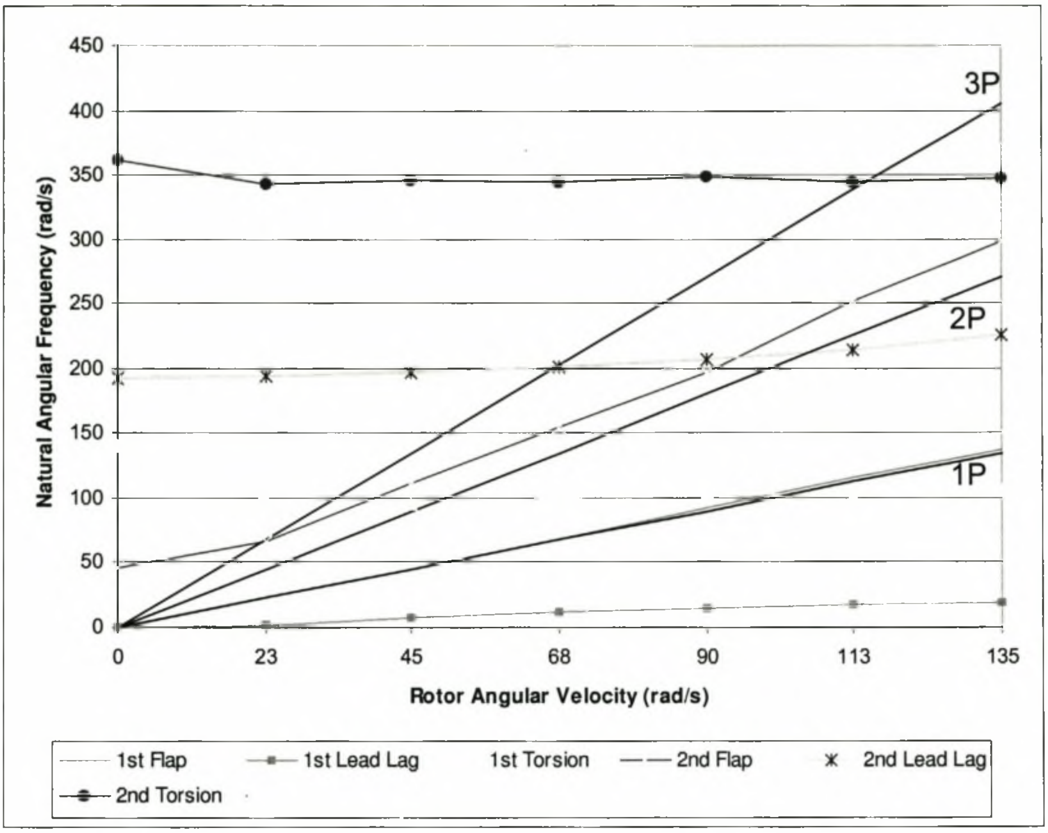

Figure 3-2: Southwell plot: fully articulated rotor

Stellenbosch University http://scholar.sun.ac.za/

CHAPTER 4: DESIGNING A NEW BEARINGLESS ROTOR

4.1 Overview

As in the design of most structures this design was also an iterative process. The final structure was analysed on MSC/NASTRAN for stresses and displacements and the Southwell plot was generated on DYMORE. The preliminary designs were done only on the DYMORE package to save time.

It was necessary to use both of these packages, because the MSC/NASTRAN for Windows package is unable to determine natural frequencies with centrifugal acceleration.

From this point on in this document the bearingless rotor hub will be called the flexbeam. The flexbeam is that part of the bearingless rotor hub that in the case of this document consists of composite material.

For more detailed design specifications of the bearingless rotor see Appendix C.

4.2 Material Selection

Certain criteria were important in selecting an adequate material for the flexbeam design, these were:

1. *Strength of the material.* The material has to withstand the forces acting on it.
2. *Flexibility.* Due to the fact that the flexbeam is replacing a bearing structure, it had to be flexible.
3. *Fatigue properties.* The flexbeam operates in a loading environment that is cyclic in nature.

Stellenbosch University http://scholar.sun.ac.za/

4 *Cost.* Although this was not a critical criteria due to the fact that the thesis turned out to be more of an academic exercise than a production prototype.

5 *Availability.* This is availability of the fibre for the University through the time-period of the thesis.

As stated in the introductory chapter it is only with the advent of composite materials that this kind of structure became possible. For this reason only composite materials were considered as a possible material.

Composite materials investigated were [6]:

1 Carbon fibre epoxy composite (67 vol %)

2 Glass fibre epoxy composite (73.3 vol %)
   a. C-glass
   b. E-glass
   c. S-glass

3 Kevlar fibre epoxy composite (82 vol %)

Table 4-1: Materials Considered

Material	*E* (GN/m^2)	Tensile Strength (MPa)	Availability	Relative Cost[1]
Carbon fibre	340-380	2200-2400	A	10
C-glass fibre	69	3100	NA	NA
E-glass fibre	72.4	3400	A	1
S-glass fibre	85.5	4800	NA	NA
Kevlar/epoxy	86	1517	A	10

A: Available *NA: Not Available*

After reviewing the options as stated in Table 4-1, E-glass/epoxy composite was finally selected as the material to be used. The reason for this choice was not only flexibility and strength to weight of E-glass/epoxy, but also the availability and cost of the E-glass during the manufacturing phase.

[1] Prices obtained from Advanced Material Technologies Cape Ltd.

Stellenbosch University http://scholar.sun.ac.za/

For purposes of analysis complete material properties were needed, for the fibre it was obtained from MATWEB [33], see Table 4-2. The epoxy used was Epolam 2020 from AMT materials [34, 35], see Table 4-3.

Table 4-2: Properties of E-glass [33]

PHYSICAL PROPERTIES	**VALUES**	**COMMENTS**
Density, g/cc	2.57	2.54-2.60 g/cm³
MECHANICAL PROPERTIES	**VALUES**	**COMMENTS**
Tensile Strength, Ultimate, MPa	3448	At 23°C (73°F); Virgin strength, 50-75% variation in finished product; 5310 MPa at -190°C (-310°F); 2620 MPa at 370°C (700°F); 1725 MPa at 540°C (1000°F)
Elongation %, break	4.8	
Poisson's Ratio	0.2	
Modulus of Elasticity, GN/m²	72.5	72.4-72.5 GN/m² at 23°C (73°F); 72.3 GN/m² at 540°C (1000°F)
Shear Modulus, GN/m²	30	Calculated
THERMAL PROPERTIES	**VALUES**	**COMMENTS**
CTE, linear 20ºC, μm/m-°C	5	
CTE, linear 250ºC, μm/m-°C	5.4	From -30 to 250°C (-20 to 480°F)
Thermal Conductivity, W/m-K	1.3	
Heat Capacity, J/g-°C	0.81	At 23°C (73°F); 1.03 J/g-°C (0.247 Btu/lbf-°F) at 200°C (390°F)
Melting Point, °C	1725	Upper limit

Stellenbosch University http://scholar.sun.ac.za/

Table 4-3: Properties of Epolam 2020 [35]

MECHANICAL PROPERTIES	VALUES
Final hardness (ISO 868), D Shore	85
Tg (DSC) (see the curves), °C	82
Flexural strength (ISO 178), MPa	120
Flexural modulus of elasticity (ISO 178), MPa	3100
HEAT PROPERTIES	**VALUES**
Tensile strength (ISO 527), MPa	80
Demoulding time at room temperature without accelerator, hr	48
Complete hardening time at room temperature, days	7

4.3 Problems Encountered from the Start

The initial goal was to attempt to place the new flexbeam into the space left by the fully articulated rotor (Figure 3-1). This proved to be a very optimistic goal, because of the torsional performance the rotor had to obtain. It was therefore decided to abandon this length constraint.

With the length constraint of 189 mm the factor of safety calculated from the stresses in the flexbeam was less than 0.1. This meant that failure of the structure was inevitable and would occur in the early stages of testing. The length was than systematically increased to the final length of 800 mm. This is a great deal more than initially intended, but inevitable due to the torsional load applied to the structure.

4.4 Calculating the Factor of Safety

As stated above, the preliminary design was analysed using the DYMORE [19] package. To compare designs the stress results from this package were extracted into three separate files, one for the nodal info, one for the elemental info and one for the stress info.

A FORTRAN [29] program, see Appendix D, was written to read in these three files and compute from them the factor of safety at every nodal position, as well as the warping, see Appendix E, of the cross-section. It was necessary to compute the warping of the cross-section to determine if the section would

Stellenbosch University http://scholar.sun.ac.za/

close on itself. The results of the factor of safety and warping calculations were then written to a FEMAP neutral file [17] and imported into MSC/NASTRAN for Windows [18] for graphical presentation.

4.4.1 Yield criteria investigated

4.4.1.1 Maximum normal stress theory

This theory states that failure will occur if any one of the principal stresses equals or exceeds the maximum allowable stress in that direction [4, 13, 26]. What this theory does not take into account is the interaction between the stresses.

For this theory the following inequalities must be satisfied [13]:

$\sigma_L < \sigma_{LU}$

$\sigma_T < \sigma_{TU}$

$\tau_{LT} < \tau_{LTU}$

4.4.1.2 Maximum strain

This theory states that failure will occur if any one of the principal strains equals or exceeds the maximum allowable in that direction [4, 13, 26]. This theory is similar to the maximum stress theory; all the stresses are now just replaced with strains.

For this theory the following inequalities must be satisfied [13]:

$\varepsilon_L < \varepsilon_{LU}$

$\varepsilon_T < \varepsilon_{TU}$

$\gamma_{LT} < \gamma_{LTU}$

4.4.1.3 Von Misses

This theory states that yielding will occur whenever the distortion energy in a unit volume equals the distortion energy in the same volume when uniaxially stressed to the yield strength [4, 25, 26]. This theory takes into account the interaction between the different stresses.

Stellenbosch University http://scholar.sun.ac.za/

For this theory the following inequality must be satisfied [26]:

$$\left[\frac{(\sigma_1-\sigma_2)^2+(\sigma_2-\sigma_3)^2+(\sigma_1-\sigma_3)^2}{2}\right]^{\frac{1}{2}}\leq\sigma_{yt}$$

In this form however the theory is not suited for composite materials.

4.4.1.4 Tsai-Hill

This theory is based on the Von Misses theory described above and expanded by Hill to include anisotropic bodies [4, 13, 25, 26].

For this theory the following inequality must be satisfied [25, 26]:

$$\left(\frac{\sigma_L}{\sigma_{LU}}\right)^2-\left(\frac{\sigma_L}{\sigma_{LU}}\right)\left(\frac{\sigma_T}{\sigma_{LU}}\right)+\left(\frac{\sigma_T}{\sigma_{TU}}\right)^2+\left(\frac{\tau_{LT}}{\tau_{LTU}}\right)^2\leq 1$$

Stellenbosch University http://scholar.sun.ac.za/

4.5 Preliminary Designs

4.5.1 Overview

The flexbeam itself went through a couple of changes throughout the thesis period. In total more than 60 iterations were done on the design. Not all these changes were major changes to the physical structure of the flexbeam, some were just changes to the fibre lay-up in the flexbeam.

In all the figures the different layers can be seen as they are presented by at least one row of elements.

Only the major design changes are mentioned in this document.

4.5.2 Designs

The first design investigated was one that was taken from work done by Prof NJ. Theron [2] on the full-scale version. This design consisted of two cross-sections; the reason for this was to isolate two distinctive zones, a flapping zone and a lead-lag zone. These two cross-sections are illustrated in Figure 4-1 and Figure 4-2. Cross-section **one** is situated in the flapping zone and cross-section **two** in the lead-lag zone.

This design resulted in a flexbeam structure with a torsional stiffness that was too high. The result of that was failure due to the applied pitch rotation.

Stellenbosch University http://scholar.sun.ac.za/

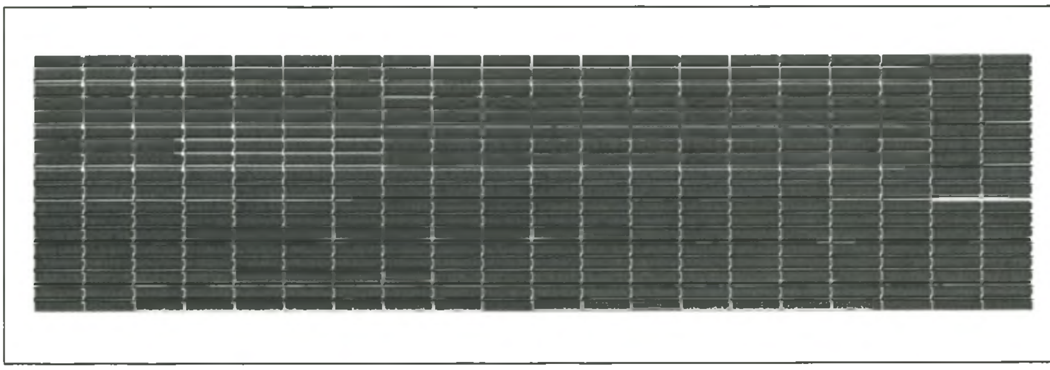

Figure 4-1: Original cross-section one

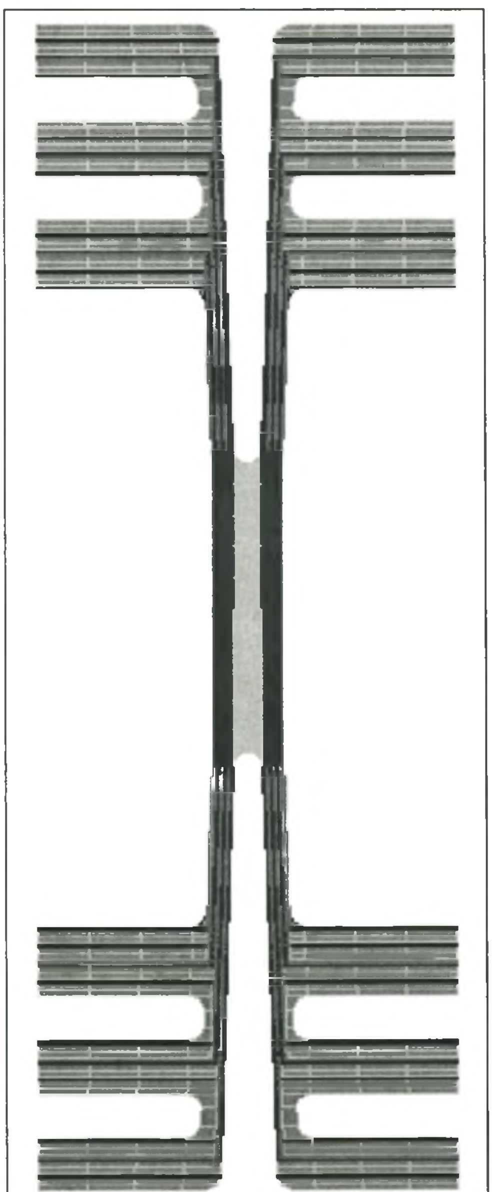

Figure 4-2: Original cross-section two

Stellenbosch University http://scholar.sun.ac.za/

Modifications to cross-section **one** was then made to try and reduce the torsional stiffness of the structure. The modification is shown in Figure 4-3. Cross-section **two** was left unchanged, this was done because the torsional stiffness of cross-section **two** was much lower than that of section **one**.

Figure 4-3: Modified cross-section one

This change was unsuccessful and also resulted in a structure with a torsional stiffness that was too high. Modifications to the lay-up of these two structures also proved to be unsuccessful. Because these changes did not result in a satisfactory structure and actually did not even improve the existing ones, the two cross-sections as shown in Figure 4-2 and Figure 4-3 were abandoned.

It was decided to start over with two simplified cross-sections and to modify them until a structure with adequate torsional stiffness was obtained.

Therefore the next cross-sections that were looked at were a flat-bar piece as the one in Figure 4-1 and a plain I-beam profile (Figure 4-4).

From the analysis it became clear that the I-beam profile had the higher torsional stiffness. For this reason it was decided to modify it to lower the overall torsional stiffness. The evolution of this I-beam is shown in Figure 4-4 to Figure 4-6.

Stellenbosch University http://scholar.sun.ac.za/

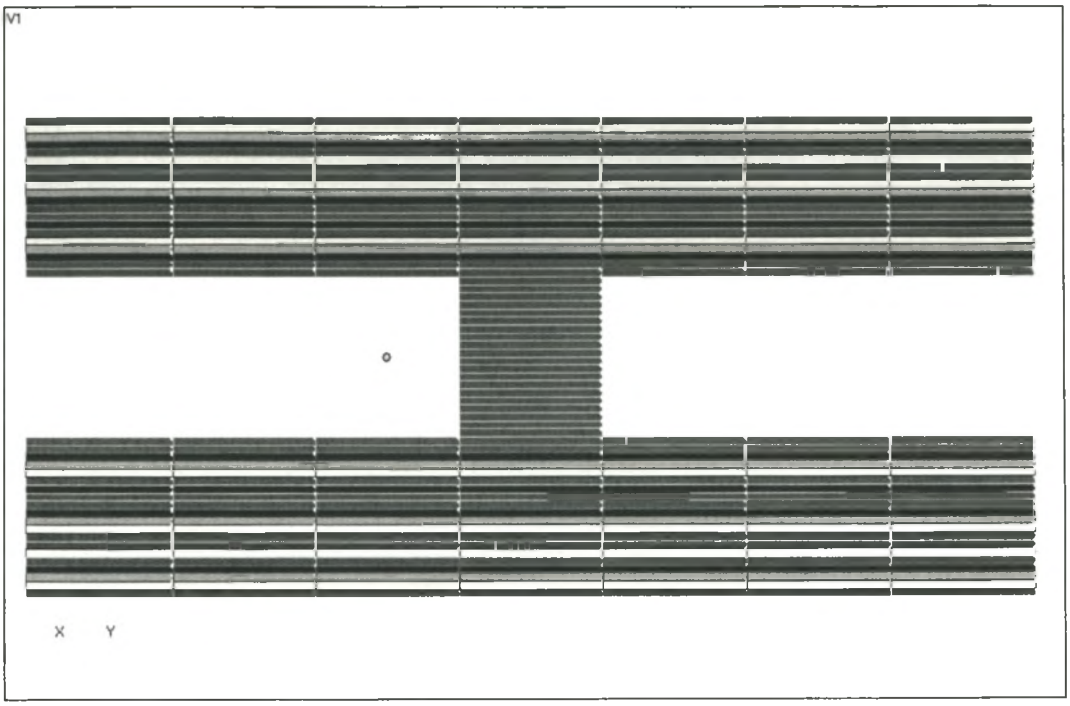

Figure 4-4: I-Beam iteration one

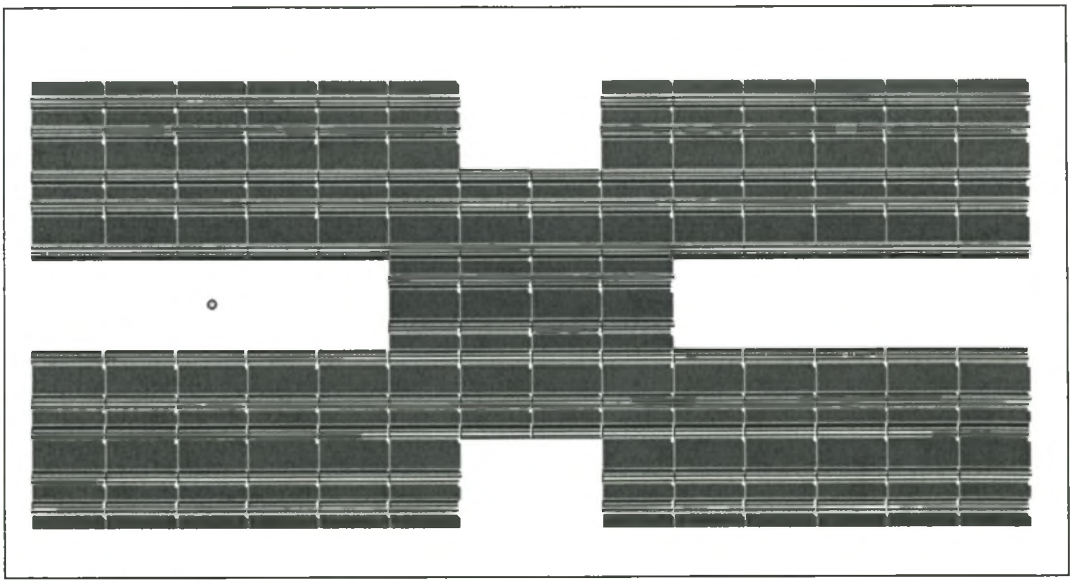

Figure 4-5: I-Beam iteration two

Stellenbosch University http://scholar.sun.ac.za/

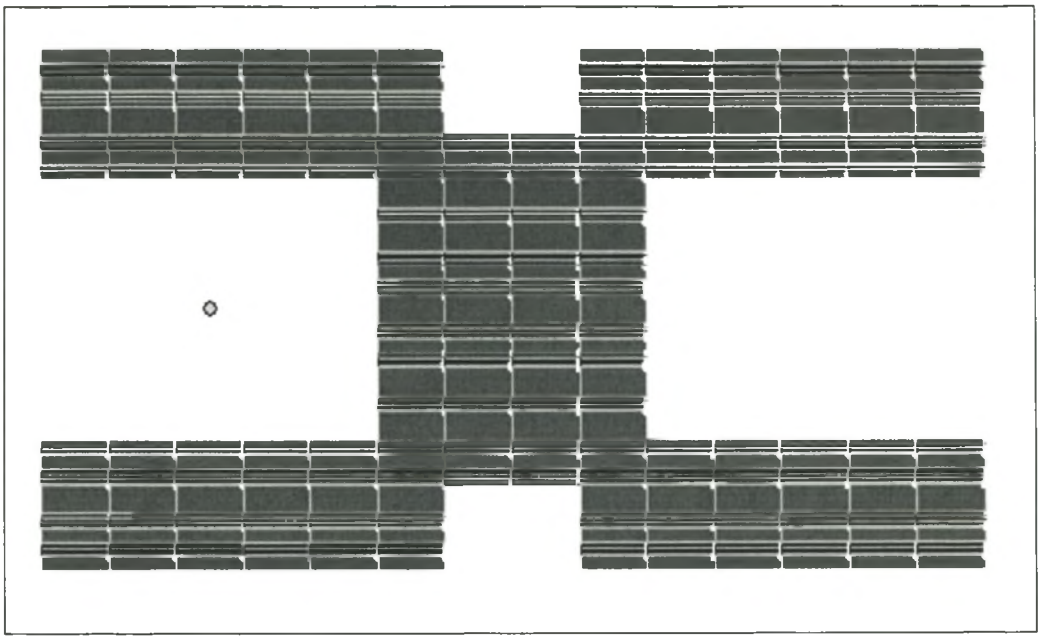

Figure 4-6: I-Beam iteration three

At this point it became clear that the I-beam had to be modified even more to "open up" the structure to reduce the torsional stiffness even more. For this reason the flanges of the I-beam were modified. The new I-beam had three thinner flanges instead of two. The new cross-section can be seen in Figure 4-7.

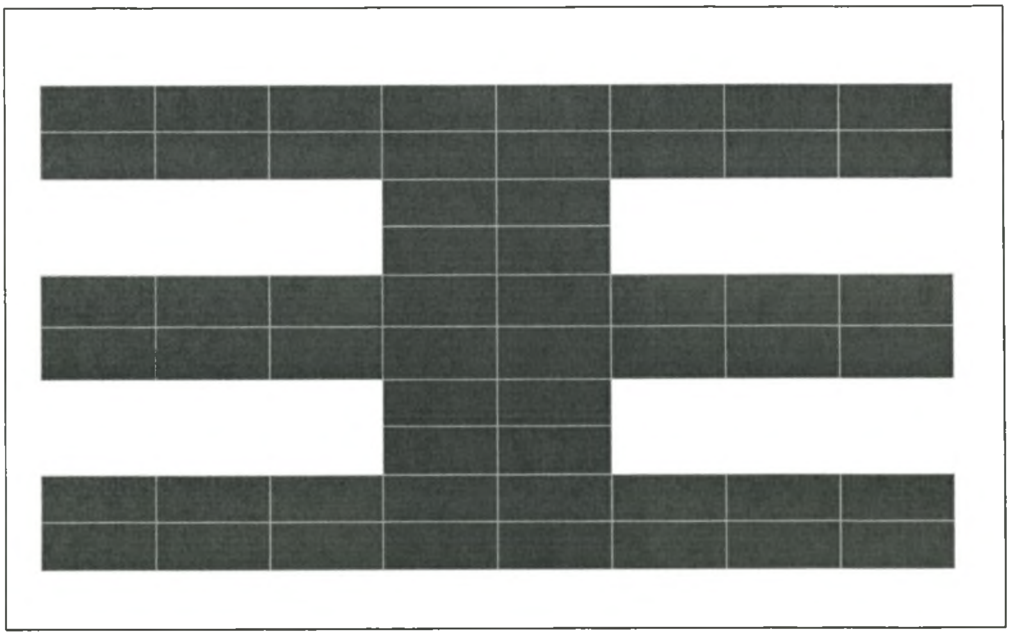

Figure 4-7: Three flange I-beam

Stellenbosch University http://scholar.sun.ac.za/

The torsional stiffness of this cross-section also proved to be too high, although it was encouraging that it was a factor of 6 lower than the original I-beam. This meant that the design was moving in the right direction. This cross-section was then modified to see whether there could be improved upon. The evolution of this cross-section can be seen in Figure 4-8 to Figure 4-12.

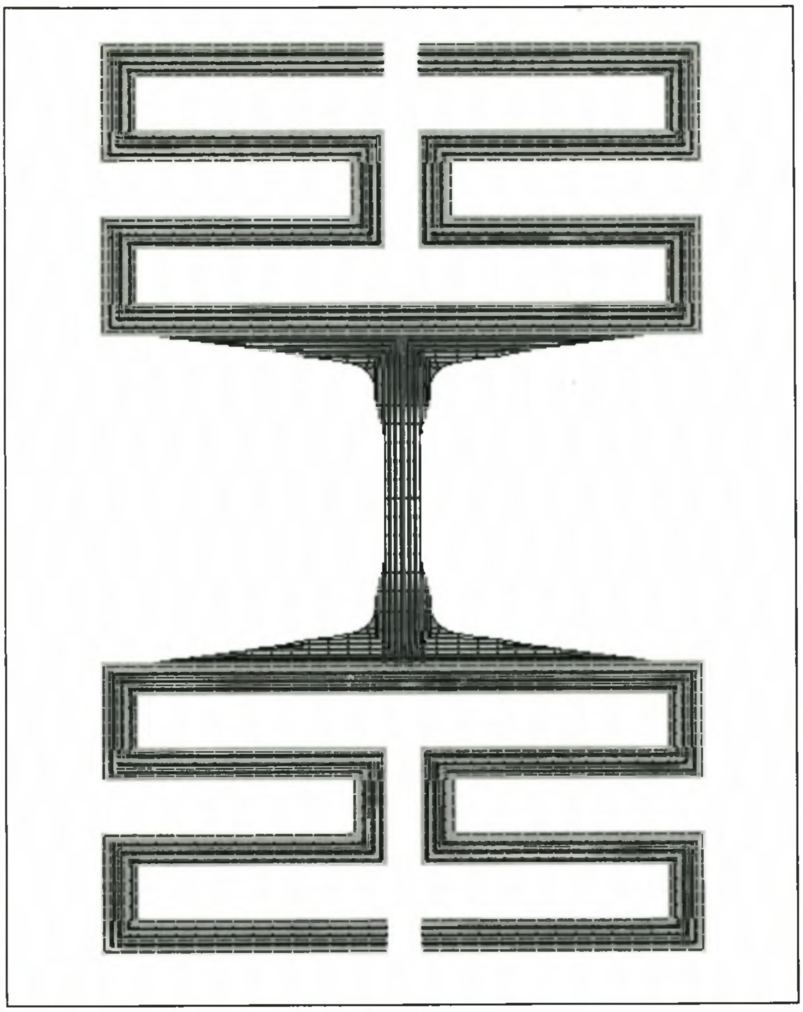

Figure 4-8: Multi-flange I-beam one

Stellenbosch University http://scholar.sun.ac.za/

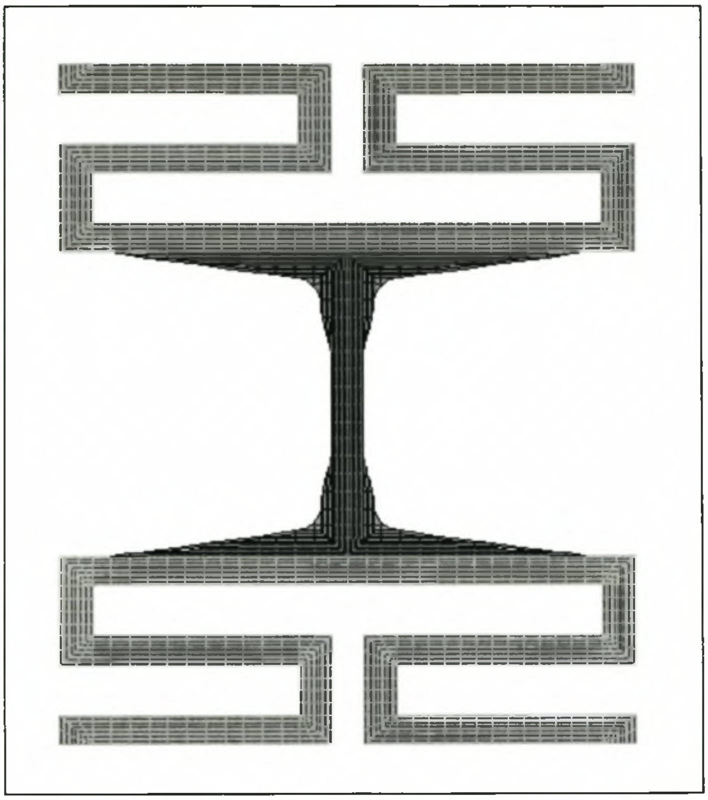

Figure 4-9: Multi-flange I-beam two

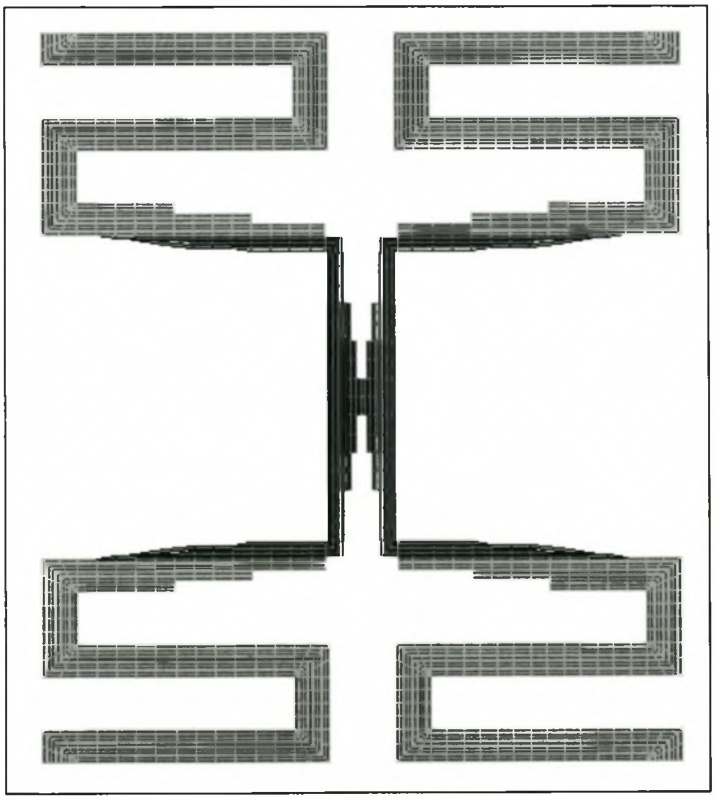

Figure 4-10:Multi-flange I-beam three

Stellenbosch University http://scholar.sun.ac.za/

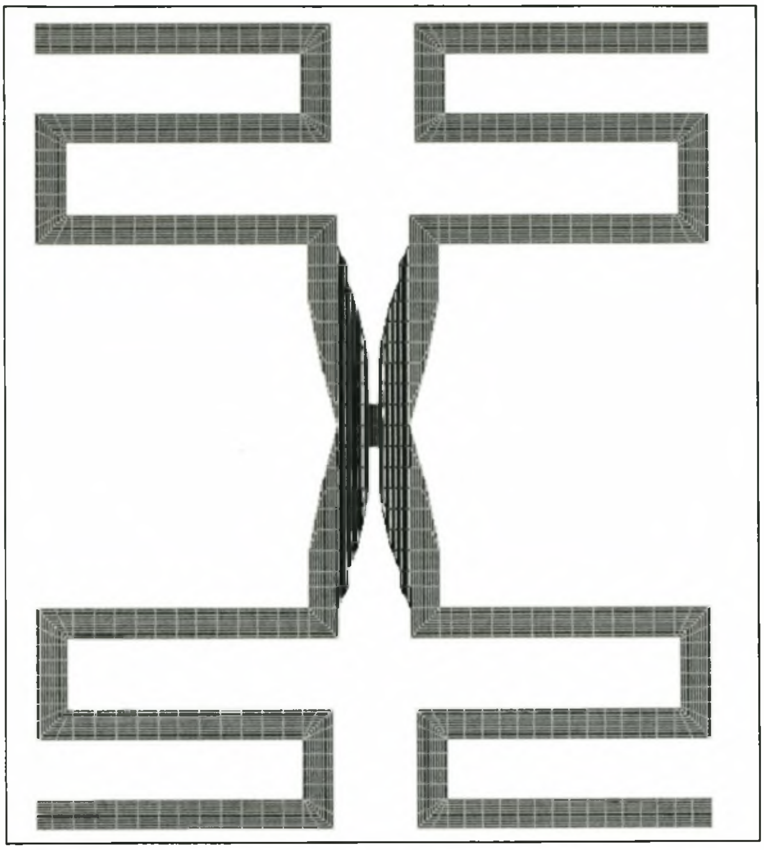

Figure 4-11: Multi-flange I-beam four

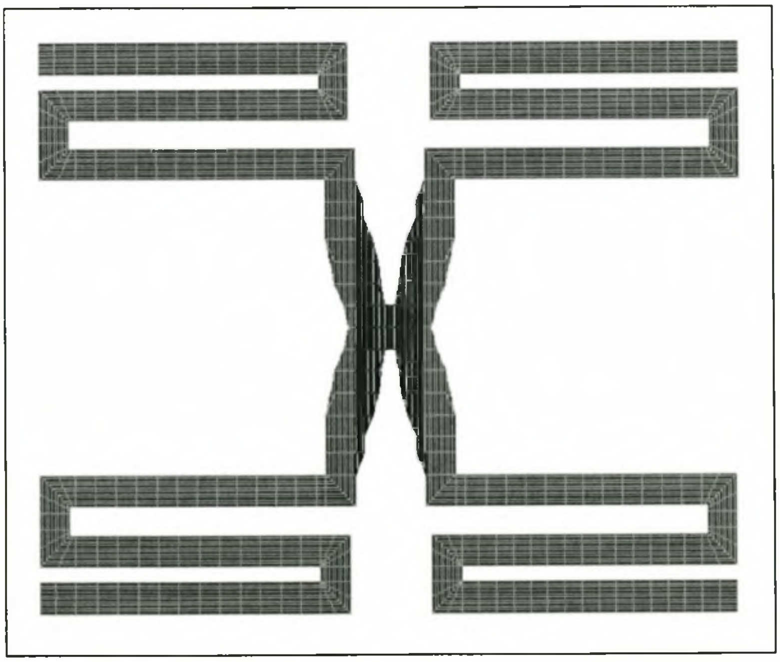

Figure 4-12: Multi-flange I-beam five

Stellenbosch University http://scholar.sun.ac.za/

Although the torsional stiffness was brought down a factor of ten relative to the original I-beam design, failure would still occur in this design due to fatigue loading, because of high torsional stiffness. It must be said that in a static environment this design would most likely not show failure, because the factor of safety calculated for this structure was 1.2.

Due to the fact stated above and the fact that the structures as shown in Figure 4-11 and Figure 4-15 became difficult to manufacture it was decided to also abandon these sections.

The next cross-section that was tried came from two articles [5, 10] in the literature. It is basically a cross-type cross-section shown in Figure 4-13. The fist cross-section that was tried failed, also due to a too high torsional stiffness. Modifications to this cross-section eventually led to a design (Figure 4-14) that gave results that was acceptable.

Further work that was done on this cross-section to model it into a three dimensional flexbeam is discussed in the next paragraph.

Stellenbosch University http://scholar.sun.ac.za/

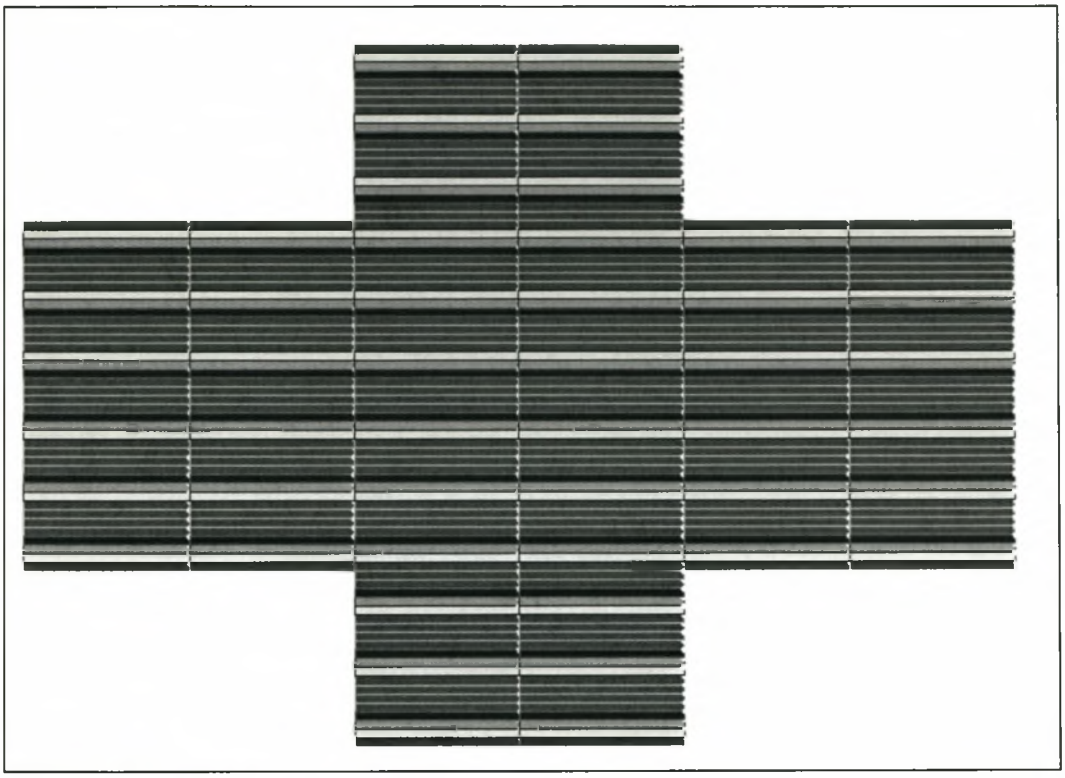

Figure 4-13: Cross type cross-section

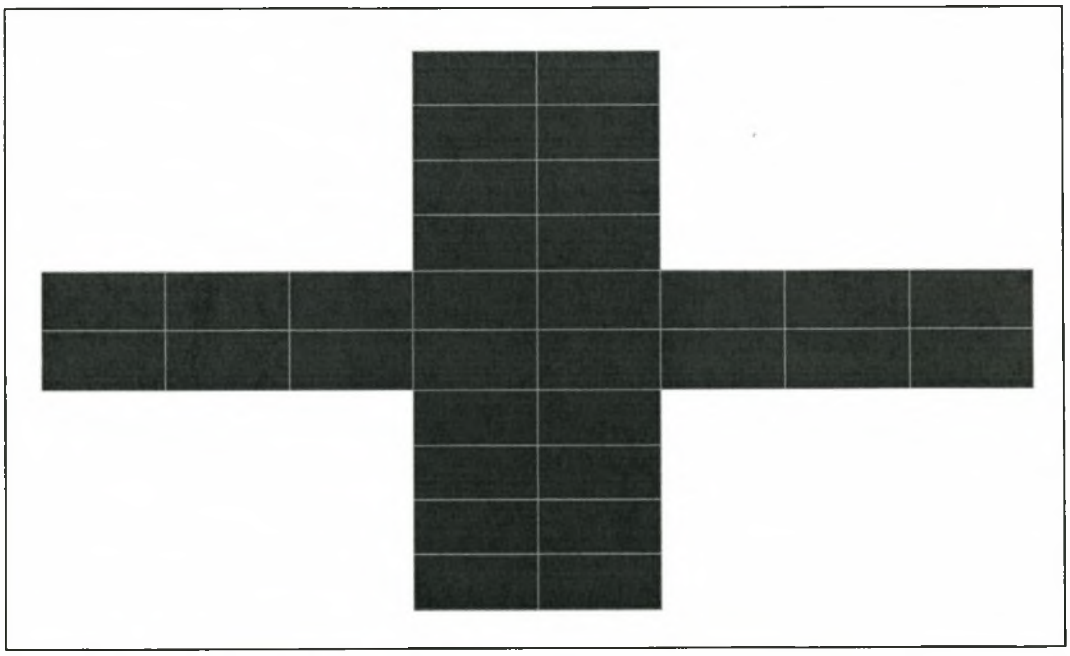

Figure 4-14: Final cross-section

Stellenbosch University http://scholar.sun.ac.za/

4.6 The final design

At the end of the iterative process it was decided to conclude with the following design. This design is by no means the optimal design, but because of time constraints on a Masters Degree and because of the ultimate goal of the thesis, this design was adequate. The design is shown in Figure 4-15.

The lay-up of this structure consists exclusively of fibres that run in the axial directions of the flexbeam.

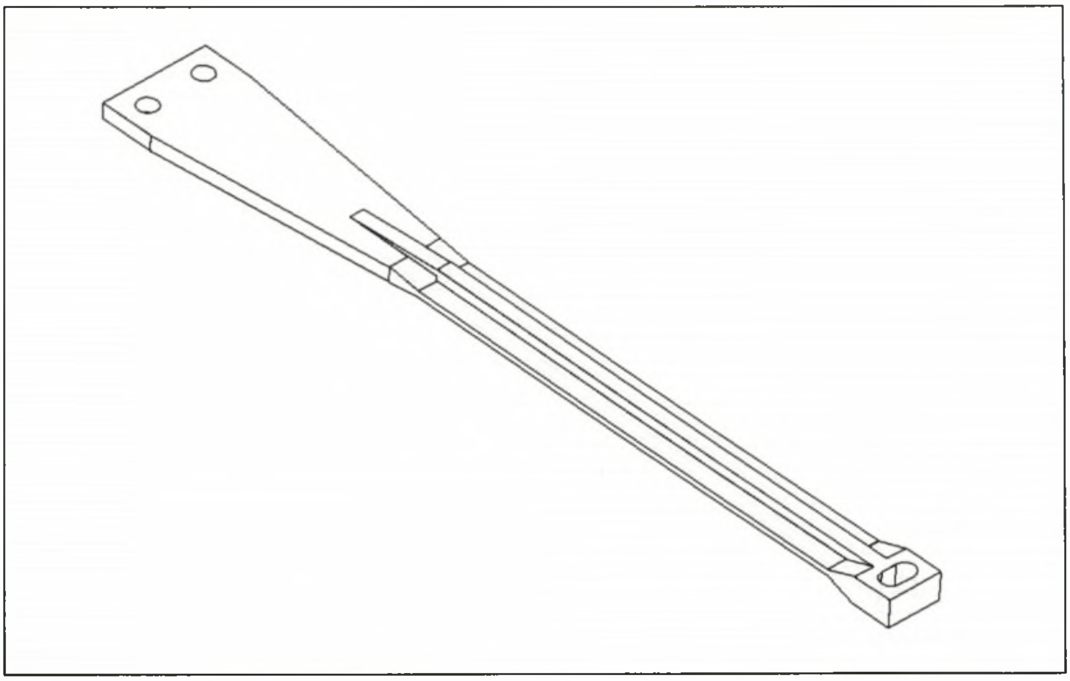

Figure 4-15: Final design

4.7 MSC/NASTRAN Model of the Final Design

The model was created using the Solid Edge Origin package and imported into MSC/NASTRAN as a *Parasolid* type. It was then meshed using this package's own solid mesher and the result was that the model consisted of 27782 nodes and 13719 CTETRA [36], 10-node tetrahedral elements. The model is shown in Figure 4-16.

Stellenbosch University http://scholar.sun.ac.za/

The model was constrained at the two holes where the flexbeam meets the drive shaft and on the other side on the intersection of the flexbeam and the blade.

The loads consisted of the peak values that the rotor would experience, as calculated from the data given by the CSIR. The axes are so defined that horizontal refers to a direction along the y-axis and vertical along the z-axis.

These included:

1) A axial load of 20000 N
2) A vertical shear force of 1000 N
3) A horizontal shear force of 1000 N
4) A vertical moment of 1000 Nm
5) A horizontal moment of 1000 Nm
6) A torsional load equivalent to a torsional angular displacement of 20° from the neutral position

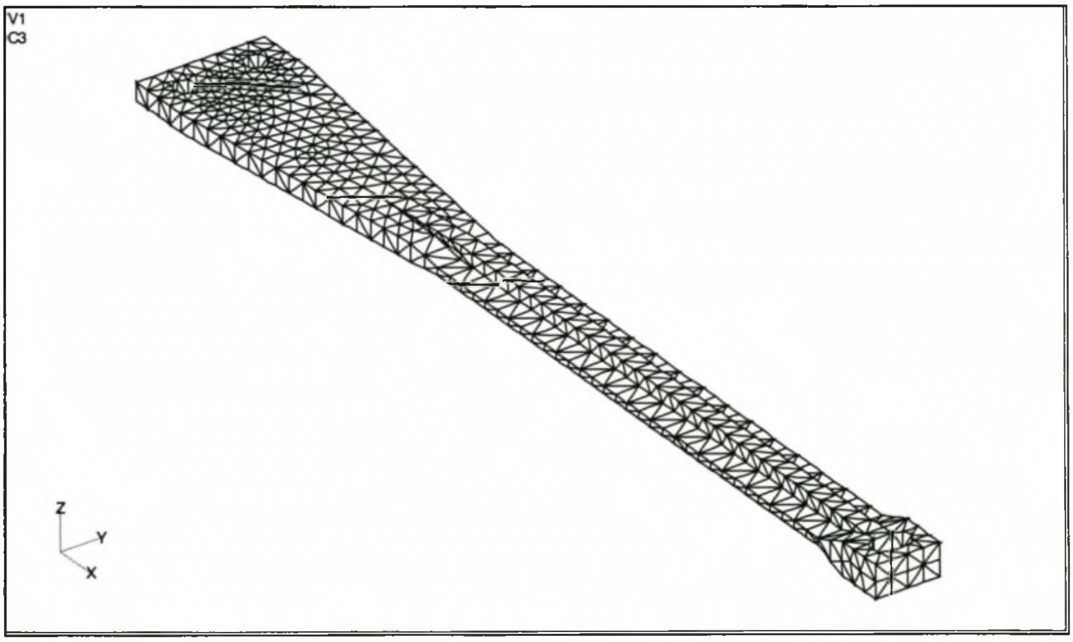

Figure 4-16: MSC/NASTRAN model

Stellenbosch University http://scholar.sun.ac.za/

4.8 Analysis Results

4.8.1 Overview

The six load cases were analysed using the static analysis method of the MSC/NASTRAN for Windows (version 4) FEA package. The results obtained from the analyses are discussed below. All results are maximum values for the stresses throughout the structure, because only the total strength of the structure was considered here.

Although all six load-cases are applied to the flexbeam at the same time during flight, they are discussed separately to establish which one of them is the crucial one for failure. In the last paragraph they are combined to investigate their effect on the stresses of the total flexbeam.

The maximum displacements of the flexbeam are not given, the reason for this is due to the fact that the constraints used in the FEA model represent the way that the model will be clamped into the test bench and are therefore not realistic deformations for the flexbeam during field operation.

Stellenbosch University http://scholar.sun.ac.za/

4.8.2 Load case 1

This load case is due to the centrifugal force that the blade exerts on the flexbeam. The rotating blades of the helicopter generate this centrifugal force during flight.

A summary of the stresses as calculated with MSC/NASTRAN for Windows are shown in Table 4-4.

Table 4-4: Load Case 1 Results

Maximum/Minimum Stress		Value (MPa)
Solid X Normal Stress	Minimum	-1.893
	Maximum	56.068
Solid Y Normal Stress	Minimum	-25.000
	Maximum	9.339
Solid Z Normal Stress	Minimum	-2.240
	Maximum	3.008
Solid XY Shear Stress	Minimum	-11.000
	Maximum	11.759
Solid YZ Shear Stress	Minimum	-2.503
	Maximum	2.357
Solid Von Mises Stress	Minimum	5.267
	Maximum	55.800

Stellenbosch University http://scholar.sun.ac.za/

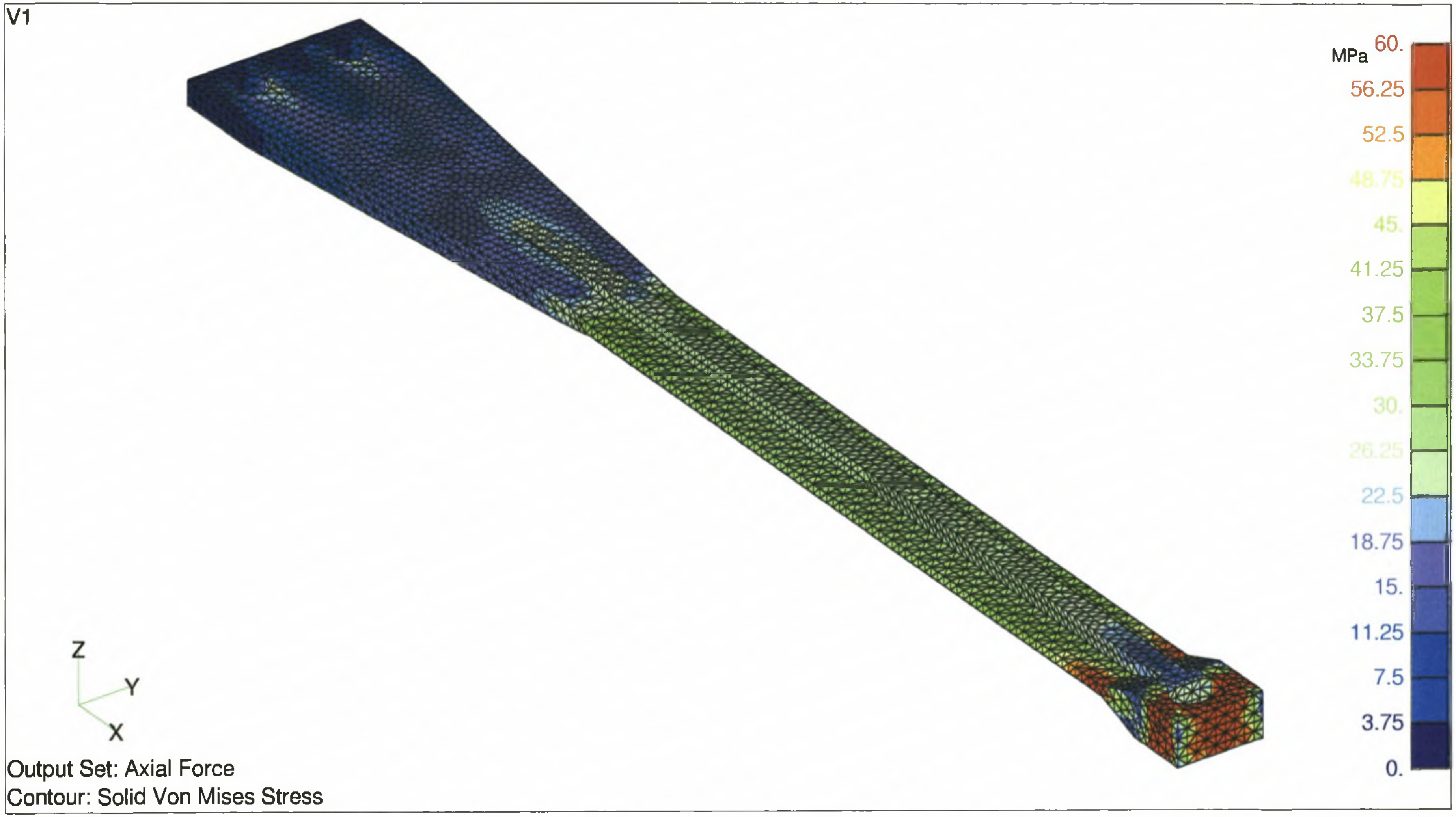

Figure 4-17: Von Mises stress distribution for load case 1

Stellenbosch University http://scholar.sun.ac.za/

4.8.3 Load case 2

The hanging fuselage of the helicopter is attached to the blade at the shaft. This connection is the flexbeam, in the current design. That means the fuselage of the helicopter is hanging from the blade by means of the flexbeam. The blades also generated lift, a force that wants to lift the helicopter upwards. The combined effect of the lift and the hanging of the fuselage generate this load case. Here only the resulting shear force is applied to the FEA model.

A summary of the stresses as calculated with MSC/NASTRAN for Windows are shown in Table 4-5.

Table 4-5: Load Case 2 Results

Maximum/Minimum Stress		Value (MPa)
Solid X Normal Stress	Minimum	-250.000
	Maximum	257.000
Solid Y Normal Stress	Minimum	-18.000
	Maximum	18.508
Solid Z Normal Stress	Minimum	-8.878
	Maximum	9.956
Solid XY Shear Stress	Minimum	-16.000
	Maximum	16.150
Solid YZ Shear Stress	Minimum	-10.000
	Maximum	10.174
Solid Von Mises Stress	Minimum	0.026
	Maximum	258.000

Stellenbosch University http://scholar.sun.ac.za/

Figure 4-18: Von Mises stress distribution for load case 2

Stellenbosch University http://scholar.sun.ac.za/

4.8.4 Load case 3

As mentioned in chapter 2 one of the forces acting on a rotating blade of a helicopter is that of drag due to air resistance. That drag causes a horizontal force along the blade. That horizontal force is then transferred into the flexbeam. Here only the resulting shear force is applied to the FEA model.

A summary of the stresses as calculated with MSC/NASTRAN for Windows are shown in Table 4-6.

Table 4-6: Load Case 3 Results

Maximum/Minimum Stress		Value (MPa)
Solid X Normal Stress	Minimum	-150.000
	Maximum	150.000
Solid Y Normal Stress	Minimum	-1.880
	Maximum	2.570
Solid Z Normal Stress	Minimum	-2.170
	Maximum	2.637
Solid XY Shear Stress	Minimum	-2.384
	Maximum	6.286
Solid YZ Shear Stress	Minimum	-0.578
	Maximum	0.578
Solid Von Mises Stress	Minimum	0.023
	Maximum	150.000

Stellenbosch University http://scholar.sun.ac.za/

Figure 4-19: Von Mises stress distribution for load case 3

Stellenbosch University http://scholar.sun.ac.za/

4.8.5 Load case 4

This load case arises from load case 2. The reason is due to the fact that the blade has a finite length, which means that any force that is acting on the blade will cause a shear force and a moment on the flexbeam. The shear force part of this load is discussed in load case 2.

A summary of the stresses as calculated with MSC/NASTRAN for Windows are shown in Table 4-7.

Table 4-7: Load Case 4 Results

Maximum/Minimum Stress		Value (MPa)
Solid X Normal Stress	Minimum	-480.000
	Maximum	484.000
Solid Y Normal Stress	Minimum	-31.000
	Maximum	29.608
Solid Z Normal Stress	Minimum	-16.000
	Maximum	17.776
Solid XY Shear Stress	Minimum	-51.000
	Maximum	44.904
Solid YZ Shear Stress	Minimum	-19.000
	Maximum	21.005
Solid Von Mises Stress	Minimum	0.007
	Maximum	485.000

Stellenbosch University http://scholar.sun.ac.za/

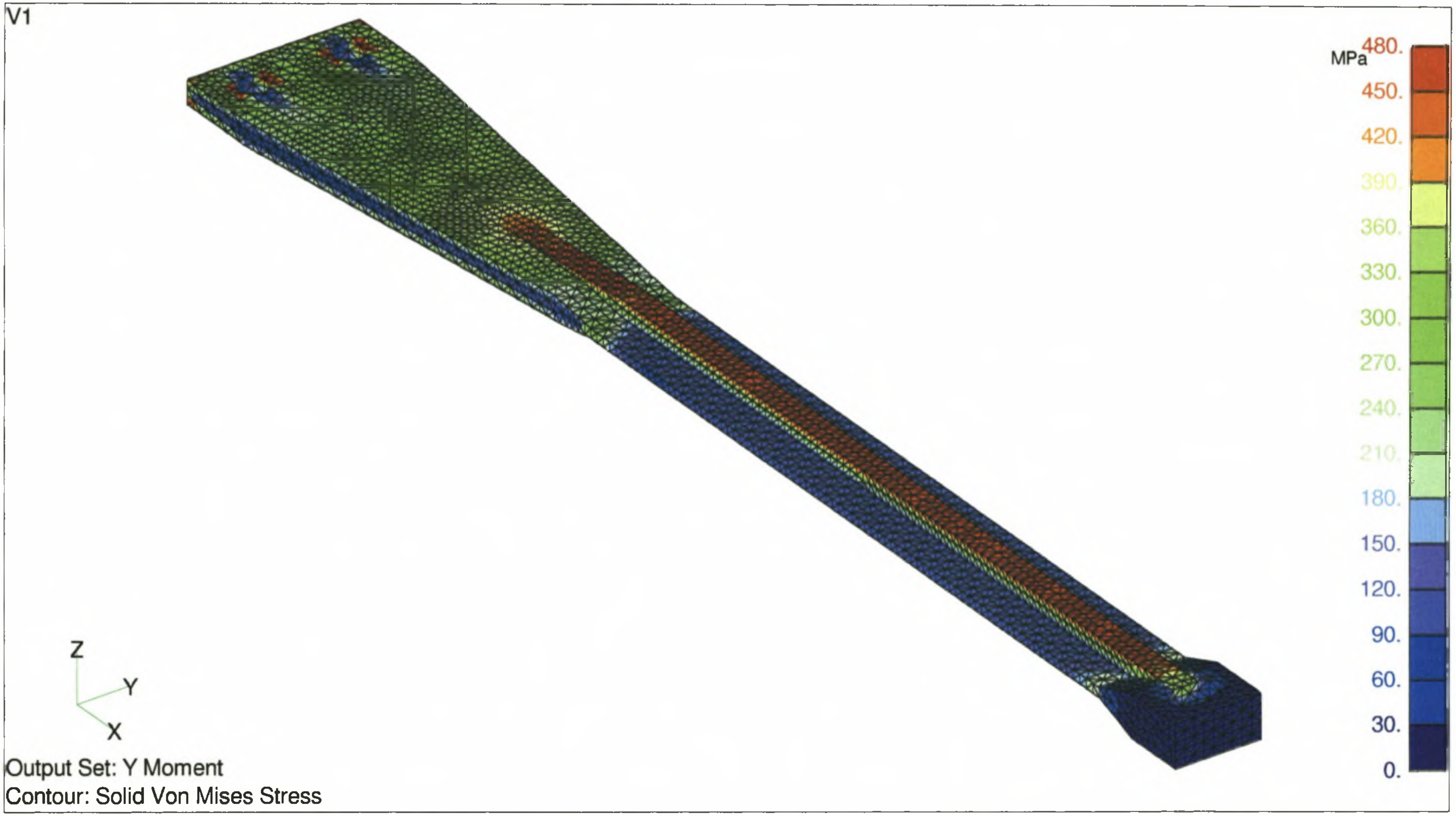

Figure 4-20: Von Mises stress distribution for load case 4

Stellenbosch University http://scholar.sun.ac.za/

4.8.6 Load case 5

This load case arises from load case 3. The reason for this is the same as mentioned in load case 4. The shear force part of this load is discussed in load case 3.

A summary of the stresses as calculated with MSC/NASTRAN for Windows are shown in Table 4-8.

Table 4-8: Load Case 5 Results

Maximum/Minimum Stress		Value (MPa)
Solid X Normal Stress	Minimum	-290.000
	Maximum	295.000
Solid Y Normal Stress	Minimum	-9.914
	Maximum	5.083
Solid Z Normal Stress	Minimum	-13.000
	Maximum	13.698
Solid XY Shear Stress	Minimum	-7.407
	Maximum	10.749
Solid YZ Shear Stress	Minimum	-2.104
	Maximum	2.009
Solid Von Mises Stress	Minimum	0.003
	Maximum	295.000

Stellenbosch University http://scholar.sun.ac.za/

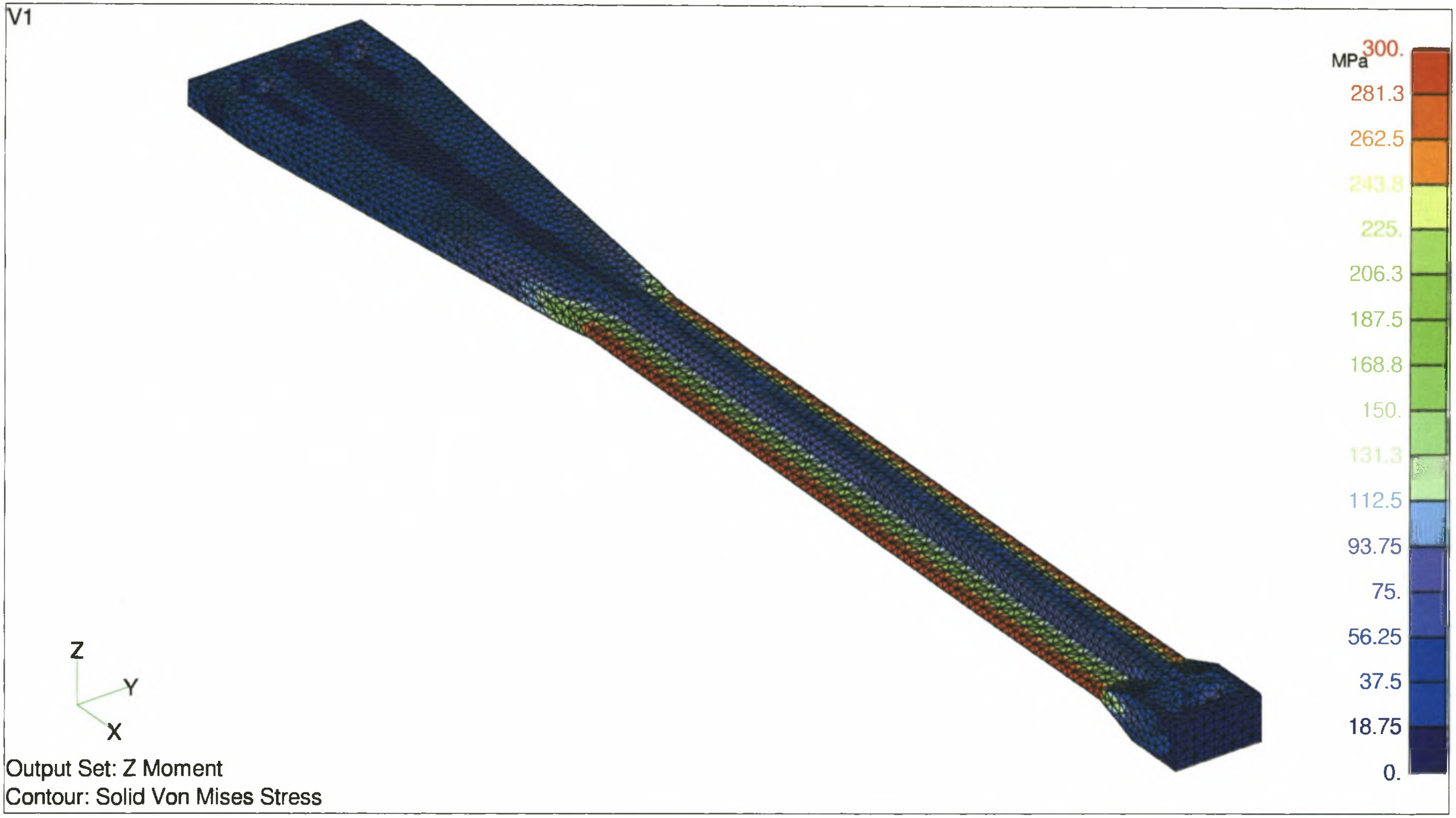

Figure 4-21: Von Mises stress distribution for load case 5

Stellenbosch University http://scholar.sun.ac.za/

4.8.7 Load case 6

The force of this load case is generated from the control stick the pilot operates. Thus the pilot has direct control over the pitch angle and the pitch force.

A summary of the stresses as calculated with MSC/NASTRAN for Windows are shown in Table 4-9.

Table 4-9: Load Case 6 Results

Maximum/Minimum Stress		Value (MPa)
Solid X Normal Stress	Minimum	-4.794
	Maximum	4.866
Solid Y Normal Stress	Minimum	-1.306
	Maximum	1.285
Solid Z Normal Stress	Minimum	-0.616
	Maximum	0.602
Solid XY Shear Stress	Minimum	-2.904
	Maximum	3.119
Solid YZ Shear Stress	Minimum	-0.540
	Maximum	0.588
Solid Von Mises Stress	Minimum	0.003
	Maximum	7.636

Stellenbosch University http://scholar.sun.ac.za/

Figure 4-22: Von Mises stress distribution for load case 6

Stellenbosch University http://scholar.sun.ac.za/

4.8.8 Combining the load cases

The linear combination of the above six load cases was done to find the combined effect of the loads on the flexbeam.

A summary of the stresses as calculated with MSC/NASTRAN for Windows are shown in Table 4-10.

Table 4-10: Combined Case Results

Maximum/Minimum Stress		**Value (MPa)**
Solid X Normal Stress	Minimum	-777.737
	Maximum	840.835
Solid Y Normal Stress	Minimum	-46.293
	Maximum	51.451
Solid Z Normal Stress	Minimum	-24.448
	Maximum	27.206
Solid XY Shear Stress	Minimum	-62.361
	Maximum	53.370
Solid YZ Shear Stress	Minimum	-28.944
	Maximum	28.673
Solid Von Mises Stress	Minimum	3.448
	Maximum	842.561

Stellenbosch University http://scholar.sun.ac.za/

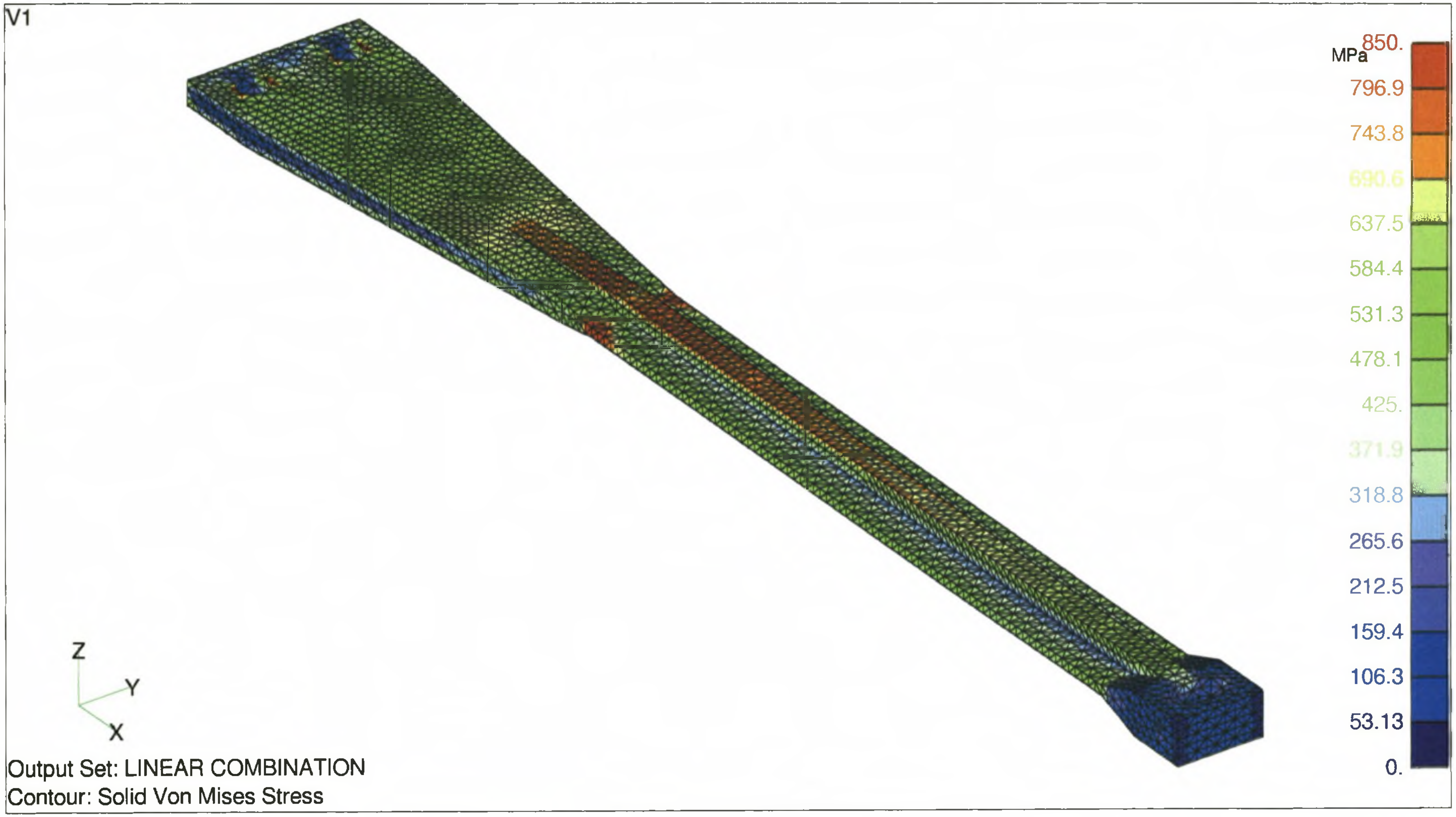

Figure 4-23: Von Mises stress distribution for combined load case

Stellenbosch University http://scholar.sun.ac.za/

4.8.9 Summary

The critical values for failure in the case of this structure are the shear stresses. This can be assumed due to the high fibre strengths and the fact that the epoxy must withstand the shear forces generated by the blade rotation.

Table 4-11: Highest Stresses Per Load Set

Final Maximum/Minimum Stress		Set	Value (MPa)
Solid X Normal Stress	Minimum	4	-480.000
	Maximum	4	484.000
Solid Y Normal Stress	Minimum	4	-31.000
	Maximum	4	29.608
Solid Z Normal Stress	Minimum	4	-16.000
	Maximum	4	17.776
Solid XY Shear Stress	Minimum	4	-51.000
	Maximum	4	44.904
Solid YZ Shear Stress	Minimum	4	-19.000
	Maximum	4	21.005
Solid Von Mises Stress	Minimum	6	0.003
	Maximum	4	485.000

The allowable values for the normal Y- and Z-stresses were taken as the maximum allowable stress value of the resin, the reason for this is that these components of the stresses act through a vector that is normal to the fibre direction.

In the case of the shear stresses, the maximum allowable stresses were also taken as the maximum allowable stress value of the resin, here the reasoning was that the resin is the predominant load-carrying member of the shear component of the force.

As can be seen from Table 4-11, load case 4 is the critical load case of the six load cases that are applied to the flexbeam.

Stellenbosch University http://scholar.sun.ac.za/

When a comparison between the maximum allowable stresses and the resulting combined stresses of Table 4-10 are made, it can be seen that the maximum stresses of the flexbeam are within the allowable values, although no great factor of safety can be expected.

With respect to the results above the design was deemed adequate as a first prototype for testing. Due to the relative high stresses, a long fatigue life for this prototype is not expected, but will serve to demonstrate whether or not the fatigue tests, as planned, are adequate.

Stellenbosch University http://scholar.sun.ac.za/

4.9 Computer Simulation on Dymore

After the stresses were determined to be in an adequate range, but by no means optimal or possibly flight ready, the dynamics of the design had to be determined. This was again done using the DYMORE [19] program. For this program the cross-sections at 8 positions, see Figure 4-24, throughout the flexbeam were taken. The PREFEM input file can be seen in Appendix F.

The individual cross-sections are illustrated in Figure 4-25 to Figure 4-32 with a summary of them in Table 4-12.

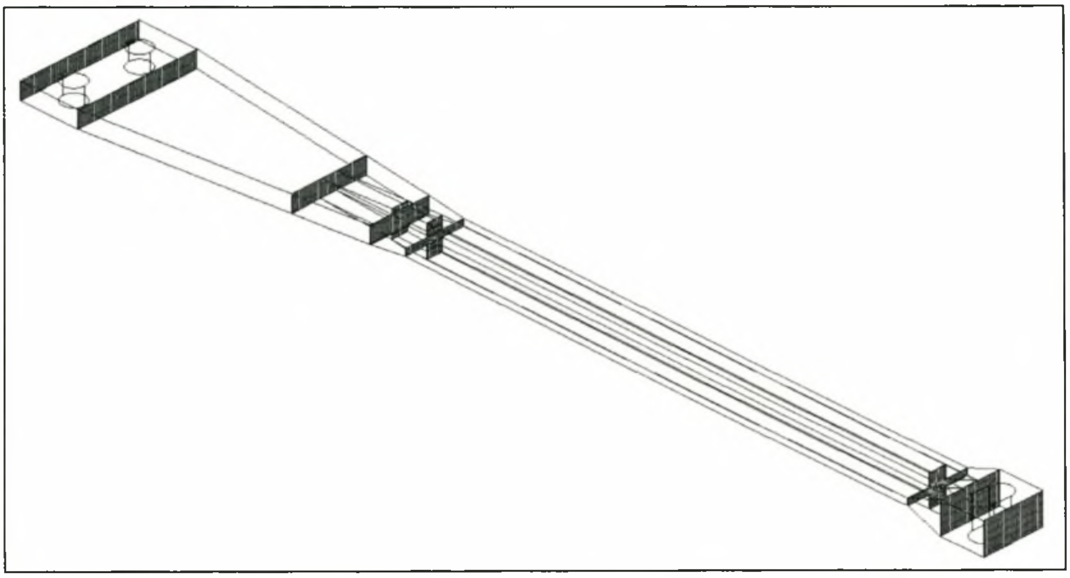

Figure 4-24: Cross-sections at 8 positions

Stellenbosch University http://scholar.sun.ac.za/

Table 4-12: Cross-Section Info for Final Design

Section	Figure	Distance (mm)[2]	Elements	Nodes
1	Figure 4-25	0	448	1473
2	Figure 4-26	54	448	1473
3	Figure 4-27	234	288	953
4	Figure 4-28	302	64	233
5	Figure 4-29	334	138	493
6	Figure 4-30	804	180	627
7	Figure 4-31	833	392	1261
8	Figure 4-32	873	392	1261

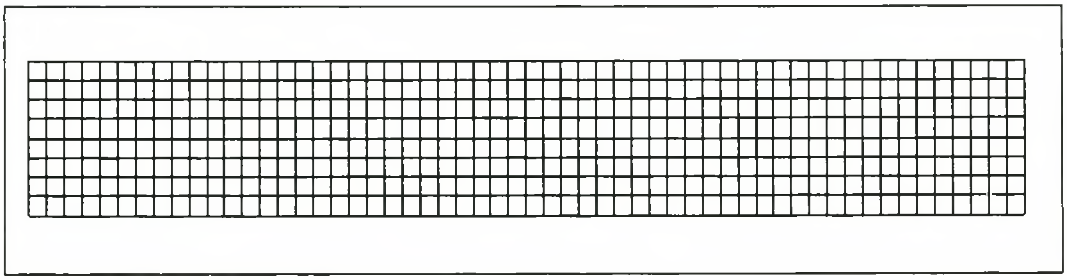

Figure 4-25: Cross-section 1

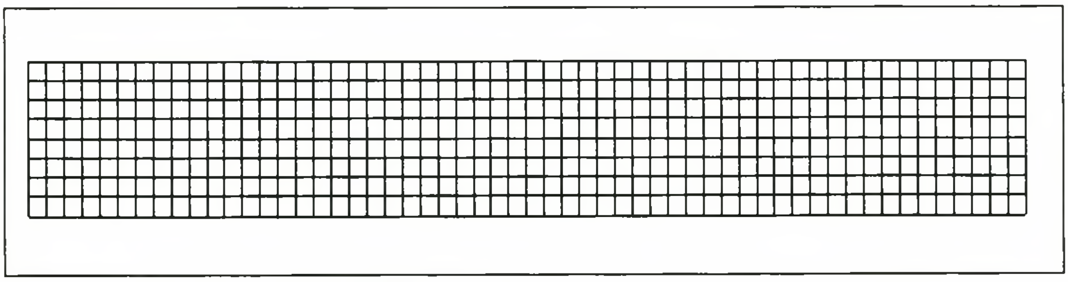

Figure 4-26: Cross-section 2

[2] This is the distance from the beginning of the flexbeam

Stellenbosch University http://scholar.sun.ac.za/

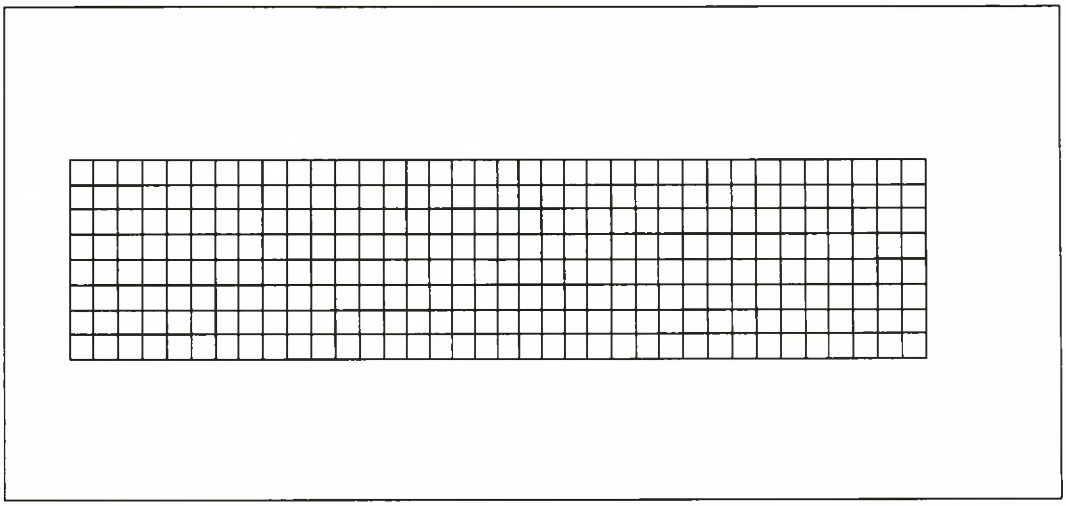

Figure 4-27: Cross-section 3

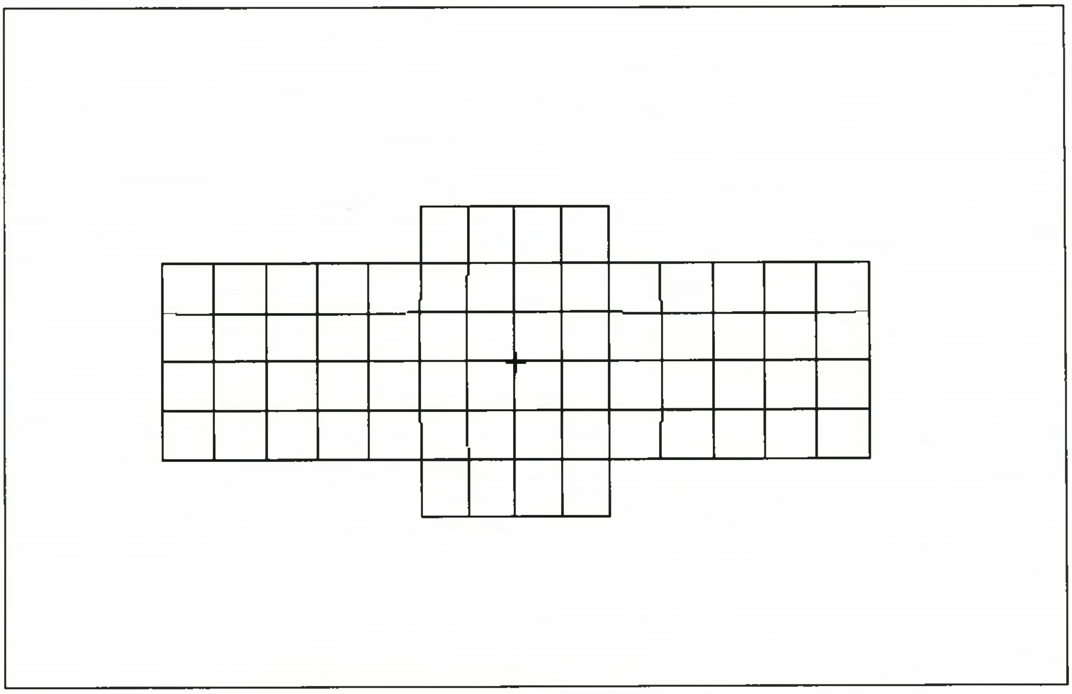

Figure 4-28: Cross-section 4

Stellenbosch University http://scholar.sun.ac.za/

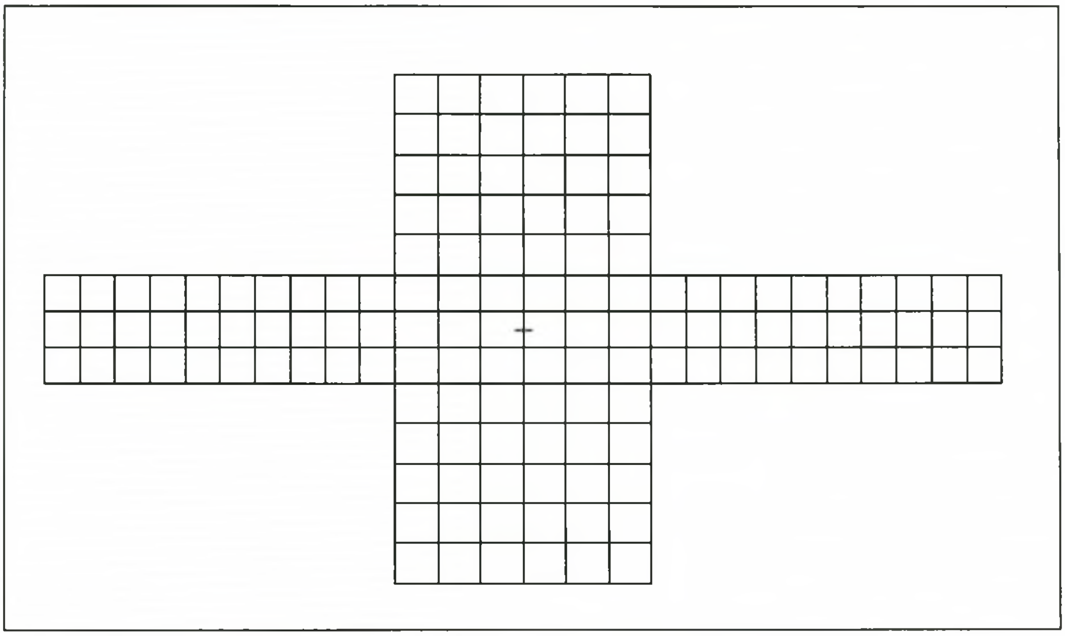

Figure 4-29: Cross-section 5

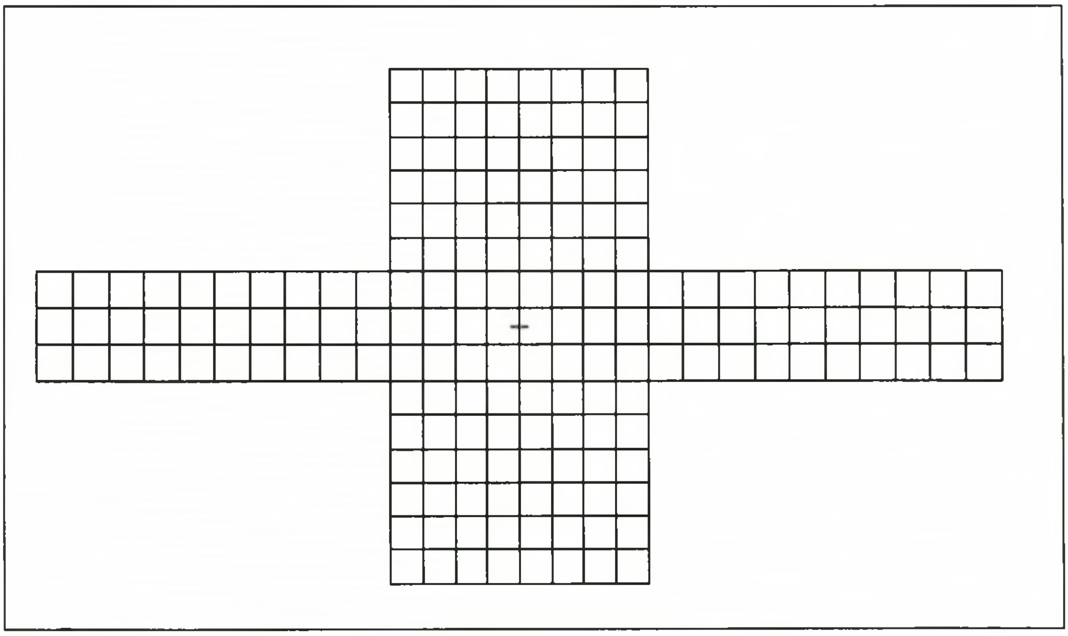

Figure 4-30: Cross-section 6

Stellenbosch University http://scholar.sun.ac.za/

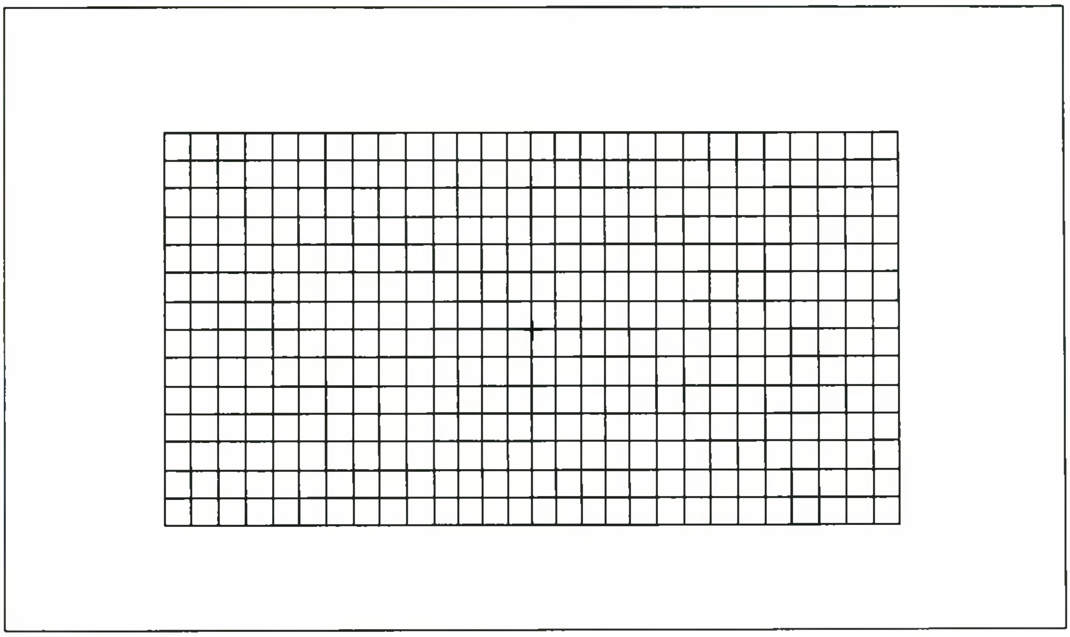

Figure 4-31: Cross-section 7

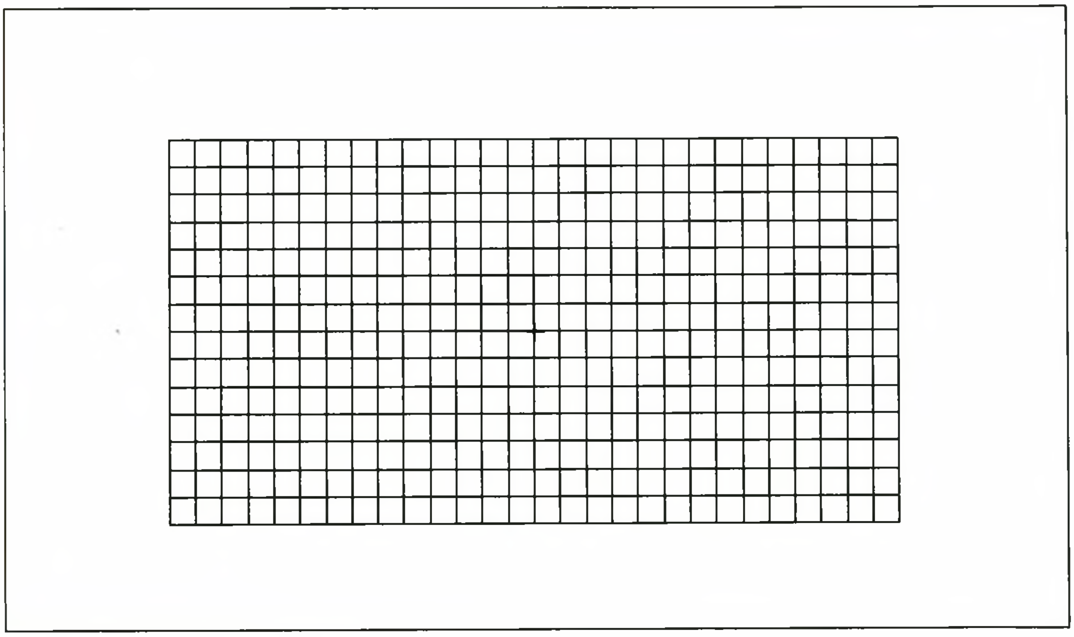

Figure 4-32: Cross-section 8

Stellenbosch University http://scholar.sun.ac.za/

They were then modelled on MSC/NASTRAN to get a 2-dimensional mesh of the section for each section. This mesh was imported into the CROSEC [21, 22] program, to get the sectional stiffness that was used in the DYMORE program.

From this the Southwell plot was generated using the DYMORE program.

Stellenbosch University http://scholar.sun.ac.za/

4.10 Southwell plot

The Southwell plot that is given in this paragraph is a comparison plot between the fully articulated rotor and the new bearingless rotor. To simplify the figure and the comparison, only the first three modes, namely flap, lead-lag and torsion, are given, see Figure 4-33.

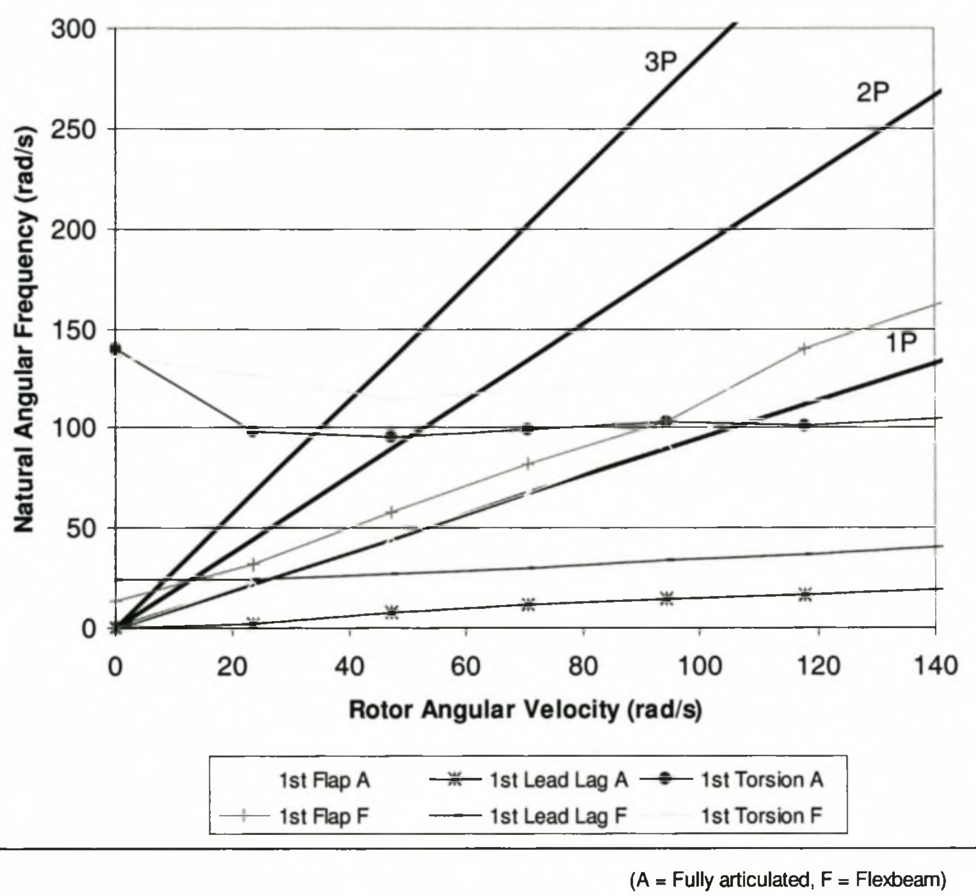

Figure 4-33: Comparison Southwell plot

As can be seen from the Southwell plot, the natural angular frequencies of the new design are considerably higher than that of the fully articulated design. Although this fact is an advantage in most cases, due to the higher manoeuvrability of the helicopter, in our case it proofs to be a disadvantage. The reason for this is that one of the design criteria stated that the dynamic response of the bearingless rotor had to correlate with that of the fully articulated rotor.

Stellenbosch University http://scholar.sun.ac.za/

CHAPTER 5: DESIGNING TESTS FOR THE NEW DESIGN

5.1 Overview

The main reason for tests is to confirm that the stiffness, which the FEA model predicted for the flexbeam, agrees with the stiffness of the actual physical hardware. No dynamic performance tests were done, because of a lack of equipment and financial resources to facilitate tests on such a scale. It was also not deemed necessary to try to obtain such funds, because of the ultimate aim of this thesis.

5.2 Strain Gauges on the Flexbeam

5.2.1 Overview

For comparison of the stresses and strains that the FEA model predicted it was decided to fit the flexbeam with a couple of strain gauges. At the end it was decided to place these strain gauges only on the surface of the flexbeam.

The reason for this was firstly to facilitate easier manufacturing of the flexbeam, secondly so that better control over the condition of the strain gauges could be achieved and thirdly so as not to include any external substances into the flexbeam, that might induce cracking.

5.2.2 Number and placement

It was decided to measure the following strains on the flexbeam. See Figure 5-1 for position detail.

1) Axial strains at positions 1, 2, 3 and 4
2) Torsional strains at positions 5 and 6

Stellenbosch University http://scholar.sun.ac.za/

The strain gauges will be wired into separate half-bridge configurations as follows:

1. At positions 1 and 2
2. At positions 3 and 4
3. At positions 5 and 6

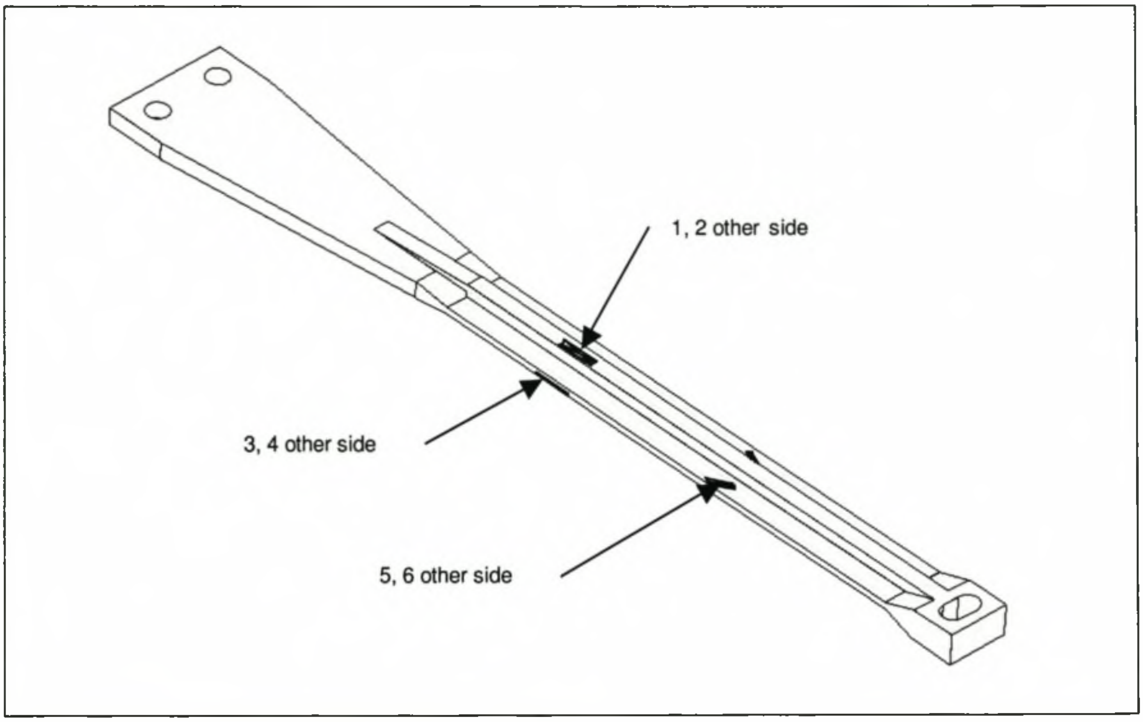

Figure 5-1: Strain gauge positions

5.3 Static Tests

5.3.1 Overview

The main reason for these tests was as mentioned above, namely to determine the behaviour of the physical structure and to see how it compares to what the FEA model predicted. And to explain any differences that may occur between them.

Stellenbosch University http://scholar.sun.ac.za/

5.3.2 Axial

In this test the specimen is clamped with its axial axis in a vertical position and a known load is applied to the other end in the axial direction. The displacement of the end is measured with a dial gauge. Strains can also be read from the strain gauges.

5.3.3 Bending

In this test the specimen is clamped horizontally at the drive shaft end and a known load will be applied in both the horizontal and vertical directions. The displacement into the direction of the loads will again be measured with a dial gauge. Strains can also be read from the strain gauges.

5.3.4 Torsion

The specimen is clamped in a horizontal position at the drive shaft end and a arm of known length is horizontally attached to the blade end. At the end of the arm a known vertical load is applied. The angular displacement of the blade end is measured using two dial gauges, one at each corner. The reason for the two dial gauges is to compensate for the vertical displacement the flexbeam will undergo.

5.4 Fatigue Test

5.4.1 Overview

It has already been stated that the flexbeam design given in this document is not the optimal design, a fatigue test is nevertheless planned to complete the methodology of the process of designing a flexbeam, the aim of the thesis.

The life cycle of a flexbeam in the aviation industry is not known, but for this thesis it is not necessary to know that. When an actual working design of a flexbeam is to be made, it would off course be necessary to know or to

Stellenbosch University http://scholar.sun.ac.za/

establish this quantity. For this test no measurements from the strain gauges will be taken, as only the lifetime of the flexbeam needs to be determined.

5.4.2 Hardware Layout

The test hardware was divided into three main parts, the control program, the control interface and the physical test bench.

The control program is the computer code written to give the necessary displacements to the control interface to ensure a realistic fatigue test.

The control interface is defined as that part of the test equipment that provides the input for the physical test bench. This includes any computer hardware, cylinders, valves, strain gauges, displacement gauges and cabling that were used.

The test bench is that part of the test equipment that forms the physical interface to the flexbeam being tested.

5.4.3 Control program

5.4.3.1 Overview

It was decided to write the program in the computer language DELPHI [23]. The reason for this is that the ADDA cards [11] that were used have very good drivers for this language.

5.4.3.2 Program operation

Sampling:

The program has to sample five strain gauges on the test bench to measure applied forces for comparison with the desired values. These strain gauges will be placed so as to measure the axial forces in the various cylinders.

Stellenbosch University http://scholar.sun.ac.za/

Then there are the five displacement transducers, one parallel to each cylinder. These transducers have a twofold purpose, namely:

1) To monitor the displacements of the cylinders
2) To act as feedback for the PID control

Controlling:

The main purpose of the control software is to supply the five hydraulic valves with the necessary input signals to ensure that the three forces and two moments are applied correctly.

Stellenbosch University http://scholar.sun.ac.za/

5.4.3.3 Flow diagrams

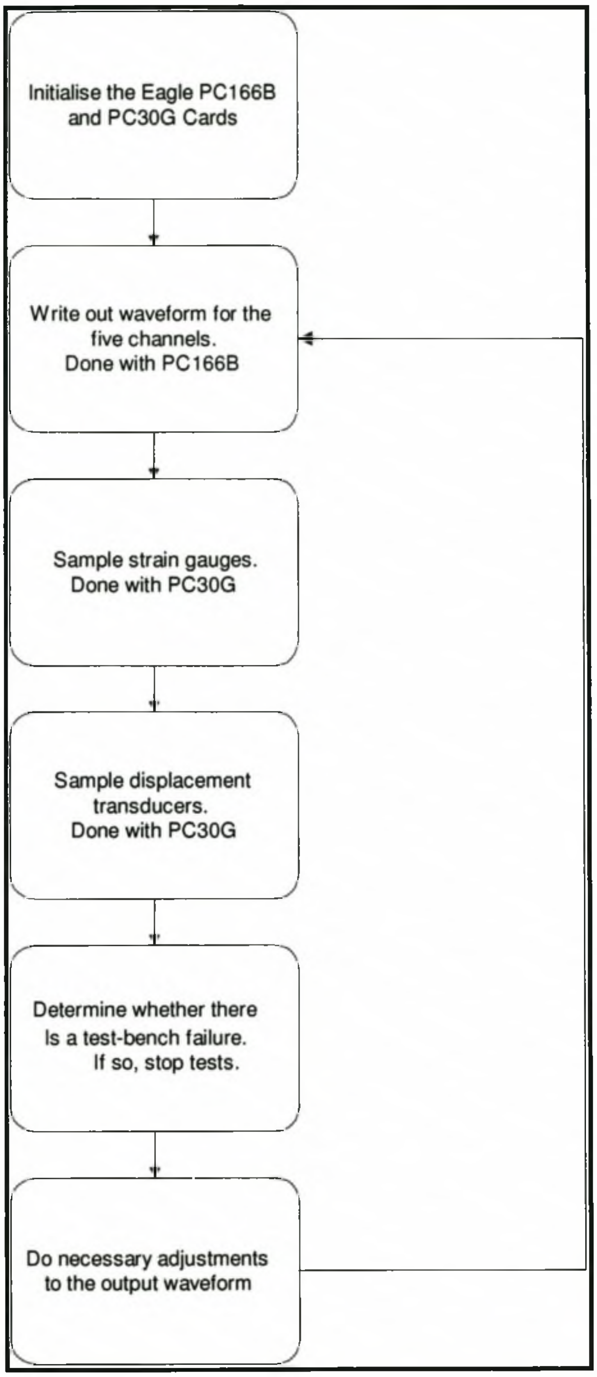

Figure 5-2: Main layout

Stellenbosch University http://scholar.sun.ac.za/

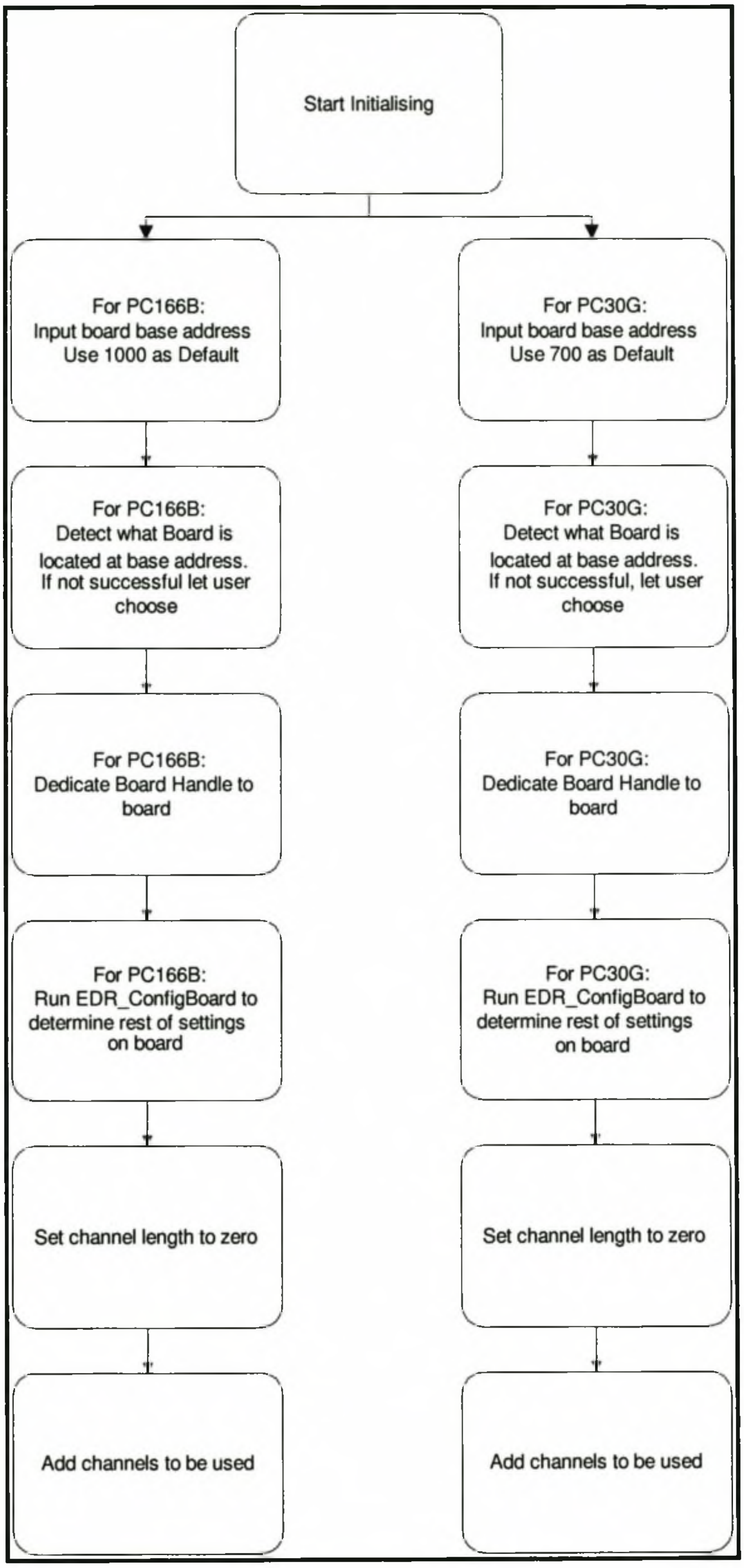

Figure 5-3: Card initialising

Stellenbosch University http://scholar.sun.ac.za/

5.4.3.4 Mathematical formulation

The translation unit on the test bench is so designed as to apply the three translations and one rotation movement to the flexbeam with the use of only three cylinders. To facilitate this, the three cylinders have to move in synchronisation with each other in a certain way. The movement is governed by the following mathematical equations.

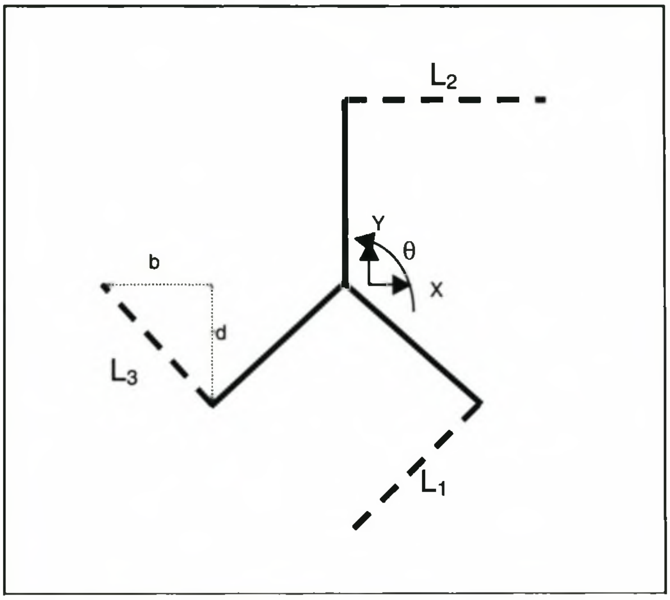

Figure 5-4: Cylinder orientation layout

For the rotation θ:

$$L_1' = L_2' = L_3' = r\theta$$

And for the translations, x and y:

$$L_1' = \sqrt{2L_1^2 + x(2b_1 + x) - y(2d_1 - y)} - L_1$$

$$L_2' = \sqrt{2L_2^2 + x(2b_2 + x) - y(2d_2 - y)} - L_2$$

$$L_3' = \sqrt{2L_3^2 + x(2b_3 + x) - y(2d_3 - y)} - L_3$$

Stellenbosch University http://scholar.sun.ac.za/

with:

L'_1	the final length of cylinder 1
L'_2	the final length of cylinder 2
L'_3	the final length of cylinder 3
L_1	the initial length of cylinder 1
L_2	the initial length of cylinder 2
L_3	the initial length of cylinder 3
b1, b2, b3	the b and d measurements for each cylinder as depicted in Figure 5-4.
x, y	the desired displacement
θ	the desired rotation

For the total length change of the cylinders the sum of the rotation and translation displacements must be used.

5.4.4 Control interface

5.4.4.1 Computer hardware

The computer hardware used, consisted of a:

1. Pentium 100 MHz computer with Windows 95 operating system. The reason for using a Windows 95 operating system is that the control programs are written in Delphi 4.
2. Eagle PC166B ADDA card [28] to establish a connection between the computer and the valve control unit. This card is an analogue output card with 8 12-bit channels.
3. Eagle PC30G ADDA card [12] to establish a connection between the computer and the strain gauges needed to monitor the forces applied. This card is an analogue input card with 16 12-bit channels.

Stellenbosch University http://scholar.sun.ac.za/

5.4.4.2 Other hardware

Except the computer hardware and physical test bench the following hardware were also used:

- Displacement gauges
- Valves
- Piping for the valves
- Cylinders
- Signal generators
- PID amplifiers

5.4.5 Test Bench

Because of the complex load condition acting on the bearingless rotor and the fact that there was not a test bench available, a special test bench had to be designed.

The load condition included a semi static axial load and 5 cyclic loads. These cyclic loads included two shear forces parallel to the cross-sections and two moments acting along the axis parallel to the cross-section. This combination gives you a five axis dynamic and one axis static load case.

To realistically simulate the fatigue problem that occurs here, all these above-mentioned forces have to act together on the flexbeam.

To simplify the operation of the test bench, it was decided to construct it in a modular fashion. One module would therefore not only apply forces to the structure, but also act as a constraint for forces applied by another module.

The test bench finally consisted of three modules, these were the

1. Airbag module.
2. Translation module.
3. Rotational module.

Stellenbosch University http://scholar.sun.ac.za/

5.4.5.1 Airbag module

The only purpose of this module is to transfer the axial load to the bearingless rotor. It was decided to use airbags in this module instead of only a preloaded cable. A length change in the flexbeam will result when bending and shear forces are also applied on the flexbeam. This length change, although very small, will cause an increase in the length of the cable (additional stretching of the cable) applying the force, increasing the preload if only a cable is used. By using airbags a constant preload can be maintained.

5.4.5.2 Translation module

The primary purpose of this module is to transfer the shear forces and the torsional force/displacement to the flexbeam. This is done with three cylinders arranged in a triangle. Its secondary purpose is to act as a constraint for the moments that are applied by the rotational unit.

5.4.5.3 Rotational module

The primary purpose of this module is the transfer of the moments to the flexbeam. This is done with two rings that can rotate within each other. The secondary purpose is to act as a constraint for the shear forces of the translation module.

5.4.5.4 How the bench works

Through the airbag module (Figure 5-5) a constant axial force is applied to the flexbeam. This is achieved by pressurising the airbags until the desired axial force is obtained in the connecting cable. This cable is on the one side connected to the airbags and on the other side to the pin on the inside of the torsional clevis (Figure 5-6). This torsional clevis is free to move up and down in the torsional plate (Figure 5-7), but is constrained for in-plane rotational movements (Figure 5-8). This torsional plate is located in the torsional module (Figure 5-9) with the use of three cylinders. With this configuration the torsion and translation can be applied to the clevis and thus the flexbeam.

Stellenbosch University http://scholar.sun.ac.za/

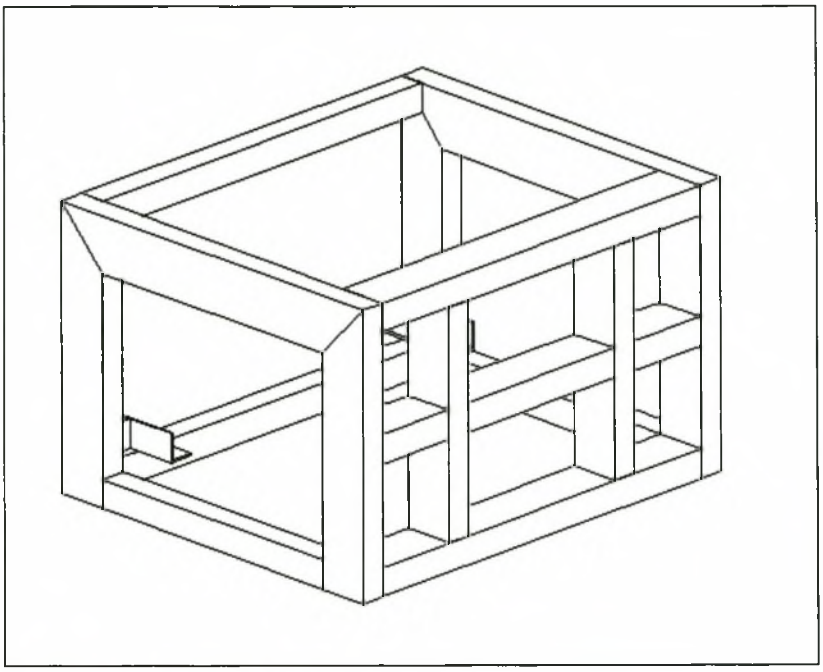

Figure 5-5: Airbag module

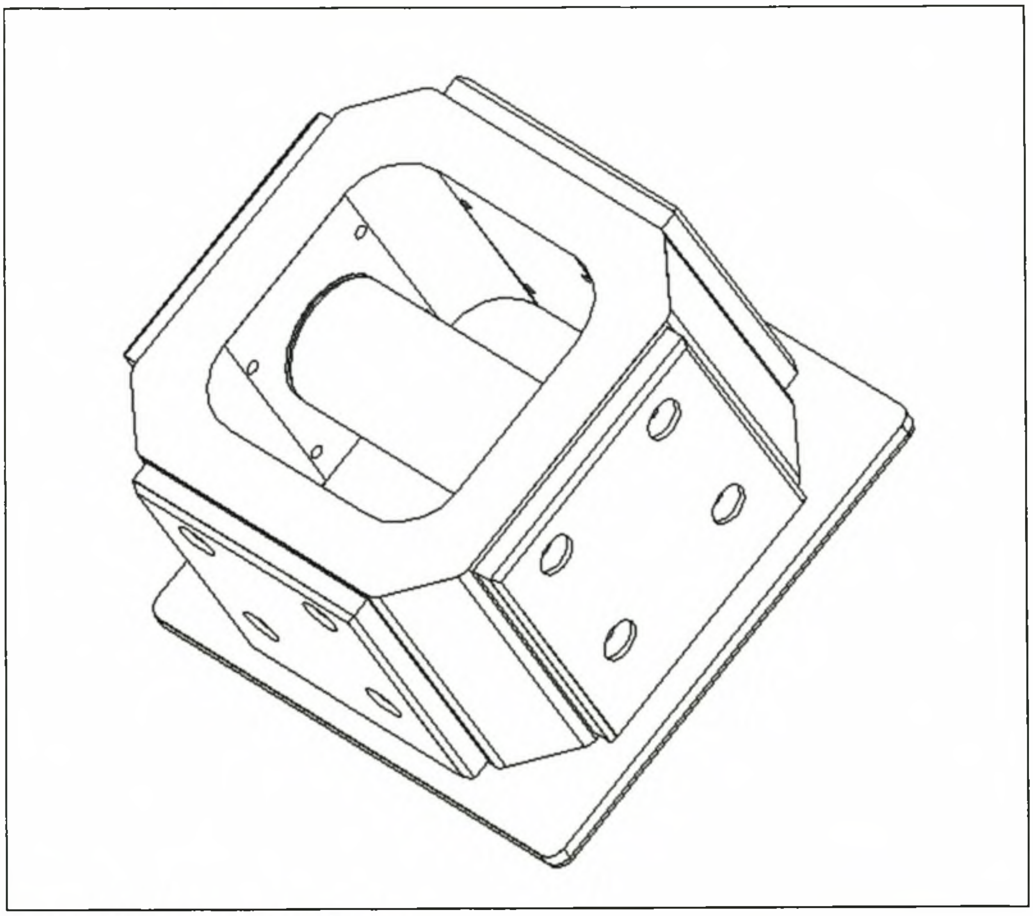

Figure 5-6: Torsional clevis pin

Stellenbosch University http://scholar.sun.ac.za/

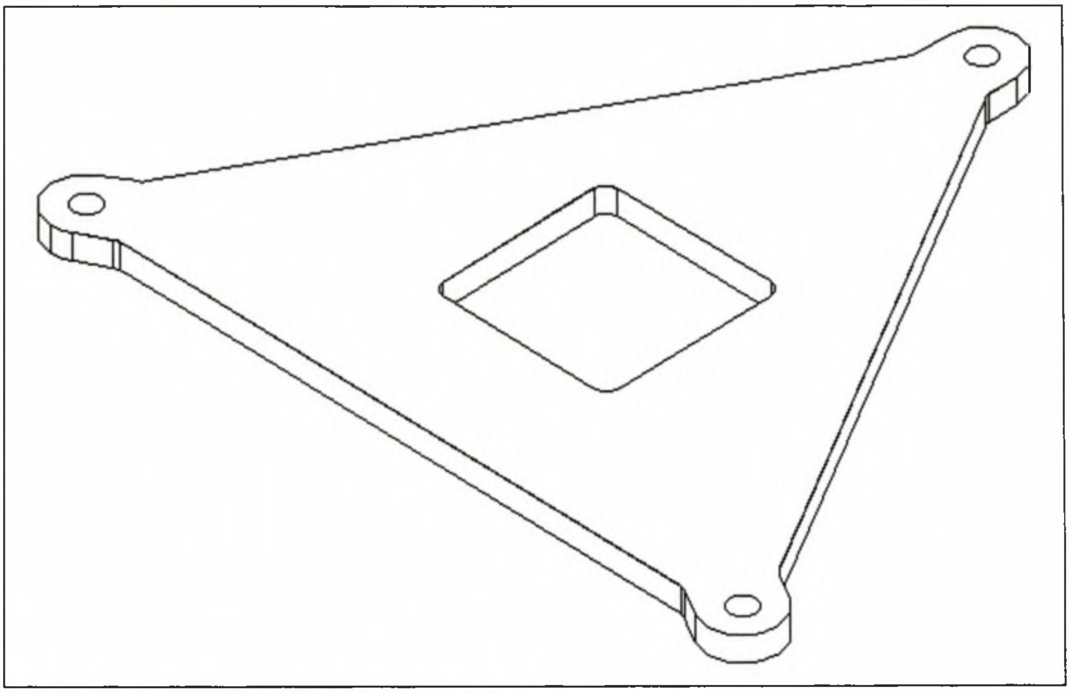

Figure 5-7: Translation and torsional plate

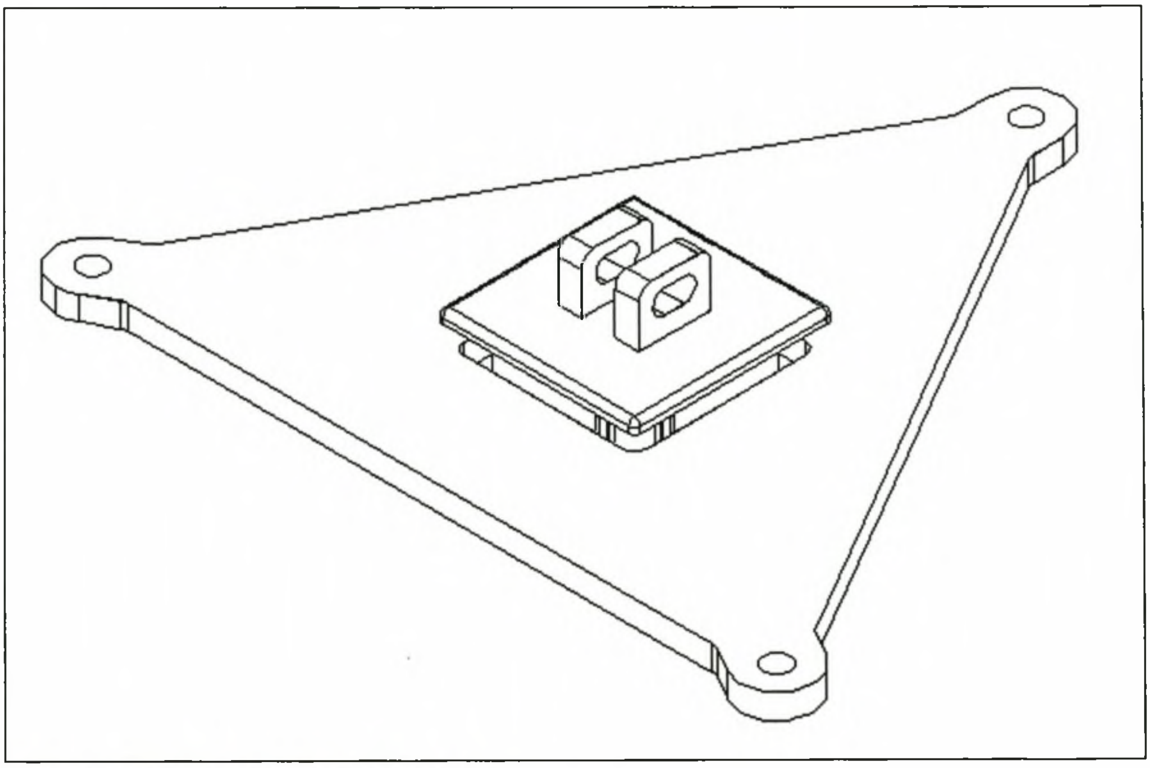

Figure 5-8: Clevis and plate assembly

Stellenbosch University http://scholar.sun.ac.za/

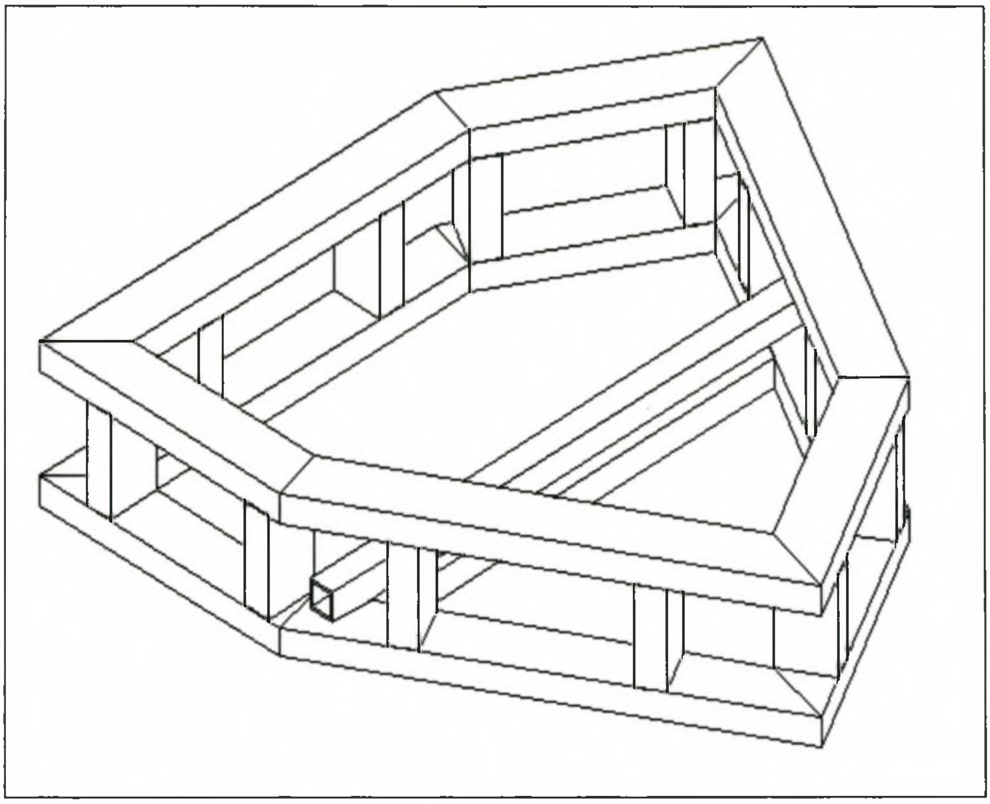

Figure 5-9: Translation and torsional module

The flexbeam is on one side connected to the torsional clevis and on the other side to the rotational clevis (Figure 5-10). This clevis is welded to the rotational module (Figure 5-11). In this module the moment forces are applied to the flexbeam by the relative motion of the two interlocking rings (Figure 5-12) with respect to each other and the rotation module as a whole.

The outer and inner rings are free to rotate around one axis provided by the two hinge pins on the outside of the outer ring. In addition to this the inner ring can also rotate around an additional axis. The combination of these two gives the system its two rotational freedoms.

When all of this is combined in a cyclic load condition, all six directional forces are applied at the same time. The complete layout of the test bench is given in Figure 5-13.

Stellenbosch University http://scholar.sun.ac.za/

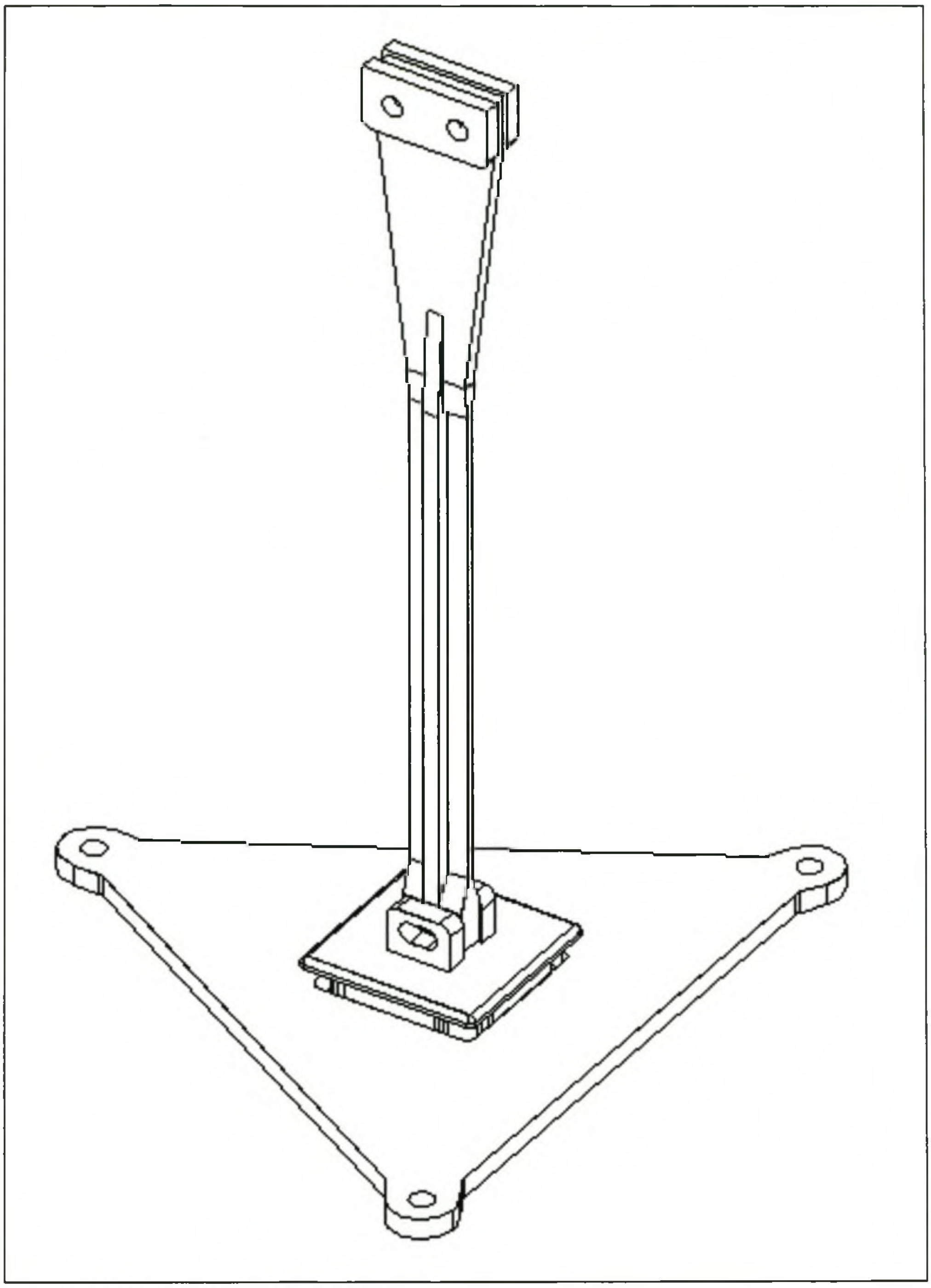

Figure 5-10: Flexbeam clevis assembly

Stellenbosch University http://scholar.sun.ac.za/

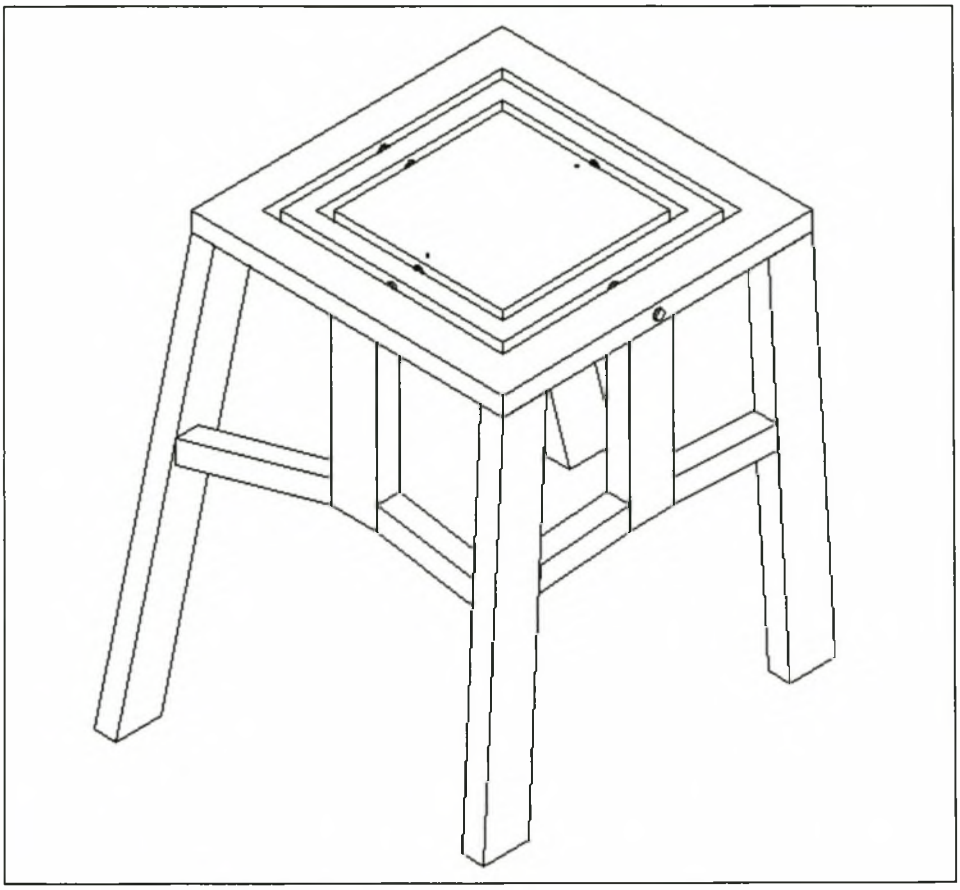

Figure 5-11: Rotational module

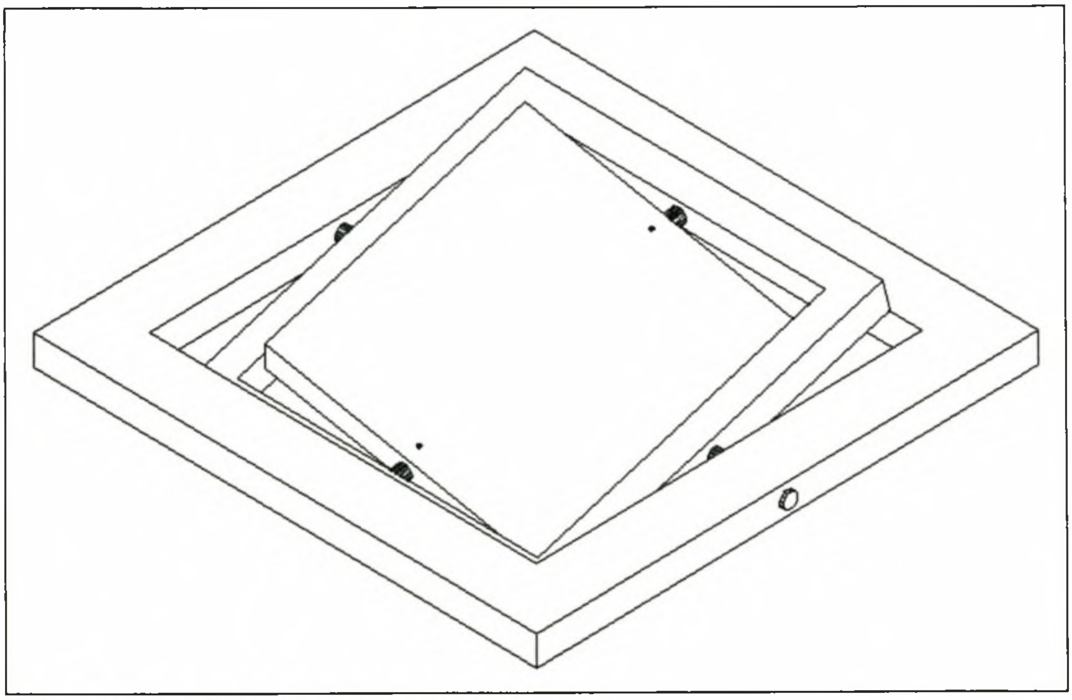

Figure 5-12: Rotation module interlocking rings

Stellenbosch University http://scholar.sun.ac.za/

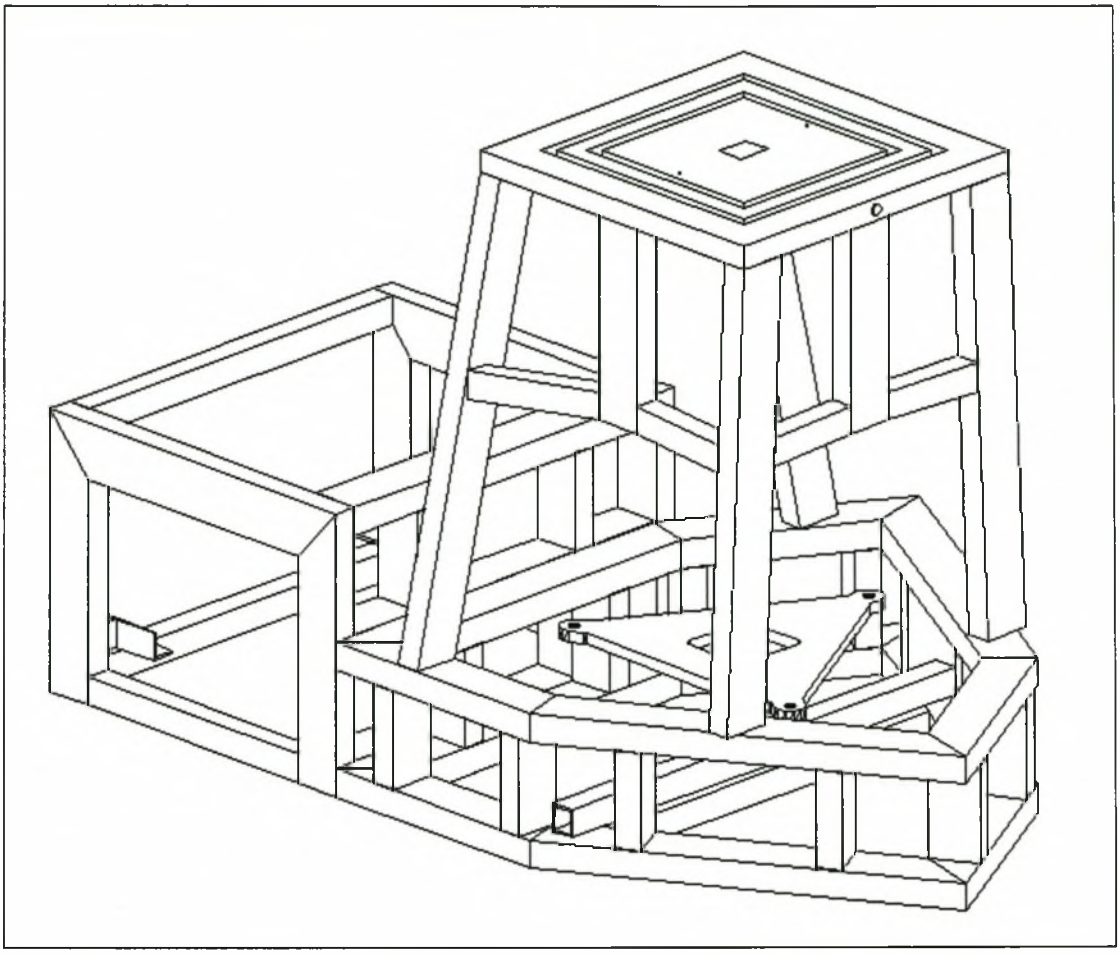

Figure 5-13: Test bench main layout

Stellenbosch University http://scholar.sun.ac.za/

CHAPTER 6: MANUFACTURING THE FLEXBEAM

6.1 Overview

As stated in Chapter 5, a unidirectional E-glass fibre and suitable epoxy resin were used to construct the flexbeam. The flexbeam was split into two halves along the z-axis neutral plane. In the manufacturing process each half was done separately, see Figure 6-1 to Figure 6-3, and then bonded together to form the whole.

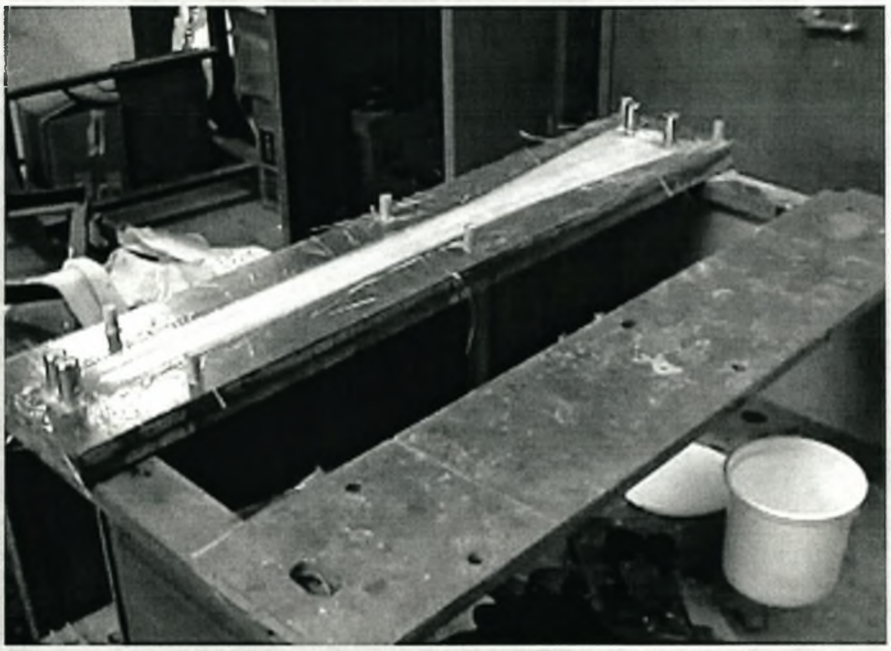

Figure 6-1: Flexbeam half still in mould

Stellenbosch University http://scholar.sun.ac.za/

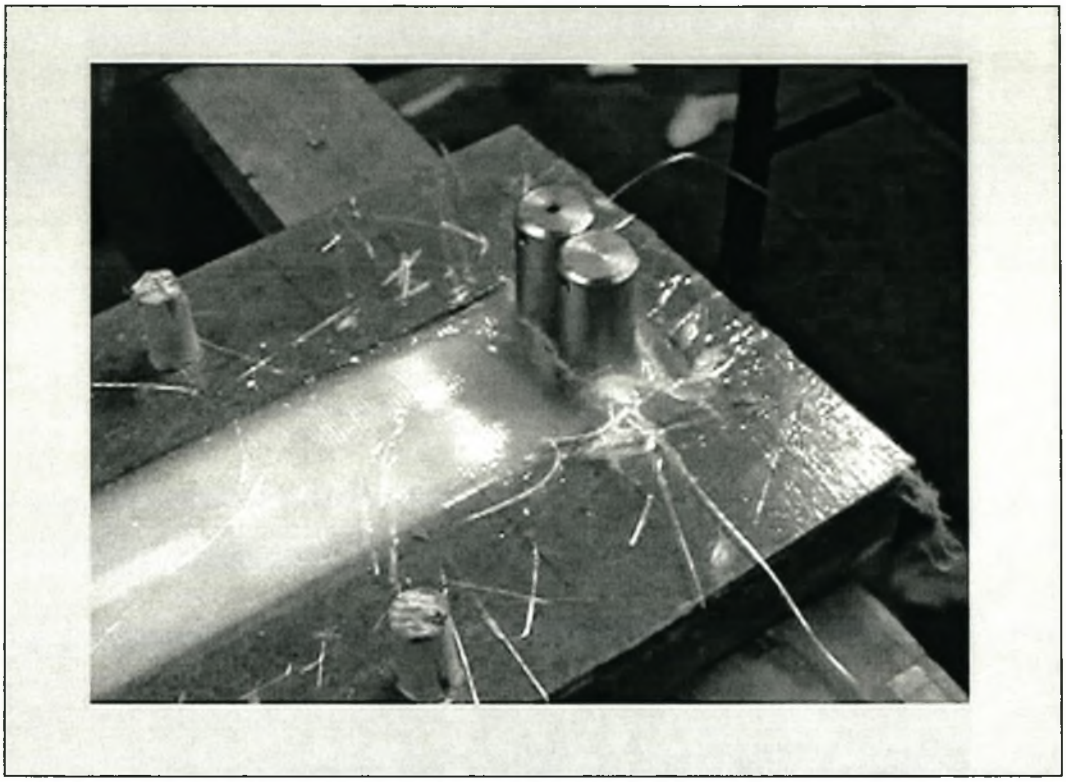

Figure 6-2: Close-up of flexbeam on blade side

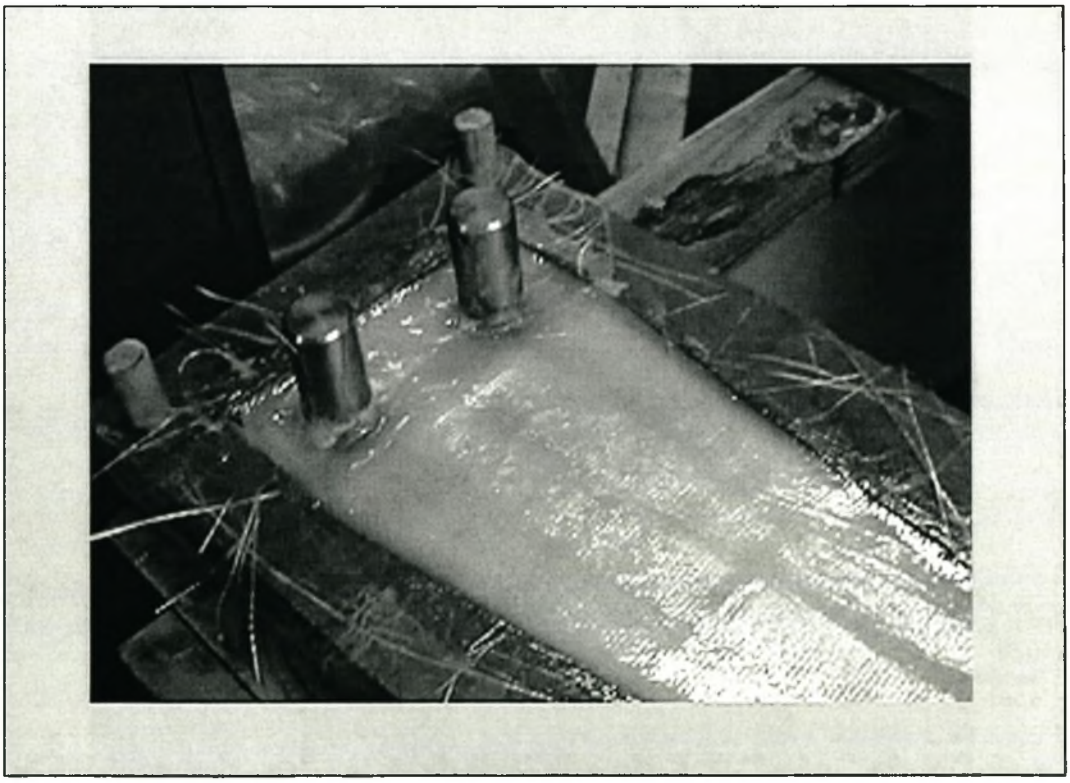

Figure 6-3: Close-up of flexbeam on drive-shaft side

Stellenbosch University http://scholar.sun.ac.za/

6.2 Materials Used

To facilitate easier hand lay-up, an 80/20% woven mat instead of a 100% fibre bundle was used. The 80/20% has 80% of the fibres in one direction and 20% of the fibres in a perpendicular direction.

The resin used as stated was an Epolam 2020 epoxy resin. This resin gave a 2¼-hour time to gel, which with hindsight proved not to be adequate, because the resin started to gel before lay-up was completed.

This problem was overcome by means of a double lay-up procedure for each half. By this is meant that the main axial load carrying part of the flexbeam was first done, where after the mould was clamped. After about five hours of curing the top of the mould was removed and the rest of the lay-up completed. This gave a complete lay-up time per half of about 4 hours.

6.3 The Mould

The mould, see Figure 6-4 to Figure 6-7, was milled from super-wood on a manual milling machine. Thereafter it was treated with sanding sealer to prevent the resin from penetrating the wood. Five layers of sanding sealer were used.

When the application of the sanding sealer was finished, a further five coats of a PVA release agent were applied. The reason for this was to facilitate easier release of the flexbeam from the mould.

6.4 The Finished Product

As stated above, bonding the two halves together made the flexbeam. The half flexbeam can be seen in Figure 6-8 to Figure 6-11, while the full flexbeam can be seen in Figure 6-12.

Stellenbosch University http://scholar.sun.ac.za/

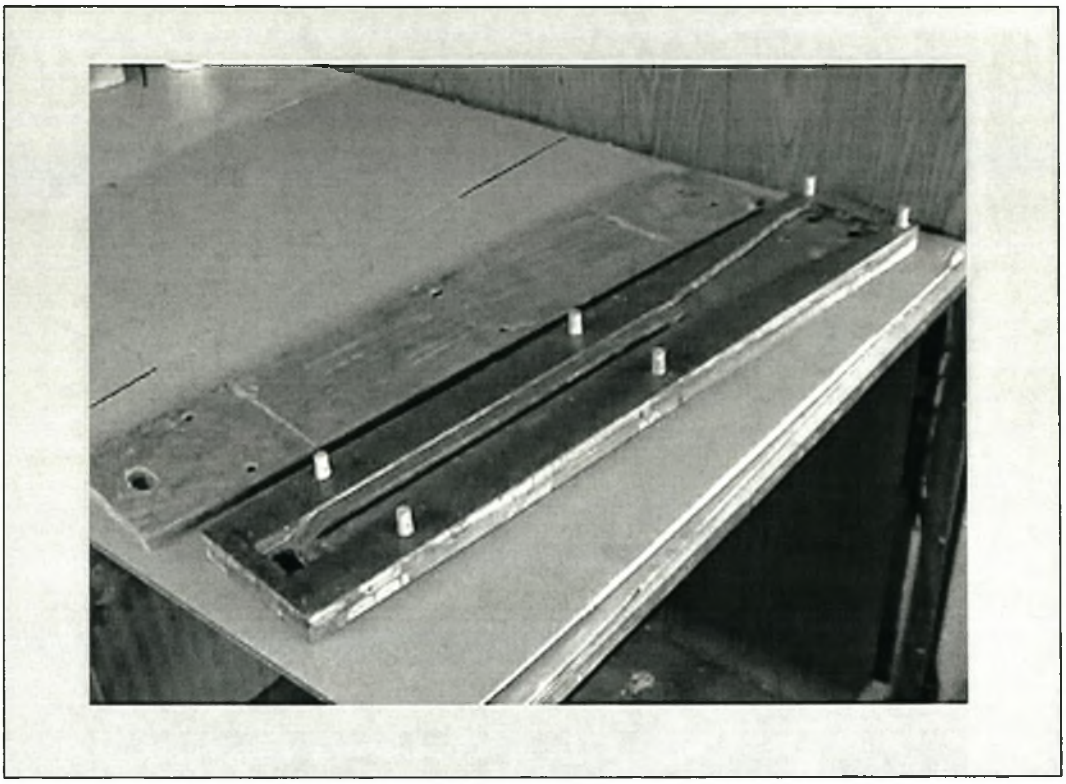

Figure 6-4: The mould for half of the flexbeam

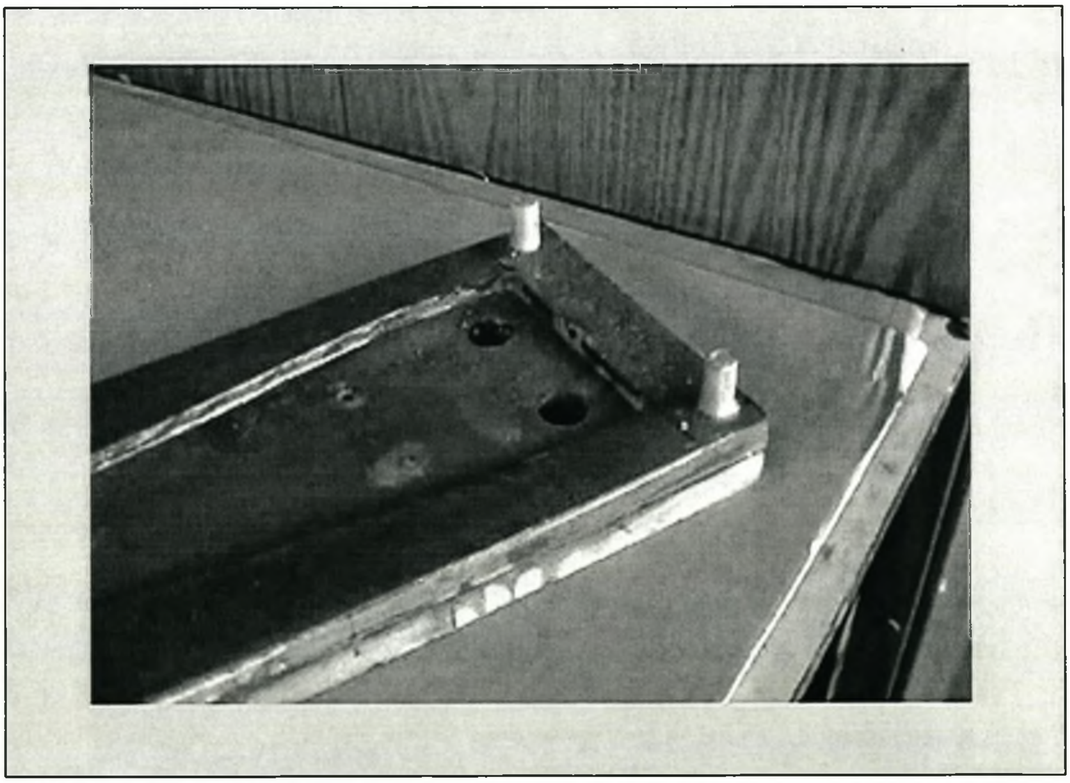

Figure 6-5: Close-up on drive-shaft end of the mould

Stellenbosch University http://scholar.sun.ac.za/

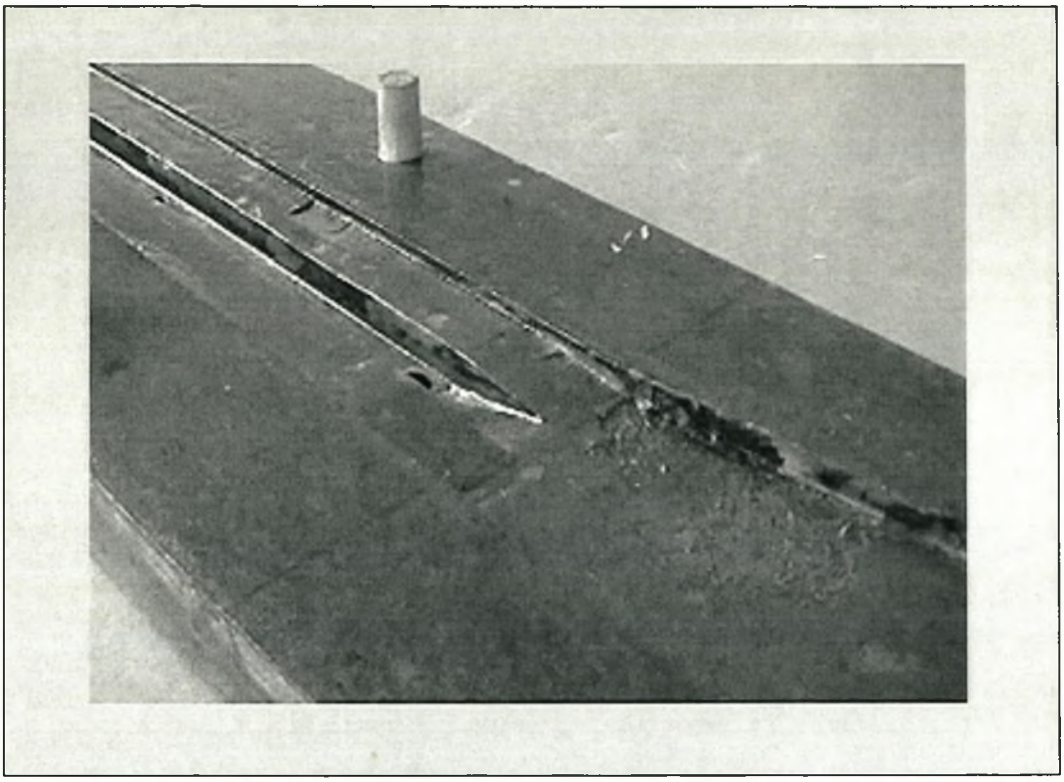

Figure 6-6: Close-up on middle part of the mould

Figure 6-7: Close-up on blade side of the mould

Stellenbosch University http://scholar.sun.ac.za/

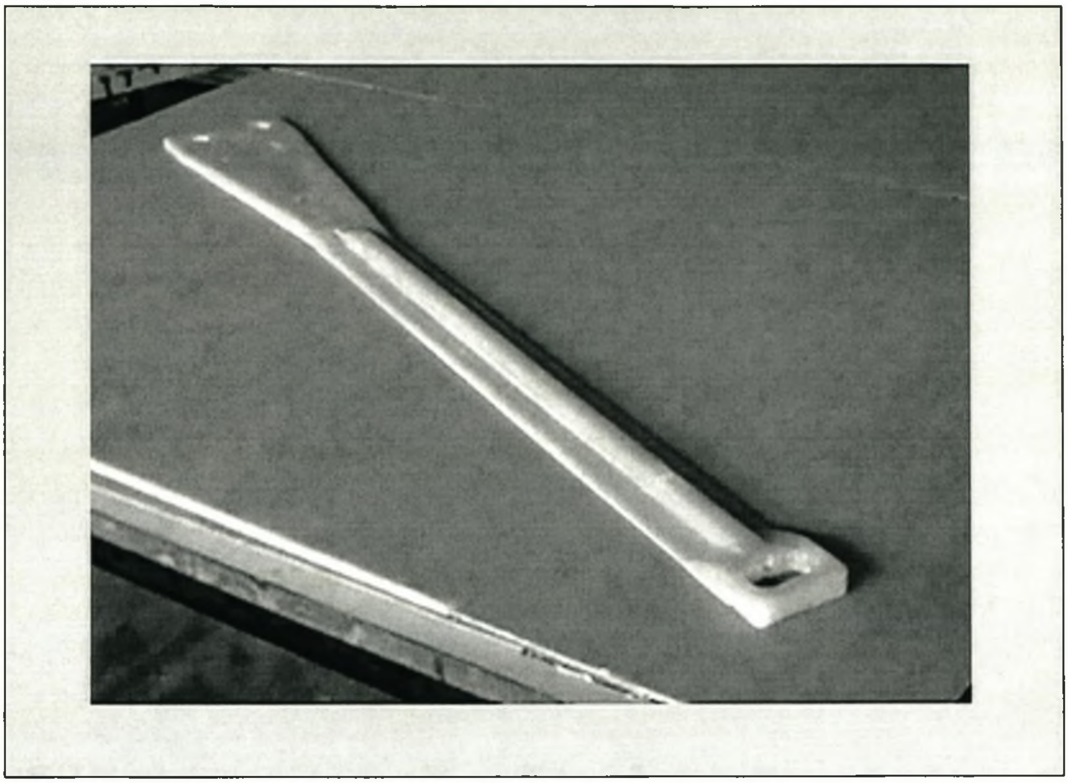

Figure 6-8: Half flexbeam

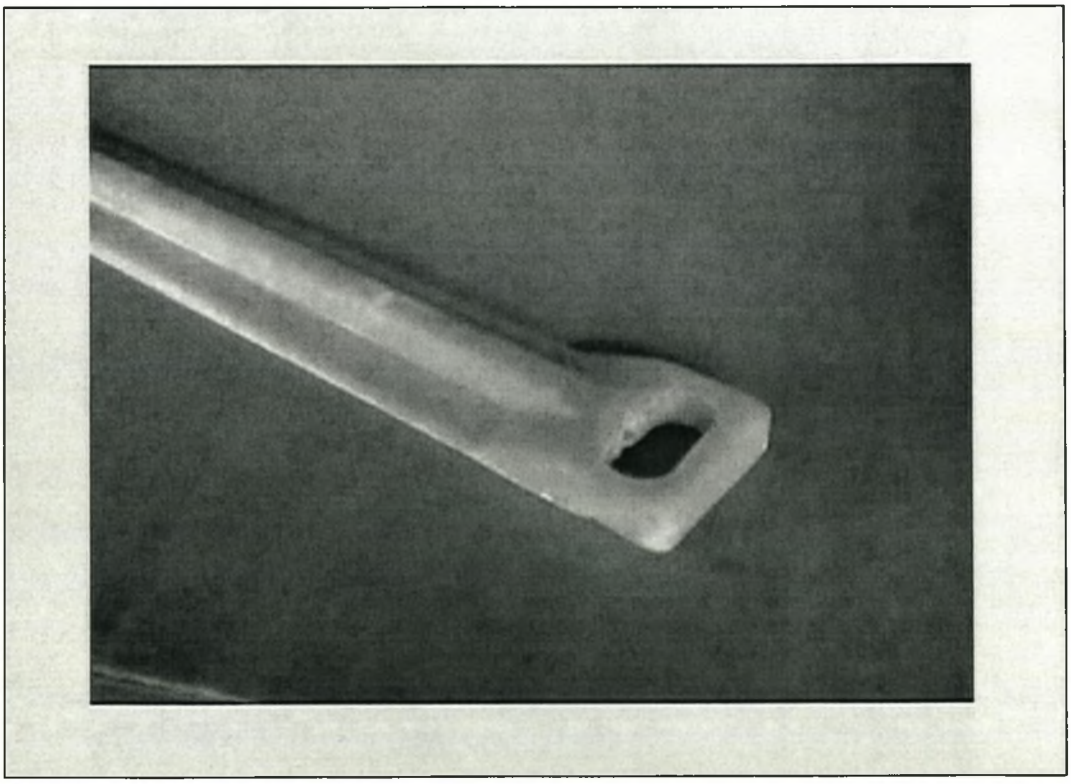

Figure 6-9: Close-up on blade side of half flexbeam

Stellenbosch University http://scholar.sun.ac.za/

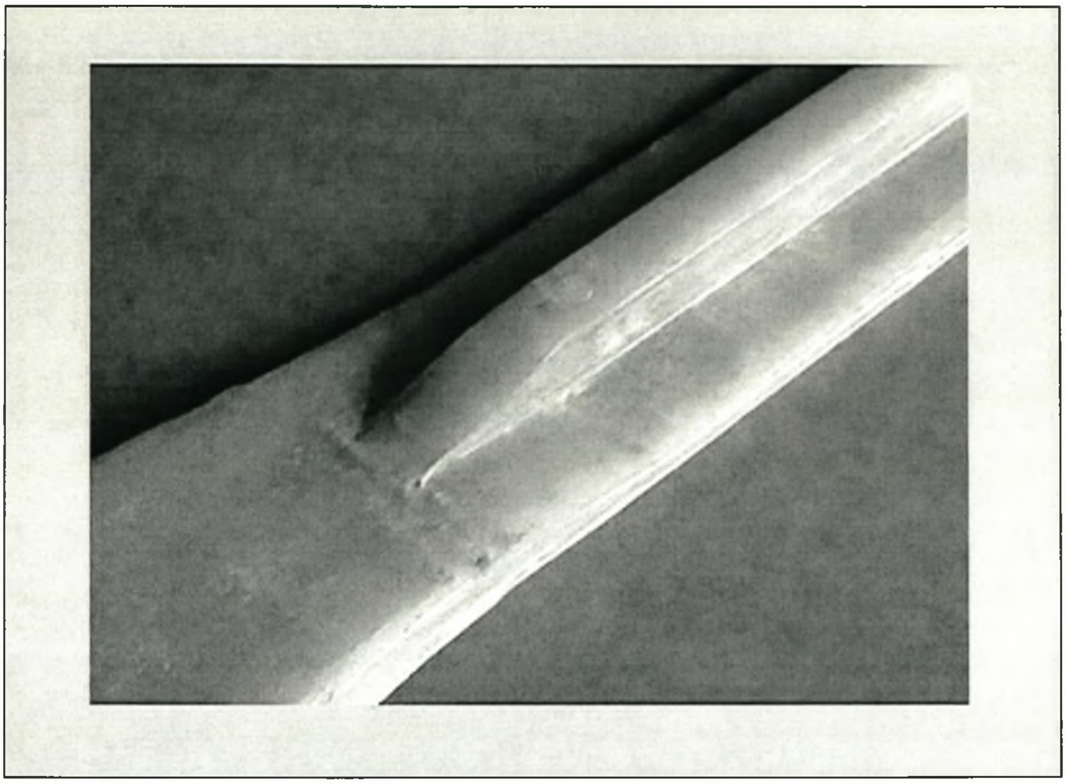

Figure 6-10: Close-up on middle part of half flexbeam

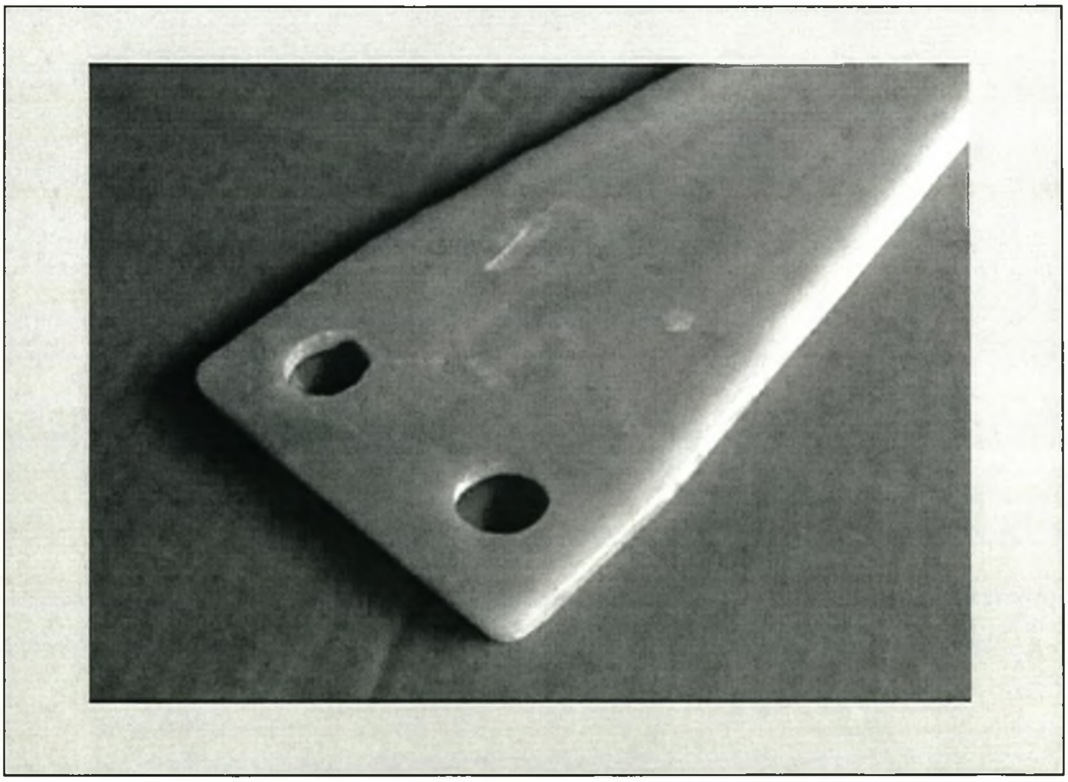

Figure 6-11: Close-up on drive-shaft side of half flexbeam

Stellenbosch University http://scholar.sun.ac.za/

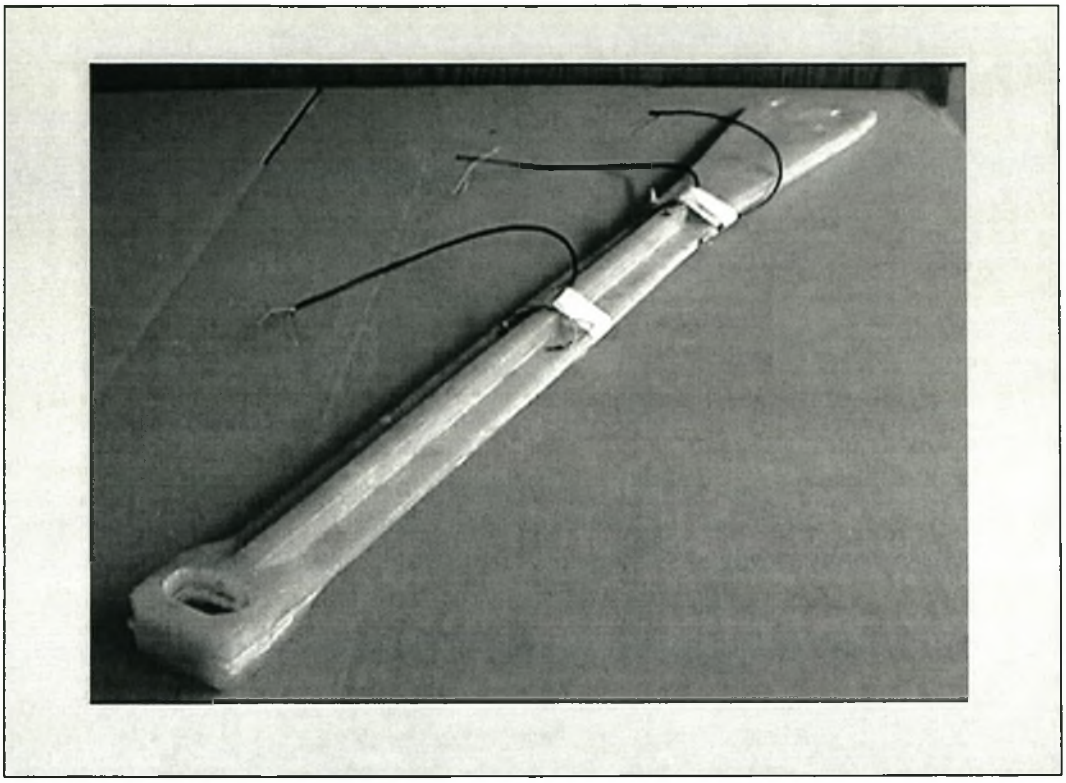

Figure 6-12: Full flexbeam with strain gauges

Stellenbosch University http://scholar.sun.ac.za/

CHAPTER 7: TEST RESULTS

7.1 Overview

In this chapter the results that were obtained from the tests as specified in Chapter 5 are presented. The static test results are compared with FEM analysis results as obtained from the MSC/NASTRAN for Windows package. For this FEM analysis the same model as used in Chapter 5 was used, but only the first three and last output sets were used in the comparison.

For all tests a 10 kg mass was used to apply the forces, for the torsional test the 10 kg mass was offset at a distance of 100 mm.

7.2 Static Tests

7.2.1 Axial

Table 7-1:Comparison Table for Axial Test

Position[3]	Measured Strain (μm/m)	Measured Stress (MPa)	FEA Stress (MPa)	Percentage difference
1, 2	5	0.154	0.15	-3%
3, 4	5	0.154	0.15	-3%

Measured displacement = 0.14 mm
FEA displacement = 0.05 mm
% Difference = -64%

[3] The position is as described in paragraph 5.2.2

Stellenbosch University http://scholar.sun.ac.za/

7.2.2 Bending (Flap)

Table 7-2: Comparison Table for Bending Test

Position[4]	Measured Strain (μm/m)	Measured Stress (MPa)	FEA Stress (MPa)	Percentage difference
1, 2	1334	41.2	24.3	-41%

Measured displacement = 28 mm
FEA displacement = 9.6 mm
% Difference = -66%

7.2.3 Bending (Lead-Lag)

Table 7-3: Comparison Table for Bending Test

Position[4]	Measured Strain (μm/m)	Measured Stress (MPa)	FEA Stress (MPa)	Percentage difference
3, 4	430	13.27	13.5	2%

Measured displacement = 2.76 mm
FEA displacement = 1.1 mm
% Difference = -60%

[4] The position is as described in paragraph 5.2.2

Stellenbosch University http://scholar.sun.ac.za/

7.2.4 Torsion

Table 7-4: Comparison Table for Torsion Test

Position[5]	Measured Strain (μm/m)	Measured Stress (MPa)	FEA Stress (MPa)	Percentage difference
5, 6	351	10.8	9.6	-11%

Measured angle = 2.38°

FEA angle = 1.042°

% Difference = -56%

7.2.5 Summary

As can be seen from the results, an average difference of around 60% is measured between the physical structure and the FEA model. This at first seems to indicate that the FEA prediction was wrong, but in fact can be explained as follows.

It must be kept in mind during the following calculations that the lay-up (fibre direction) is constant throughout the flexbeam cross-section.

FEA Orthotropic Moduli of Elasticity[6]

Longitudinal modulus used in FEA model (E_L)	78 GN/m^2
Transverse modulus used in FEA model (E_T)	26 GN/m^2
Shear modulus used in FEA model (G_{LT})	13 GN/m^2
Assumed fibre % in FEA model	60%

[5] The position is as described in paragraph 5.2.2

[6] Values here were taken as first assumption before final material selection was made.

Stellenbosch University http://scholar.sun.ac.za/

Physical Structure Orthotropic Moduli of Elasticity

E-glass fibre Modulus of Elasticity (E_f) [Table 4-2]	72.5 GN/m^2
E-glass fibre Shear Modulus (G_f)	30 GN/m^2
Epolam 2020 Modulus of Elasticity (E_m) [Table 4-3]	3.1 GN/m^2
Epolam 2020 Shear Modulus (G_m)	1.24 GN/m^2
Cloth: E-glass fibre % in x-direction	80%
Cloth: E-glass fibre % in y-direction	20%
Physical structure fibre % (measured during the lay-up procedure)	50%
Total fibre % in x-direction	40%
Total fibre % in y-direction	10%

The cloth and resin matrix can schematically be presented as two laminas. Where v_{Lf} is the fibre volume fraction of the x-direction fibres and v_{Tf} is the fibre volume fraction of the y-direction fibres. The average of the two is 0.5 as it must be according to physical mass measurements.

$v_{Lf} = 0.8$, $v_{Lm} = 0.2$

$v_{Tf} = 0.2$, $v_{Tm} = 0.8$

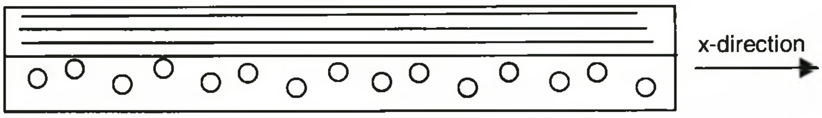

By using micromechanics equations:

$$E_L = \tfrac{1}{2}(v_{Lf} \times E_f + v_{Lm} \times E_m) + \tfrac{1}{2}\left(\frac{v_{Tf}}{E_f} + \frac{v_{Tm}}{E_m}\right)^{-1}$$

$$E_L = \tfrac{1}{2}(0.8 \times 72.5 + 0.2 \times 3.1) + \tfrac{1}{2}\left(\frac{0.2}{72.5} + \frac{0.8}{3.1}\right)^{-1} = 31.23\ \text{GN/m}^2$$

$$E_T = \tfrac{1}{2}\left(\frac{v_{Lf}}{E_f} + \frac{v_{Lm}}{E_m}\right)^{-1} + \tfrac{1}{2}(v_{Tf} \times E_f + v_{Tm} \times E_m)$$

$$E_T = \tfrac{1}{2}\left(\frac{0.8}{72.5} + \frac{0.2}{3.1}\right)^{-1} + \tfrac{1}{2}(0.2 \times 72.5 + 0.8 \times 3.1) = 15.11\ \text{GN/m}^2$$

Stellenbosch University http://scholar.sun.ac.za/

$$G_{LT} = (\frac{V_f}{G_f} + \frac{V_m}{G_m})^{-1}$$

$$G_{LT} = (\frac{0.5}{30} + \frac{0.5}{1.24})^{-1} = 2.38 \text{ GN/m}^2$$

Thus

Physical structure Modulus of Elasticity in axial direction	31.23 GN/m^2
Physical structure Modulus of Elasticity in transverse direction	15.11 GN/m^2
Physical structure Shear Modulus of Elasticity	2.38 GN/m^2

% Difference in Modulus of Elasticity in axial direction	-60%
% Difference in Modulus of Elasticity in transverse direction	-42%
% Difference in Shear Modulus of Elasticity	-82%

Thus the Modulus of Elasticity in the axial direction of the physical structure differs by about 60% from that of the FEA model and therefore explains the 60% difference in measured displacement values (axial and bending test cases), the same can be said for the Shear Modulus of Elasticity (torsion test case). The transverse Modulus of Elasticity has a negligible effect on the values compared here.

As can be seen from Table 7-1 to Table 7-4 the stresses for the axial, bending (lead-lag) and torsional tests correlate very well with that of the FEA model, lying within 11%.

The stress of the bending (flap) test on the other hand does not correlate well at all with the FEA model. Seeing that the FEA model gave accurate results for all the other cases, the model can be assumed to be accurate. The model was also checked for defects with none found. Baring this in mind the only reason for the lack in stress correlation must be in measuring of the strains during the flap bending-test. Therefore this test was done four times, each time resulting in the same reading.

Stellenbosch University http://scholar.sun.ac.za/

The reason for this difference in the stresses can therefore not be explained and present a point of concern. It is advised that this deviation in correlation be studied further to determine its possible cause.

7.2.6 FEA Correlation by Using Revised Moduli of Elasticity

To verify the deduction that was made in paragraph 7.2.5 with respect to the Moduli of Elasticity, it was decided to rerun the FEA model with this newly determined material properties. The results of this analysis are presented in this paragraph in the same way as was done in the previous one.

7.2.6.1 Axial

Table 7-5: Comparison Table for Axial Test

Position[7]	Measured Strain (μm/m)	Measured Stress (MPa)	FEA Stress (MPa)	Percentage difference
1, 2	5	0.154	0.15	-3%
3, 4	5	0.154	0.15	-3%

Measured displacement = 0.14 mm
FEA displacement = 0.12 mm
% Difference = -14%

[7] The position is as described in paragraph 5.2.2

Stellenbosch University http://scholar.sun.ac.za/

7.2.6.2 Bending (Flap)

Table 7-6: Comparison Table for Bending Test

Position[8]	**Measured Strain (μm/m)**	**Measured Stress (MPa)**	**FEA Stress (MPa)**	**Percentage difference**
1, 2	1334	41.2	24.0	-41.7%

Measured displacement = 28 mm
FEA displacement = 24.4 mm
% Difference = -13%

7.2.6.3 Bending (Lead-Lag)

Table 7-7: Comparison Table for Bending Test

Position[4]	**Measured Strain (μm/m)**	**Measured Stress (MPa)**	**FEA Stress (MPa)**	**Percentage difference**
3, 4	430	13.27	14	5%

Measured displacement = 2.76 mm
FEA displacement = 2.62 mm
% Difference = -5%

[8] The position is as described in paragraph 5.2.2

Stellenbosch University http://scholar.sun.ac.za/

7.2.6.4 Torsion

Table 7-8: Comparison Table for Torsion Test

Position[9]	Measured Strain (μm/m)	Measured Stress (MPa)	FEA Stress (MPa)	Percentage difference
5, 6	351	10.8	9.6	-11%

Measured angle = 2.38°

FEA angle = 2.44°

% Difference = 2.5%

7.2.6.5 Summary

Thus the assumption made about the Moduli of Elasticity reduction was a correct assumption, as can be seen from the above results.

[9] The position is as described in paragraph 5.2.2

Stellenbosch University http://scholar.sun.ac.za/

7.3 Fatigue Test

Due to the prolong period of this type of test and the number of specimens that need to be tested, no life span for the flexbeam are given in this document. The main reasons for this are the time constraints that are put on an MSc Ing degree and the availability of the hydraulic power packs and equipment at the time of testing.

A shortened form of the test was none the less done to verify whether the test bench, more than the flexbeam, are working and if it would be adequate to handle these prolonged tests. The outcome of this test seems to indicate that the test bench is adequate for the type of tests that it was designed for.

It is recommended that more specimens of the flexbeam are build and tested to destruction on the test bench. This way an accurate life span for the flexbeam can be determined.

Stellenbosch University http://scholar.sun.ac.za/

CHAPTER 8: CONCLUSION

Due to the shift from a fully articulated rotor to a bearingless rotor it was deemed necessary to do a design for the 24% scale model of the Rooivalk attack helicopter at the CSIR in Pretoria.

Design specifications were drawn up for the proposed bearingless rotor system, specifying everything from the dimensions to the manufacturing and serviceability of the system. This document was drawn up using military specifications due to the fact that it was destined for ARMSCOR.

A numeric model of the scale model's blade was done on the DYMORE package and various designs for bearingless rotor hubs were included in a full numeric model of the system. At this point only quasi-static analyses were run.

From these analyses it were found that the length constraint put on the design was not feasible, due to the torsional twist of 20 degrees that had to be obtained and was subsequently dropped. Various designs and fibre direction lay-ups were tried, most proved inadequate due to their high torsional stiffness.

After numerous iterations the final design was obtained. This design is not an optimal design for the problem, but would serve to validate the tests that would be decided upon. This design was then modelled on MSC/NASTRAN for Windows, a finite element analysis package, to determine the three dimensional stresses in the structure. From the DYMORE package a Southwell plot was generated.

Stellenbosch University http://scholar.sun.ac.za/

The next phase of the thesis could then start. This included the identifying of various tests to verify the design. A number of static tests were identified, this included:

- Axial
- Bending
- Torsional

It also seemed necessary to do fatigue tests on the structure, due to its operational environment. For this test to be conducted a special test bench had to be designed and constructed. The tests bench had to apply oscillating loads in five directions and a static load in the axial direction.

Due to the time limitation on the MSc Ing degree it was decided that the fatigue tests would only be taken as far as to validate the usefulness of both the test and test-bench.

The last phase of the thesis was to manufacture the flexbeam from the specified E-glass/epoxy and the testing thereof.

To conclude: This thesis successfully contributed to the knowledge base for designing a bearingless rotor system and laid out procedures and methodologies to this effect.

Stellenbosch University http://scholar.sun.ac.za/

REFERENCES

1. Sehgal, A, 1999, Design and development of a four-bladed bearingless main rotor system for the USMC H-1 upgrade programs, Journal of the American Helicopter Society.
2. Theron, N. J., 1997, KT 470 826 and 7. Item 33. HOOVER 1B. Feasibility study of various flexbeam hub concepts with final recommendation., University of Stellenbosch.
3. Bielawa, Richard L., 1992, Rotary wing structural dynamics and aeroelasticity, AIAA Educational Series.
4. Tsai, Stephan W. and Hahn, Thomas H., 1980, Introduction to composite materials, Technomic AG.
5. Bousman, William G., 1983, Design considerations for bearingless rotor hubs, Army Research and Technology Labs, California.
6. Shackelford, James F, 1992,Introduction to Material Science for Engineers, MacMillan.
7. Whitney, James M., 1987, Structural analysis of laminated anisotropic plates, Technomic Publishing co Inc.
8. Kaw, Autar K., 1997, Mechanics of Composite Materials, CRC Press.
9. Swanson, Stephan R., 1997, Introduction to Design and Analysis with Advanced Composite Materials, Prentice Hall.
10. Murri, Gretchen B., O'Brien, T. Kevin and Rousseau, Carl Q., 1997, Fatigue Life Methodology for Tapered Composite Flexbeam Laminates, Journal of the American Helicopter Society.
11. Tinker, David, 1997, Software developer's kit for Eagle Technology boards, Eagle Technology.
12. Eagle Technology, 1996, User Manual for the PC30F and PC30G Series Boards, Eagle Technology.
13. Agarwal, B.D. and Broutman, L.J., 1990, Analysis and Performance of fiber composites, John Wiley & Sons INC.
14. Greenberg, M.D., 1988, Advanced Engineering Mathematics, Prentice Hall.

Stellenbosch University http://scholar.sun.ac.za/

15. Van Rensburg, I.W.J. and Brodie, A., 1991, System Specifications for a helicopter rotor test facility, Renkor Technology.
16. Steyn, J., 1999, Prime Item Specifications For Bearingless Rotor Hub For The 24% Scale Model Of The Rooivalk Attack Helicopter, University of Stellenbosch.
17. FEMAP PROGRAM, 1985-1998, Enterprise Software Products Inc.
18. The MacNeal Schwendler Corporation, 1994, MSC/NASTRAN Reference Manual version 1, The MacNeal Schwendler Corporation.
19. DYMORE PROGRAM, 1994, Rensselaer Polythechnic Institute.
20. Bauchau, O.A., 1994, DYMORE: User's Manual, Rensselaer Polytechnic Institute, Department of Engineering.
21. CROSEC PROGRAM, 1994, Rensselaer Polythechnic Institute.
22. Bauchau, O.A., 1994, CROSEC: User's Manual, Rensselaer Polythechnic Institute,.
23. Teixeira, Steve and Pacheco, Xavier, 1998, Delphi 4 Developer's Guide, SAMS.NET Publishing.
24. CSIR technical drawings.
25. Benham, P.P., Crawford, R.J. and Armstrong, C.G., 1996, Mechanics of Engineering Materials, second edition, Longman.
26. Shigley, J.E. and Mischke, C.R., 1989, Mechanical Engineering Design, fifth edition, McGraw-Hill.
27. MIL-STD-490A, 1985, Military Standard: Specification Practices.
28. Eagle Technology, 1998, User Manual for the PC166 Series Boards, Eagle Technology.
29. Zirkel, G and Berlinger, E, 1994, Understanding Fortran 77 & 90, PWS Publishing Company, Boston.
30. Encyclopedia Britannica, 1969, Encyclopedia Britannica INC.
31. http://www.britannica.com.
32. http://www.helis.com.
33. http://www.matweb.com.
34. Soper John, 2000, AMT Materials, Cape Town.
35. Epolam 2020 Datasheet, 2000, AMT Materials, Cape Town.
36. The MacNeal Schwendler Corporation, 1996, MSC/NASTRAN Quick Reference Guide v69, The MacNeal Schwendler Corporation.

Stellenbosch University http://scholar.sun.ac.za/

APPENDIX A: BLADE CROSS-SECTION PROPERTIES

Table A- 1: Blade Cross-Sections

Segment	Obrd end	Ref station	Radial station		Mass	Elzz	Elxx	Glyy
	m	m			kg/m	Nm^2	Nm^2	Nm^2
1	0.0336	0.0168	0.017968	0.008984	0	23890.17	23890.17	7962.978
2	0.0672	0.0372	0.035936	0.019893	0	23890.17	15926.78	7962.978
3	0.1032	0.0852	0.055187	0.045561	14.78	9397.38	9397.38	3025.923
4	0.144	0.1236	0.077005	0.066096	14.78	310.5599	3105.599	63684.4
5	0.1896	0.1668	0.10139	0.089198	14.78	398.1282	4301.967	63684.4
6	0.24	0.2148	0.128342	0.114866	3.24	644.6751	1194.302	172.0002
7	0.288	0.264	0.154011	0.141176	2.68	132.1997	1035.2	118.6492
8	0.336	0.312	0.179679	0.166845	1.21	114.6778	1512.92	113.0744
9	0.384	0.36	0.205348	0.192513	0.9072	94.75898	2548.12	99.53619
10	0.4512	0.4176	0.241283	0.223316	0.815	77.23704	5335.1	86.79559
11	0.528	0.4896	0.282353	0.261818	0.769	75.66668	6211.197	86.79559
12	0.624	0.576	0.33369	0.308021	0.6941	72.4433	6050.028	86.79559
13	0.72	0.672	0.385027	0.359358	0.6451	71.65812	5496.269	86.79559
14	0.756	0.738	0.404278	0.394652	0.6123	68.47607	5335.1	86.79559
15	0.8016	0.7788	0.428663	0.416471	0.9297	67.69089	5173.931	85.99801
16	0.84	0.8208	0.449198	0.43893	0.9112	66.0792	5095.413	85.99801
17	0.8784	0.8592	0.469733	0.459465	0.561	64.50884	5016.895	85.99801
18	0.936	0.9072	0.500535	0.485134	0.5437	62.89715	4855.726	85.99801
19	0.1008	0.972	0.053904	0.519786	0.5196	60.50028	4698.69	85.20456
20	1.1044	1.056	0.590588	0.564706	0.5115	58.92992	4301.967	83.60941
21	1.2	1.152	0.641711	0.616043	0.5023	58.14474	4140.798	78.8322
22	1.296	1.248	0.693048	0.66738	0.4954	56.53305	4061.04	73.25741
23	1.392	1.344	0.744385	0.718717	0.4856	42.19316	3503.561	67.68676
24	1.488	1.44	0.795722	0.770053	0.4666	39.01938	3424.217	58.92579
25	1.584	1.536	0.847059	0.82139	0.4435	31.05599	2707.222	49.37137
26	1.68	1.632	0.898396	0.872727	0.432	28.66738	3185.356	46.98277
27	1.752	1.716	0.936898	0.917647	1.221	25.4812	4301.967	31.8515
28	1.8	1.7766	0.962567	0.950053	1.475	20.70399	5256.582	29.46289
29	1.838	1.8192	0.982888	0.972834	0.2592	13.53818	3264.701	19.1109
30	1.87	1.854	1	0.991444	0.144	4.105258	1035.2	6.3703

Stellenbosch University http://scholar.sun.ac.za/

Izz	Iyy	Ixx	Twist	Twist rel.	CG offset		Shear centre offset	
Kgm^2	Kgm^2	Kgm^2	degrees	to 75% R	mm	radial	mm	radial
0.2032	0.2032	0.4064	0	6.118	0	0	0	0
0.2032	0.2032	0.4064	0	6.118	0	0	0	0
0.2032	0.2032	0.4064	0	6.118	0	0	0	0
0.2032	0.2032	0.4064	0	6.118	0	0	0	0
0.2032	0.2032	0.4064	0	6.118	0	0	0	0
0.0261	0.2	0.2261	0	6.118	7	0.000899	0.8	0.000103
0.0235	0.263	0.2865	0	6.118	21	0.002696	2.5	0.000321
0.0208	0.326	0.3468	0	6.118	35	0.004493	4	0.000513
0.0182	0.388	0.4062	0	6.118	49	0.00629	5.6	0.000719
0.015	0.462	0.477	0	6.118	65	0.008344	7.5	0.000963
0.0133	0.484	0.4973	-0.2322	5.885805	53	0.006804	17	0.002182
0.0115	0.424	0.4355	-0.78946	5.328535	43	0.00552	20.7	0.002657
0.0105	0.359	0.3695	-1.40865	4.709347	31	0.003979	17.6	0.002259
0.0101	0.315	0.3251	-1.83434	4.283656	23	0.002953	15.5	0.00199
0.0147	0.305	0.3197	-2.0975	4.020501	18	0.002311	14.3	0.001836
0.0145	0.282	0.2965	-2.36839	3.749606	13	0.001669	5.4	0.000693
0.0094	0.257	0.2664	-2.61607	3.501931	11	0.001412	5	0.000642
0.0092	0.248	0.2572	-2.92566	3.192337	8	0.001027	4.5	0.000578
0.009	0.236	0.245	-3.34362	2.774385	6	0.00077	4	0.000513
0.0088	0.233	0.2418	-3.8854	2.232595	5	0.000642	1.6	0.000205
0.0086	0.23	0.2386	-4.50459	1.613408	4	0.000513	-0.9	-0.00012
0.0084	0.226	0.2344	-5.12378	0.99422	5	0.000642	-3	-0.00039
0.0075	0.222	0.2295	-5.74313	0.374871	5	0.000642	-15.5	-0.00199
0.0064	0.221	0.2274	-6.36248	-0.24448	8	0.001027	-16.9	-0.00217
0.0052	0.204	0.2092	-6.98184	-0.86384	4	0.000513	-28.5	-0.00366
0.0058	0.2	0.2058	-7.60119	-1.48319	3	0.000385	-26.8	-0.00344
0.0161	0.2358	0.2519	-8.14313	-2.02513	2	0.000257	-17.2	-0.00221
0.0191	0.2458	0.2649	-8.5341	-2.4161	1	0.000128	-10.5	-0.00135
0.0022	0.1885	0.1907	-8.615	-2.497	0	0	-5.6	-0.00072
0.0005	0.1829	0.1834	-8.615	-2.497	0	0	-1.8	-0.00023

Stellenbosch University http://scholar.sun.ac.za/

APPENDIX B: AERODYNAMIC LOADS

Table B- 1 : Aerodynamic Loads

Azimuth	15	30	45	60	75	90	105	120
Station	1	r/R=	0.18					
Fx	-22.4788	-19.2161	-14.9971	-13.6713	-16.839	-21.9929	-24.7676	-23.1063
Fz	-2.54448	-1.83661	-1.64881	-1.85762	-1.91595	-1.37717	-0.48131	0.044121
Mt	-0.33936	-0.31147	-0.42977	-0.56885	-0.60367	-0.5049	-0.368	-0.34532
Station	2	r/R=	0.26					
Fx	-14.6552	-12.1176	-9.03673	-8.42157	-11.3769	-15.7557	-18.0905	-16.8795
Fz	-1.13357	-0.42199	-0.81151	-1.38315	-0.88433	1.045624	3.294188	4.168043
Mt	-0.21734	-0.18847	-0.28729	-0.41549	-0.46789	-0.40713	-0.29898	-0.27149
Station	3	r/R=	0.335					
Fx	-9.70275	-7.7901	-5.95209	-6.01417	-8.41424	-11.5348	-13.1491	-12.5015
Fz	-2.70796	-1.8209	-1.84347	-2.05464	-1.43731	0.29803	2.219996	2.913587
Mt	-0.13005	-0.10229	-0.18769	-0.30476	-0.36239	-0.32122	-0.22997	-0.19991
Station	4	r/R=	0.405					
Fx	-6.57628	-5.1961	-4.50198	-5.15759	-6.95059	-8.80214	-9.70968	-9.62516
Fz	-3.55143	-2.67707	-2.42182	-2.3568	-1.86669	-0.74446	0.472848	0.903353
Mt	-0.07583	-0.04866	-0.12177	-0.22721	-0.28583	-0.25805	-0.17979	-0.14797
Station	5	r/R=	0.47					
Fx	-3.44139	-2.59324	-3.06342	-4.29043	-5.37738	-5.8415	-6.01163	-6.57796
Fz	-0.78141	-0.17208	-0.33831	-0.68068	-0.57618	0.171003	1.158958	1.666077
Mt	-0.03373	-0.00711	-0.06832	-0.16262	-0.22255	-0.20843	-0.1438	-0.1111
Station	6	r/R=	0.53					
Fx	-0.88454	-0.33202	-1.37793	-2.88634	-3.64751	-3.46805	-3.30313	-4.17387
Fz	-0.24225	-0.01854	-0.69688	-1.33341	-1.14956	-0.1054	1.099272	1.54492
Mt	0.001966	0.027216	-0.02401	-0.10851	-0.16938	-0.16739	-0.11534	-0.08235
Station	7	r/R=	0.585					
Fx	1.230107	1.51589	-0.01445	-1.75295	-2.24023	-1.52061	-1.05732	-2.14198
Fz	-0.07553	-0.13582	-1.15621	-1.97895	-1.73173	-0.48706	0.861374	1.279148
Mt	0.028847	0.05209	0.008643	-0.06718	-0.1272	-0.13355	-0.09125	-0.05845
Station	8	r/R=	0.635					
Fx	2.624236	2.673311	0.721908	-1.19975	-1.42122	-0.20491	0.544649	-0.69376
Fz	-0.20735	-0.39459	-1.46127	-2.2986	-2.09555	-0.92845	0.369981	0.812198
Mt	0.04383	0.064998	0.027782	-0.03999	-0.09706	-0.10774	-0.07224	-0.04012
Station	9	r/R=	0.685					
Fx	3.362497	3.211605	0.919722	-1.11891	-1.06633	0.612864	1.634991	0.290238
Fz	-0.14119	-0.3695	-1.35177	-2.16184	-2.1082	-1.18786	-0.03305	0.48986
Mt	0.048265	0.067482	0.036243	-0.02301	-0.0752	-0.0876	-0.05744	-0.02686
Station	10	r/R=	0.733					
Fx	3.545063	3.263788	0.788663	-1.27202	-0.99477	1.01606	2.237735	0.849644
Fz	0.234177	-0.0028	-0.93637	-1.76196	-1.85399	-1.14032	-0.09419	0.533653
Mt	0.04501	0.06258	0.036738	-0.01439	-0.06098	-0.07357	-0.04778	-0.01953
Station	11	r/R=	0.77					

Stellenbosch University http://scholar.sun.ac.za/

Fx	3.488708	3.121116	0.590362	-1.42404	-0.98951	1.212768	2.555243	1.178439
Fz	0.295288	0.124161	-0.73443	-1.51809	-1.6495	-1.06376	-0.13396	0.543316
Mt	0.038917	0.054859	0.033737	-0.00989	-0.05086	-0.06304	-0.04121	-0.01581
Station	12	r/R=	0.81					
Fx	3.347326	2.909628	0.411088	-1.50727	-0.97031	1.307396	2.705874	1.392204
Fz	-0.4475	-0.43029	-1.0655	-1.64152	-1.68019	-1.18773	-0.44125	0.176247
Mt	0.031844	0.04576	0.029	-0.00713	-0.0421	-0.05345	-0.03562	-0.01356
Station	13	r/R=	0.845					
Fx	3.2505	2.747609	0.31878	-1.49399	-0.91704	1.33007	2.721462	1.50835
Fz	-2.07868	-1.75672	-1.97578	-2.16977	-2.02121	-1.60074	-1.08621	-0.68513
Mt	0.025832	0.037528	0.024128	-0.00557	-0.03505	-0.04536	-0.03094	-0.01203
Station	14	r/R=	0.875					
Fx	3.1736	2.618525	0.285044	-1.42208	-0.85017	1.298075	2.644605	1.558989
Fz	-4.08384	-3.41164	-3.10006	-2.79399	-2.40811	-2.09312	-1.92807	-1.95793
Mt	0.02077	0.030282	0.019533	-0.0046	-0.02904	-0.03815	-0.02673	-0.01084
Station	15	r/R=	0.905					
Fx	2.76874	2.247114	0.230603	-1.22433	-0.70899	1.163843	2.352789	1.464191
Fz	-4.54257	-3.75874	-3.2293	-2.69545	-2.15415	-1.79962	-1.76528	-2.12843
Mt	0.015599	0.022812	0.014885	-0.00332	-0.02237	-0.03019	-0.02194	-0.00929
Station	16	r/R=	0.93					
Fx	1.953654	1.598205	0.195584	-0.81741	-0.43396	0.923923	1.797309	1.180963
Fz	-2.21193	-1.83617	-1.77079	-1.6126	-1.09383	-0.34755	0.143768	-0.12562
Mt	0.01092	0.016275	0.011124	-0.00168	-0.01602	-0.02287	-0.01752	-0.0076
Station	17	r/R=	0.95					
Fx	1.071929	0.929741	0.194042	-0.35748	-0.13377	0.657175	1.178172	0.834551
Fz	0.714525	0.518939	-0.04387	-0.38759	0.029743	1.12976	2.108611	2.087931
Mt	0.006982	0.010915	0.008128	-0.00025	-0.01082	-0.01699	-0.01406	-0.00641
Station	18	r/R=	0.97					
Fx	0.370867	0.393607	0.16466	-0.03665	0.059421	0.400752	0.634513	0.497065
Fz	1.872077	1.433615	0.719105	0.24924	0.523681	1.483801	2.401618	2.499696
Mt	0.003576	0.006018	0.005123	0.000604	-0.00645	-0.01173	-0.01094	-0.00565
Station	19	r/R=	0.99					
Fx	0.090681	0.118114	0.062103	0.003229	0.036299	0.150659	0.230004	0.187025
Fz	0.634296	0.475599	0.236527	0.100177	0.210715	0.517949	0.785287	0.79599
Mt	0.001032	0.00186	0.001764	0.000332	-0.00236	-0.00471	-0.00474	-0.00268

135	150	165	180	195	210	225	240	255
-19.2383	-17.4045	-19.583	-23.6054	-25.3991	-22.9985	-18.4967	-16.0629	-17.9616
-0.12596	-0.4825	-0.38965	0.044078	0.156761	-0.40738	-1.37145	-2.28396	-3.06802
-0.50674	-0.74717	-0.86316	-0.75732	-0.55592	-0.48437	-0.61913	-0.80085	-0.81931
-13.9582	-12.5776	-14.1531	-17.0032	-18.1384	-16.1457	-12.5251	-10.3331	-11.3936
2.996431	0.848814	-0.40964	0.11888	1.574843	2.2888	1.347467	-0.72682	-2.6668
-0.39951	-0.60978	-0.72879	-0.65759	-0.48897	-0.41511	-0.5137	-0.66107	-0.68092
-10.9126	-10.3382	-11.4124	-12.9758	-13.3423	-11.8689	-9.5082	-8.01777	-8.49652
1.810616	-0.18906	-1.46164	-1.17127	-0.0261	0.515857	-0.32336	-2.00798	-3.39651

Stellenbosch University http://scholar.sun.ac.za/

-0.30624	-0.49554	-0.6159	-0.56917	-0.42494	-0.3509	-0.42528	-0.55073	-0.57529
-9.32645	-9.48701	-10.0094	-10.2981	-9.96099	-9.08198	-8.0388	-7.28551	-7.1917
0.154324	-1.2264	-2.18853	-2.17813	-1.6561	-1.54937	-2.25036	-3.25896	-3.85655
-0.23618	-0.4062	-0.52472	-0.49623	-0.37229	-0.29978	-0.356	-0.46425	-0.49234
-7.67916	-8.57667	-8.41533	-7.29177	-6.28352	-6.22794	-6.75243	-6.80027	-5.96907
1.26999	0.294658	-0.42548	-0.35718	0.135567	0.143716	-0.72135	-1.82028	-2.26957
-0.18139	-0.33047	-0.44381	-0.43039	-0.32592	-0.25684	-0.29733	-0.3884	-0.41688
-5.90463	-7.10275	-6.58021	-4.78671	-3.51111	-3.92066	-5.22783	-5.62689	-4.36454
0.845773	-0.44494	-1.24872	-0.93047	0.028628	0.431698	-0.32798	-1.56477	-2.16374
-0.13626	-0.26491	-0.37123	-0.36968	-0.28273	-0.21795	-0.24525	-0.32064	-0.3483
-4.35711	-5.79658	-4.99807	-2.66918	-1.15477	-1.90658	-3.84507	-4.5834	-3.05856
0.416453	-1.03553	-1.87133	-1.39484	-0.122	0.599303	0.006676	-1.23325	-1.87994
-0.09917	-0.21019	-0.30912	-0.31613	-0.24349	-0.1829	-0.19997	-0.26275	-0.28995
-3.29925	-4.9386	-3.92067	-1.15263	0.578132	-0.42417	-2.88068	-3.95484	-2.30589
0.034795	-1.32304	-2.10405	-1.60061	-0.27255	0.556595	0.111096	-0.9741	-1.48856
-0.07117	-0.16793	-0.25962	-0.27207	-0.21044	-0.15376	-0.16355	-0.21687	-0.24385
-2.62316	-4.41791	-3.22159	-0.10685	1.787409	0.572703	-2.321	-3.70335	-1.99476
-0.0268	-1.09279	-1.69614	-1.16866	0.098766	0.883089	0.48232	-0.48772	-0.9111
-0.05047	-0.13441	-0.21811	-0.23378	-0.18162	-0.12945	-0.13399	-0.1792	-0.20519
-2.23281	-4.10502	-2.79342	0.521201	2.489911	1.114259	-2.07932	-3.67724	-1.94198
0.315358	-0.4114	-0.81379	-0.27612	0.907207	1.635479	1.238222	0.242885	-0.31907
-0.03794	-0.11083	-0.18622	-0.20309	-0.15884	-0.11176	-0.11315	-0.15151	-0.1753
-1.94523	-3.82273	-2.44961	0.945117	2.930742	1.460584	-1.89975	-3.62795	-1.89945
0.580279	0.143804	-0.16639	0.23674	1.260855	1.979524	1.658011	0.605478	-0.22177
-0.03031	-0.09314	-0.15991	-0.17663	-0.1393	-0.09777	-0.09744	-0.12975	-0.15055
-1.65472	-3.46906	-2.07708	1.302661	3.27375	1.787542	-1.61818	-3.42274	-1.76758
0.357914	0.076816	-0.32693	-0.25326	0.500235	1.231438	1.094177	0.105499	-0.87134
-0.02456	-0.07701	-0.13411	-0.14967	-0.11908	-0.08382	-0.08261	-0.10907	-0.12636
-1.36429	-3.06057	-1.69405	1.578278	3.50674	2.103016	-1.18932	-2.9933	-1.49118
-0.62322	-1.00383	-1.59993	-1.80741	-1.29792	-0.65528	-0.71953	-1.54214	-2.30481
-0.02013	-0.06325	-0.11119	-0.12499	-0.10005	-0.07059	-0.06918	-0.09086	-0.10508
-1.07616	-2.62476	-1.32928	1.744174	3.581608	2.333901	-0.68356	-2.37611	-1.06842
-2.27577	-2.89025	-3.53936	-3.71948	-3.30341	-2.95794	-3.32509	-4.1098	-4.35169
-0.01659	-0.05132	-0.09067	-0.1024	-0.08219	-0.05799	-0.0567	-0.07447	-0.08617
-0.75386	-2.06365	-0.96661	1.63729	3.200673	2.182983	-0.31029	-1.72641	-0.69741
-2.86892	-3.72352	-4.24339	-4.10851	-3.62027	-3.61917	-4.41374	-5.18856	-4.83739

Stellenbosch University http://scholar.sun.ac.za/

-0.01255	-0.03831	-0.06846	-0.07792	-0.06273	-0.0441	-0.043	-0.05674	-0.06602
-0.3992	-1.35033	-0.59669	1.219322	2.291721	1.567676	-0.16387	-1.16067	-0.504
-1.14417	-2.21732	-2.55651	-2.03731	-1.40455	-1.55325	-2.41172	-2.90285	-2.15404
-0.00843	-0.02613	-0.04825	-0.05597	-0.04542	-0.03174	-0.03067	-0.04078	-0.04802
-0.0805	-0.65266	-0.25912	0.725354	1.276544	0.84381	-0.11504	-0.67876	-0.37681
1.047616	-0.04763	-0.23196	0.471679	1.136558	1.008194	0.403127	0.29349	1.110718
-0.00527	-0.01641	-0.03195	-0.03821	-0.03144	-0.02181	-0.02077	-0.02785	-0.03332
0.10888	-0.15109	-0.03454	0.294525	0.445135	0.255034	-0.09177	-0.31085	-0.27084
1.765636	0.997591	0.937397	1.498656	1.968853	1.903524	1.629881	1.749257	2.336183
-0.00315	-0.00841	-0.01757	-0.02199	-0.01844	-0.01264	-0.01177	-0.01595	-0.01941
0.062382	-0.02389	-0.00113	0.077153	0.104145	0.046645	-0.04335	-0.10416	-0.11234
0.572621	0.357712	0.355517	0.5278	0.666652	0.648446	0.569619	0.604271	0.778785
-0.00123	-0.00256	-0.00561	-0.00727	-0.00616	-0.00415	-0.00381	-0.00524	-0.00644

270	285	300	315	330	345	360
-22.5105	-25.8263	-25.4941	-22.6358	-20.4746	-20.9091	-22.5955
-3.99784	-5.15052	-6.10774	-6.35193	-5.7859	-4.735	-3.57785
-0.65726	-0.50607	-0.53987	-0.71813	-0.83797	-0.757	-0.53093
-14.6848	-17.354	-17.3691	-15.3153	-13.577	-13.7275	-14.8596
-3.73951	-4.23967	-4.78894	-5.43613	-5.57018	-4.63605	-2.84435
-0.55268	-0.43036	-0.45527	-0.59184	-0.67329	-0.58734	-0.38553
-10.4788	-12.3534	-12.7751	-11.8165	-10.7024	-10.3726	-10.4352
-3.98228	-4.25885	-4.90676	-5.88546	-6.43287	-5.8764	-4.34816
-0.47431	-0.37321	-0.39033	-0.49594	-0.5506	-0.4628	-0.27996
-7.84508	-8.89698	-9.73425	-9.9489	-9.58174	-8.8722	-7.88931
-3.99085	-4.27046	-5.12665	-6.22019	-6.75177	-6.24298	-4.94087
-0.4126	-0.32794	-0.33916	-0.4222	-0.45939	-0.37444	-0.20985
-5.05694	-5.17563	-6.49666	-8.03381	-8.52305	-7.45046	-5.3768
-2.04752	-2.02011	-2.83042	-4.03758	-4.56213	-3.81449	-2.22512
-0.35419	-0.28383	-0.29054	-0.35476	-0.37821	-0.29816	-0.15219
-2.62413	-2.25653	-3.8068	-5.98124	-6.87741	-5.63485	-3.06856
-1.93144	-1.78733	-2.5355	-3.76205	-4.26677	-3.37707	-1.62744
-0.29995	-0.24246	-0.24596	-0.29425	-0.30596	-0.23065	-0.1018
-0.71437	0.02839	-1.68377	-4.33079	-5.51473	-4.10736	-1.13718
-1.59817	-1.31631	-1.97297	-3.23036	-3.84043	-3.03671	-1.33719
-0.25376	-0.20719	-0.20827	-0.24376	-0.24642	-0.17584	-0.06194

Stellenbosch University http://scholar.sun.ac.za/

0.465939	1.504791	-0.31817	-3.33975	-4.76429	-3.22053	0.097717
-1.09725	-0.73159	-1.34434	-2.60817	-3.31209	-2.70965	-1.25867
-0.21712	-0.17897	-0.17822	-0.20444	-0.20158	-0.13654	-0.03585
1.105158	2.394871	0.493495	-2.8491	-4.50738	-2.88319	0.708789
-0.50104	-0.15047	-0.73101	-1.89592	-2.56427	-2.12288	-0.96476
-0.18562	-0.15409	-0.15197	-0.1715	-0.16611	-0.10832	-0.02089
1.371753	2.837117	0.896199	-2.65816	-4.49378	-2.86519	0.848149
-0.10078	0.150733	-0.34662	-1.30403	-1.83194	-1.44657	-0.46244
-0.1601	-0.13331	-0.13048	-0.14584	-0.1402	-0.09016	-0.01489
1.513063	3.071371	1.12756	-2.5102	-4.43157	-2.84458	0.846
-0.28684	-0.11152	-0.45726	-1.20623	-1.65073	-1.32294	-0.40871
-0.13803	-0.11499	-0.112	-0.12462	-0.11961	-0.07692	-0.01265
1.612715	3.18804	1.294499	-2.28979	-4.20294	-2.69172	0.852249
-1.09879	-0.90122	-1.08883	-1.74637	-2.2739	-2.10326	-1.247
-0.11589	-0.0965	-0.09378	-0.10418	-0.10002	-0.0646	-0.01122
1.69246	3.189518	1.400378	-1.9947	-3.80704	-2.37855	0.95287
-2.2925	-1.89655	-2.03041	-2.83097	-3.6363	-3.73073	-2.98537
-0.09629	-0.08017	-0.07797	-0.08664	-0.08315	-0.05377	-0.00969
1.767162	3.074719	1.417804	-1.67489	-3.30819	-1.96964	1.100185
-3.60621	-2.72887	-2.87946	-4.06742	-5.32501	-5.72798	-5.09496
-0.079	-0.06585	-0.0642	-0.0714	-0.06845	-0.04421	-0.00812
1.56308	2.576778	1.204848	-1.31061	-2.62368	-1.49108	1.065646
-3.32155	-2.02326	-2.26987	-3.84788	-5.46984	-6.07852	-5.54153
-0.06083	-0.05102	-0.04995	-0.05546	-0.0529	-0.03399	-0.0063
0.989653	1.672452	0.780403	-0.88728	-1.76632	-0.99025	0.770154
-0.5582	0.467192	-0.03077	-1.56695	-2.93829	-3.36848	-2.91217
-0.04483	-0.03814	-0.03756	-0.04139	-0.03905	-0.02489	-0.00477
0.378338	0.75962	0.355532	-0.47744	-0.94395	-0.55017	0.395873
2.226561	2.607348	1.915234	0.789992	0.0596	0.023966	0.420141
-0.03165	-0.02743	-0.0272	-0.02968	-0.02761	-0.01747	-0.00363
-0.07187	0.079131	0.036947	-0.17076	-0.33288	-0.24109	0.079026
2.849774	2.773918	2.181662	1.597033	1.414273	1.604568	1.86883
-0.01869	-0.01645	-0.01646	-0.01781	-0.01624	-0.01008	-0.00223
-0.08178	-0.04133	-0.02425	-0.04998	-0.08952	-0.08136	-0.0031
0.941098	0.935313	0.766152	0.578516	0.504068	0.555509	0.64009
-0.0062	-0.00546	-0.00552	-0.00598	-0.00538	-0.00327	-0.00075

Stellenbosch University http://scholar.sun.ac.za/

APPENDIX C: DESIGN SPECIFICATIONS OF THE 24% SCALE ROTOR [16, 27]

C.1 Scope

These specifications establish the performance, design, development and testing requirements for a bearingless rotor hub for the 24% scale model of the Rooivalk attack helicopter. The bearingless rotor hub is primarily intended as a technology demonstrator, and secondarily to be tested on the actual 24% scale model.

C.2 Applicable Documents

C.2.1 Military Standards

MIL-STD-490A	Military Standard Specification Practices
RSA-MIL-STD-8	Software Development, Minimum Requirements for

C.2.2 Other Documents

DOC.NO. 103-000-00-28 System Specification for a Helicopter Rotor Test Facility

C.3 Requirements

C.3.1 Prime Item Definition

C.3.1.1 General Definition

A bearingless rotor hub is a structure, usually manufactured of composite materials, that allows blade motion of flap, lead-lag and pitch through the elastic deformation of the structure rather than the use of discrete bearings that allow rotation between components.

Stellenbosch University http://scholar.sun.ac.za/

The prime item will be the bearingless rotor hub to be constructed primarily of composite materials. The dynamic performance of the bearingless rotor hub shall be, within tolerances, the same as that of the fully articulated hub.

C.3.1.2 Geometric Diagram of the Bearingless Rotor Hub

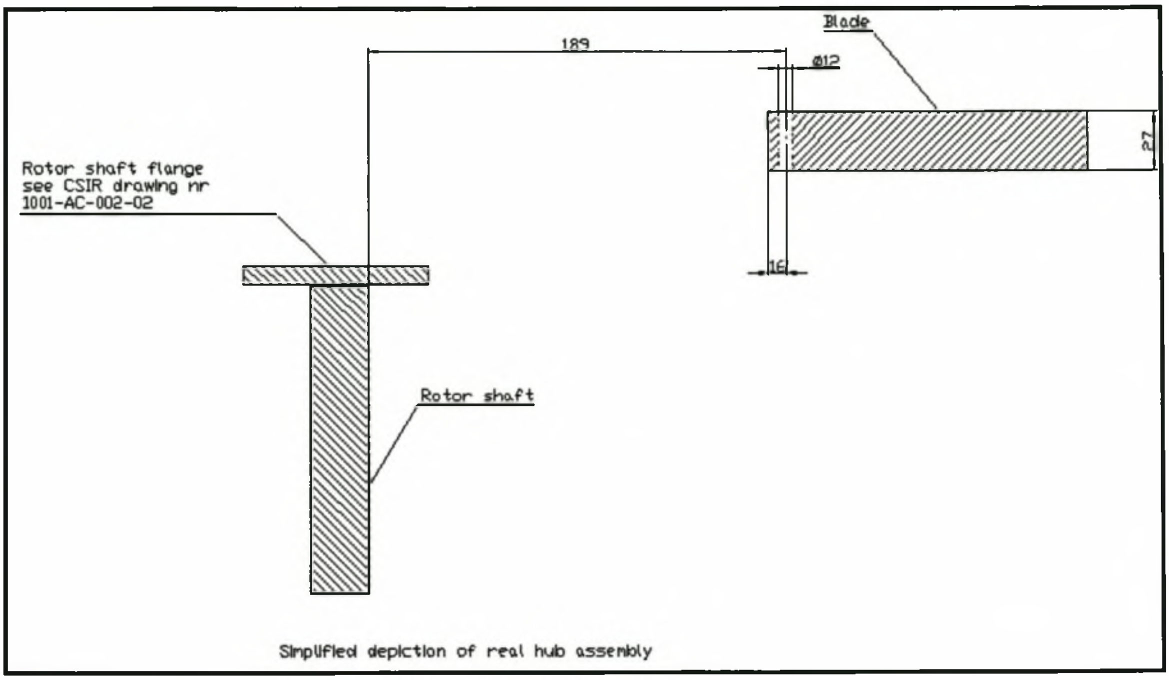

Figure C-1: Hub layout

C.3.1.3 Interface definition

C.3.1.3.1 Prime item shaft interface

The interface between the bearingless rotor hub and the rotor shaft of the helicopter shall be changed to accommodate the new design. The hub shall however interface with the existing shaft without changing it.

C.3.1.3.2 Prime item blade interface

The interface between the bearingless rotor hub and the blade shall be determined by the interface on the side of the blade, ensuring that the blade interface shall not have to be altered.

Stellenbosch University http://scholar.sun.ac.za/

C.3.2 Characteristics

C.3.2.1 Performance

C.3.2.1.1 Operational envelope

The bearingless rotor hub shall be capable of a dynamic response equivalent to that of the original rotor hub. It shall be capable of angular velocities in the range of 0 to 125 rad/s and be able to withstand blade pitch inputs of up to 20 degrees.

C.3.2.1.2 Structural envelope

The bearingless rotor hub shall withstand the static and dynamic loads imposed upon it by the blades. For the purpose of design and testing, an air load data set will be supplied by the CSIR. When the blades are in rest the hub shall ensure that the blades do not droop to a level that may cause a blade strike at start-up or shutdown with any part of the model or the ground.

C.3.2.2 Physical

C.3.2.2.1 Dimensions

The bearingless rotor hub shall preferably have dimensions as depicted in Figure C-1, fitting into the space of the fully articulated hub. If this would not be possible then the bearingless hub shall have the smallest possible outside diameter.

C.3.2.2.2 Weight

The weight of the bearingless rotor hub shall not exceed that of the fully articulated hub.

C.3.2.2.3 Blade interface

The interface at the blade side shall be determined by the blade itself and the design of the bearingless rotor hub shall be altered to fit in with it.

Stellenbosch University http://scholar.sun.ac.za/

C.3.2.2.4 Shaft interface

The interface at the shaft end shall be altered according to the design of the bearingless rotor hub. A necessary interface shall be designed to replace the existing one.

C.3.2.2.5 Finish

The bearingless rotor hub shall be given a smooth polished finish to minimize the affects of air resistance.

C.3.2.3 Reliability

C.3.2.3.1 Failure identification

A failure of the structure shall be defined if any of the following happens;

- Delamination of composite fibres or layers
- Any cracking of the composite matrix
- Fracture of the structure

C.3.2.4 Maintainability

C.3.2.4.1 General

The bearingless rotor hub shall have no maintenance done on it. When a failure of the structure is detected it shall be replaced and not repaired.

C.3.2.5 Downtime

The downtime shall not be more than with the fully articulated hub

C.3.3 Design and construction

C.3.3.1 Materials

The materials used shall be primarily a composite fibre mat bonded together with an appropriate resin.

C.3.3.2 Processes

The process that shall the used is a hand lay-up procedure with the mould being put under pressure during the curing phase.

Stellenbosch University http://scholar.sun.ac.za/

C.4 Quality assurance provisions

C.4.1 Interface Definition

C.4.1.1 Prime Item Shaft Interface

It shall be checked with physical inspection.

C.4.1.2 Prime Item Blade Interface

It shall be checked with physical inspection.

C.4.2 Characteristics

C.4.2.1 Performance

C.4.2.1.1 Operational envelope

It shall be verified with a comparison between the fully articulated and bearingless rotor hubs. This comparison shall be done with finite element analysis of both the models.

C.4.2.1.2 Structural envelope

It shall be verified by means of physical testing of the flexbeam structure to determine its stiffness and strength.

C.4.2.2 Physical

C.4.2.2.1 Dimensions

It shall be verified by means of measuring the final structure.

C.4.2.2.2 Weight

It shall be verified by weighing the final structure.

C.4.2.2.3 Blade interface

It shall be verified by physical inspection.

C.4.2.2.4 Shaft interface

It shall be verified by physical inspection.

Stellenbosch University http://scholar.sun.ac.za/

C.4.2.2.5 Finish

It shall be verified by physical inspection.

C.4.2.3 Reliability

C.4.2.3.1 Failure identification

It shall be verified by physical inspection as well as with measurement equipment.

C.4.2.4 Maintainability

C.4.2.4.1 General

Not Applicable

C.4.2.4.2 Downtime

Not Applicable

C.4.3 Design and Construction

C.4.3.1 Materials

Not Applicable

C.4.3.2 Processes

Not Applicable

Stellenbosch University http://scholar.sun.ac.za/

APPENDIX D: SOURCE CODE FOR CALCULATING THE FACTOR OF SAFETY

Program vfber

```
      use dfport

c-------------------------------------------------------------------
c     Die program is geskryf deur Johannes Steyn  (9308873)
c     Die datum is 06 Mei 1999
c
c     Dit is geskryf as deel van my MSCEng Tesis om die veiligheids faktor
c     uit te werk van spannings data verkry deur crosec
c-------------------------------------------------------------------
      parameter maxnodes=20000
      parameter maxelements=20000
      common /iotp/ nr,nw
      integer idum
      real idumr
      character*60 idumc
      Integer nnode, nelement
      Integer i ,j , pos, nr, nw
      double precision TM1(6,6), TM2(6,6)
      double precision node(9), AA(1:6), BB(1:6), BBtemp(6,6)
      double precision stress(10*maxelements,6)
      double precision stresst(10*maxelements,6)
      double precision gaussepunt(10*maxelements,2)
      double precision nodelt(maxnodes,2)
      integer elem(maxelements,9), upper , vfplek
      double precision elemm(maxelements*9,3)
      double precision vf(10*maxelements), vftemp(4) , vfmin
      double precision sigma1p,sigma1m,sigma2p,sigma2m,sigma3p,sigma3m
      double precision toult,touhars
      character*8 Hour ,begintime, endtime
      double precision phi , pi
      double precision m2,n2,k2,l2
c-------------------------------------------------------------------
      nr  = 5
      nw  = 6
      pi = 3.141592653589793

c      tho = 1.0d+03
      open (nr ,file='vf.inp',status='old')
      open (nw ,file='vf.out',status='new')
      call time(Hour)
      call time(begintime)
      write (nw,*) Hour, "    :Begining Analysis"

c-----read number of nodes and elements
      call time(Hour)
      write (nw,*) Hour, "    :Started reading number of nodes and elements"
      write (nw,*)
      read  (nr,*,err=900) nnode, nelement
c     write (nw,*) nnode, nelement
      read  (nr,*,err=900)
      call time(Hour)
      write (nw,*) Hour, "    :Finished reading number of nodes and elements"
      write (nw,*)
c-----read nodal coordinates
      call time(Hour)
      write (nw,*) Hour, "    :Started reading nodal coordinates"
      write (nw,*)
      do 200 i = 1 , nnode
```

Stellenbosch University http://scholar.sun.ac.za/


```
      read  (nr,2000,err=900)   idum,nodelt(i,1),nodelt(i,2)
 200  continue
      read  (nr,*,err=900)
      call time(Hour)
      write (nw,*) Hour, "    :Finished reading nodal coordinates"
      write (nw,*)

c     do 201 i=1,nnode
c     write  (nw,2000,err=900)   idum,nodelt(i,1),nodelt(i,2)
c 201  continue

c-----read element info
      call time(Hour)
      write (nw,*) Hour, "    :Started reading element info"
      write (nw,*)
      do 300 i = 1 , nelement
      read  (nr,3000,err=900)   idum,idum,elemm(i,1),idum,elemm(i,2),
     2                          elemm(i,3),elem(i,1),elem(i,2),elem(i,3),
     3                        elem(i,4),elem(i,5),elem(i,6),
     4                        elem(i,7),elem(i,8),elem(i,9)
 300  continue
      call time(Hour)
      write (nw,*) Hour, "    :Finished reading element info"
      write (nw,*)

c     do 301 i = 1 , nelement
c     write  (nw,3000,err=900)  idum,idum,elemm(i,1),idum,elemm(i,2),
c    2                          elemm(i,3),elem(i,1),elem(i,2),elem(i,3),
c    3                        elem(i,4),elem(i,5),elem(i,6),
c    4                        elem(i,7),elem(i,8),elem(i,9)
c 301  continue

c-----read stress info
      call time(Hour)
      write (nw,*) Hour, "    :Started reading Stress and Gaussian info"
      write (nw,*)
      i=0
      DO while (.NOT. EOF(nr))
      i=i+1
      read  (nr,*)

      read  (nr,4000,err=900) idum, gaussepunt(i,1)
      read  (nr,5000,err=900) idum, gaussepunt(i,2),stresst(i,1),
     1                           stresst(i,6),stresst(i,5),stresst(i,2),
     2                         stresst(i,3),stresst(i,4)

      End DO
      upper=i
      call time(Hour)
      write (nw,*) Hour, "    :Finished reading Stress and Gaussian info"
      write (nw,*)
c ---------------------------------------------------------------------------

      call time(Hour)
      write (nw,*) Hour, "    :Beginning analysys"
      write (nw,*)
      pos=0
c
      do 800 j = 1 , nelement
c ------------------------------------------------------
c Konvergeer die spannings van XY na LT
c ------------------------------------------------------

      if ((elem(j,5) .EQ. 0) .AND. (elem(j,4) .NE. 0)) then
c ------------------------------------------------------
c Reghoekige element met 4 nodes
c ------------------------------------------------------
```

Stellenbosch University http://scholar.sun.ac.za/


```
c Bereken hoek phi
c -------------------------------------------------------
      z1=gaussepunt(pos+1,2)
      z2=gaussepunt(pos+2,2)
      z3=gaussepunt(pos+3,2)
      z4=gaussepunt(pos+4,2)
      y1=gaussepunt(pos+1,1)
      y2=gaussepunt(pos+2,1)
      y3=gaussepunt(pos+3,1)
      y4=gaussepunt(pos+4,1)

      z8=(z3+z4)/2
      y8=(y3+y4)/2
      z5=(z1+z2+z3+z4)/4
      y5=(y1+y2+y3+y4)/4

      phi=atan((z8-z5)/(y8-y5))

c Transformasie matriks1

      k2=cos(phi)
      l2=sin(phi)

      TM1(2,2)=k2**2;
      TM1(2,3)=l2**2;
      TM1(2,4)=2*k2*l2;
      TM1(3,2)=l2**2;
      TM1(3,3)=k2**2;
      TM1(3,4)=-2*k2*l2;
      TM1(1,1)=1;
      TM1(5,5)=k2;
      TM1(5,6)=-l2;
      TM1(6,5)=l2;
      TM1(6,6)=k2;
      TM1(4,2)=-k2*l2;
      TM1(4,3)=k2*l2;
      TM1(4,4)=(k2**2-l2**2);

c Transformasie Matriks2

      m2=cos(elemm(j,3)*pi/180)
      n2=sin(elemm(j,3)*pi/180)

      TM2(1,1)=m2**2;
      TM2(1,2)=n2**2;
      TM2(1,6)=2*m2*n2;
      TM2(2,1)=n2**2;
      TM2(2,2)=m2**2;
      TM2(2,6)=-2*m2*n2;
      TM2(3,3)=1;
      TM2(4,4)=m2;
      TM2(4,5)=-n2;
      TM2(5,4)=n2;
      TM2(5,5)=m2;
      TM2(6,1)=-m2*n2;
      TM2(6,2)=m2*n2;
      TM2(6,6)=(m2**2-n2**2);

      do 410, i = 1, 6
       AA(i)=stresst(pos+1,i)
  410 continue

      BBtemp=matmul(TM2,TM1)
      BB=matmul(BBtemp,AA)
      do 411, i = 1 , 6
       stress(pos+1,i)=BB(i)
  411 continue
```

Stellenbosch University http://scholar.sun.ac.za/


```
      do 412, i = 1, 6
       AA(i)=stresst(pos+2,i)
  412 continue

      BBtemp=matmul(TM2,TM1)
      BB=matmul(BBtemp,AA)
      do 413, i = 1 , 6
       stress(pos+2,i)=BB(i)
  413 continue

      do 414, i = 1, 6
       AA(i)=stresst(pos+3,i)
  414 continue

      BBtemp=matmul(TM2,TM1)
      BB=matmul(BBtemp,AA)
      do 415, i = 1 , 6
       stress(pos+3,i)=BB(i)
  415 continue

      do 416, i = 1, 6
       AA(i)=stresst(pos+4,i)
  416 continue

      BBtemp=matmul(TM2,TM1)
      BB=matmul(BBtemp,AA)
      do 417, i = 1 , 6
       stress(pos+4,i)=BB(i)
  417 continue

      pos=pos+4

      elseif ((elem(j,5) .NE. 0) .AND. (elem(j,4).EQ. 0)) then
c-------------------------------------------------------
c Driehoekige element met 6 nodes

      z1=gaussepunt(pos+1,2);
      z2=gaussepunt(pos+2,2);
      y1=gaussepunt(pos+1,1);
      y2=gaussepunt(pos+2,1);

      phi=atan((z2-z1)/(y2-y1));

c Transformasie matriks1

      k2=cos(phi);
      l2=sin(phi);

      TM1(2,2)=k2**2;
      TM1(2,3)=l2**2;
      TM1(2,4)=2*k2*l2;
      TM1(3,2)=l2**2;
      TM1(3,3)=k2**2;
      TM1(3,4)=-2*k2*l2;
      TM1(1,1)=1;
      TM1(5,5)=k2;
      TM1(5,6)=-l2;
      TM1(6,5)=l2;
      TM1(6,6)=k2;
      TM1(4,2)=-k2*l2;
      TM1(4,3)=k2*l2;
      TM1(4,4)=(k2**2-l2**2);

c Transformasie Matriks2

      m2=cos(elemm(j,3)*pi/180)
```

Stellenbosch University http://scholar.sun.ac.za/


```
      n2=sin(elemm(j,3)*pi/180)

      TM2(1,1)=m2**2;
      TM2(1,2)=n2**2;
      TM2(1,6)=2*m2*n2;
      TM2(2,1)=n2**2;
      TM2(2,2)=m2**2;
      TM2(2,6)=-2*m2*n2;
      TM2(3,3)=1;
      TM2(4,4)=m2;
      TM2(4,5)=-n2;
      TM2(5,4)=n2;
      TM2(5,5)=m2;
      TM2(6,1)=-m2*n2;
      TM2(6,2)=m2*n2;
      TM2(6,6)=(m2**2-n2**2);

      do 418, i = 1, 6
       AA(i)=stresst(pos+1,i)
418   continue

      BBtemp=matmul(TM2,TM1)
      BB=matmul(BBtemp,AA)
      do 419, i = 1 , 6
       stress(pos+1,i)=BB(i)
419   continue

      do 420, i = 1, 6
       AA(i)=stresst(pos+2,i)
420   continue

      BBtemp=matmul(TM2,TM1)
      BB=matmul(BBtemp,AA)
      do 421, i = 1 , 6
       stress(pos+2,i)=BB(i)
421   continue

      do 422, i = 1, 6
       AA(i)=stresst(pos+3,i)
422   continue

      BBtemp=matmul(TM2,TM1)
      BB=matmul(BBtemp,AA)
      do 423, i = 1 , 6
       stress(pos+3,i)=BB(i)
423   continue

      do 424, i = 1, 6
       AA(i)=stresst(pos+4,i)
424   continue

      BBtemp=matmul(TM2,TM1)
      BB=matmul(BBtemp,AA)
      do 425, i = 1 , 6
       stress(pos+4,i)=BB(i)
425   continue

      do 426, i = 1, 6
       AA(i)=stresst(pos+5,i)
426   continue

      BBtemp=matmul(TM2,TM1)
      BB=matmul(BBtemp,AA)
      do 427, i = 1 , 6
       stress(pos+5,i)=BB(i)
427   continue
```

Stellenbosch University http://scholar.sun.ac.za/


```
      do 428, i = 1, 6
       AA(i)=stresst(pos+6,i)
 428 continue

      BBtemp=matmul(TM2,TM1)
      BB=matmul(BBtemp,AA)
      do 429, i = 1 , 6
       stress(pos+6,i)=BB(i)
 429 continue

      do 430, i = 1, 6
       AA(i)=stresst(pos+7,i)
 430 continue

      BBtemp=matmul(TM2,TM1)
      BB=matmul(BBtemp,AA)
      do 431, i = 1 , 6
       stress(pos+7,i)=BB(i)
 431 continue

      pos=pos+7

      elseif ((elem(j,5) .EQ. 0) .AND. (elem(j,4) .EQ. 0)) then

c ---------------------------------------------------------
c Driehoekige element met 4 nodes

      z1=gaussepunt(pos+1,2);
      z2=gaussepunt(pos+2,2);
      y1=gaussepunt(pos+1,1);
      y2=gaussepunt(pos+2,1);

      phi=atan((z2-z1)/(y2-y1));

c Transformasie matriks1

      k2=cos(phi);
      l2=sin(phi);

      TM1(2,2)=k2**2;
      TM1(2,3)=l2**2;
      TM1(2,4)=2*k2*l2;
      TM1(3,2)=l2**2;
      TM1(3,3)=k2**2;
      TM1(3,4)=-2*k2*l2;
      TM1(1,1)=1;
      TM1(5,5)=k2;
      TM1(5,6)=-l2;
      TM1(6,5)=l2;
      TM1(6,6)=k2;
      TM1(4,2)=-k2*l2;
      TM1(4,3)=k2*l2;
      TM1(4,4)=(k2**2-l2**2);

c Transformasie Matriks2

      m2=cos(elemm(j,3)*pi/180)
      n2=sin(elemm(j,3)*pi/180)

      TM2(1,1)=m2**2;
      TM2(1,2)=n2**2;
      TM2(1,6)=2*m2*n2;
      TM2(2,1)=n2**2;
      TM2(2,2)=m2**2;
      TM2(2,6)=-2*m2*n2;
      TM2(3,3)=1;
      TM2(4,4)=m2;
```

Stellenbosch University http://scholar.sun.ac.za/


```
      TM2(4,5)=-n2;
      TM2(5,4)=n2;
      TM2(5,5)=m2;
      TM2(6,1)=-m2*n2;
      TM2(6,2)=m2*n2;
      TM2(6,6)=(m2**2-n2**2);

      do 432, i = 1, 6
       AA(i)=stresst(pos+1,i)
  432 continue

      BBtemp=matmul(TM2,TM1)
      BB=matmul(BBtemp,AA)
      do 433, i = 1 , 6
       stress(pos+1,i)=BB(i)
  433 continue

      do 434, i = 1, 6
       AA(i)=stresst(pos+2,i)
  434 continue

      BBtemp=matmul(TM2,TM1)
      BB=matmul(BBtemp,AA)
      do 435, i = 1 , 6
       stress(pos+2,i)=BB(i)
  435 continue

      do 436, i = 1, 6
       AA(i)=stresst(pos+3,i)
  436 continue

      BBtemp=matmul(TM2,TM1)
      BB=matmul(BBtemp,AA)
      do 437, i = 1 , 6
       stress(pos+3,i)=BB(i)
  437 continue


      pos=pos+3

      elseif ((elem(j,5) .NE. 0) .AND. (elem(j,4) .NE. 0))  then
c ---------------------------------------------------------
c Reghoekige element met 8 nodes

      z5=gaussepunt(pos+5,2);
      z8=gaussepunt(pos+8,2);
      y5=gaussepunt(pos+5,1);
      y8=gaussepunt(pos+8,1);

      phi=atan((z8-z5)/(y8-y5));

c Transformasie matriks1

      k2=cos(phi);
      l2=sin(phi);

      TM1(2,2)=k2**2;
      TM1(2,3)=l2**2;
      TM1(2,4)=2*k2*l2;
      TM1(3,2)=l2**2;
      TM1(3,3)=k2**2;
      TM1(3,4)=-2*k2*l2;
      TM1(1,1)=1;
      TM1(5,5)=k2;
      TM1(5,6)=-l2;
      TM1(6,5)=l2;
      TM1(6,6)=k2;
```

Stellenbosch University http://scholar.sun.ac.za/


```
      TM1(4,2)=-k2*l2;
      TM1(4,3)=k2*l2;
      TM1(4,4)=(k2**2-l2**2);

c Transformasie Matriks2

      m2=cos(elemm(j,3)*pi/180)
      n2=sin(elemm(j,3)*pi/180)

      TM2(1,1)=m2**2
      TM2(1,2)=n2**2
      TM2(1,6)=2*m2*n2
      TM2(2,1)=n2**2
      TM2(2,2)=m2**2
      TM2(2,6)=-2*m2*n2
      TM2(3,3)=1
      TM2(4,4)=m2
      TM2(4,5)=-n2
      TM2(5,4)=n2
      TM2(5,5)=m2
      TM2(6,1)=-m2*n2
      TM2(6,2)=m2*n2
      TM2(6,6)=(m2**2-n2**2)

      do 438, i = 1, 6
       AA(i)=stresst(pos+1,i)
  438 continue

      BBtemp=matmul(TM2,TM1)
      BB=matmul(BBtemp,AA)
      do 439, i = 1 , 6
       stress(pos+1,i)=BB(i)
  439 continue

      do 440, i = 1, 6
       AA(i)=stresst(pos+2,i)
  440 continue

      BBtemp=matmul(TM2,TM1)
      BB=matmul(BBtemp,AA)
      do 441, i = 1 , 6
       stress(pos+2,i)=BB(i)
  441 continue

      do 442, i = 1, 6
       AA(i)=stresst(pos+3,i)
  442 continue

      BBtemp=matmul(TM2,TM1)
      BB=matmul(BBtemp,AA)
      do 443, i = 1 , 6
       stress(pos+3,i)=BB(i)
  443 continue

      do 444, i = 1, 6
       AA(i)=stresst(pos+4,i)
  444 continue

      BBtemp=matmul(TM2,TM1)
      BB=matmul(BBtemp,AA)
      do 445, i = 1 , 6
       stress(pos+4,i)=BB(i)
  445 continue

      do 446, i = 1, 6
       AA(i)=stresst(pos+5,i)
  446 continue
```

Stellenbosch University http://scholar.sun.ac.za/


```
      BBtemp=matmul(TM2,TM1)
      BB=matmul(BBtemp,AA)
      do 447, i = 1 , 6
       stress(pos+5,i)=BB(i)
 447 continue

      do 448, i = 1, 6
       AA(i)=stresst(pos+6,i)
 448 continue

      BBtemp=matmul(TM2,TM1)
      BB=matmul(BBtemp,AA)
      do 449, i = 1 , 6
       stress(pos+6,i)=BB(i)
 449 continue

      do 450, i = 1, 6
       AA(i)=stresst(pos+7,i)
 450 continue

      BBtemp=matmul(TM2,TM1)
      BB=matmul(BBtemp,AA)
      do 451, i = 1 , 6
       stress(pos+7,i)=BB(i)
 451 continue

      do 452, i = 1, 6
       AA(i)=stresst(pos+8,i)
 452 continue

      BBtemp=matmul(TM2,TM1)
      BB=matmul(BBtemp,AA)
      do 453, i = 1 , 6
       stress(pos+8,i)=BB(i)
 453 continue

      do 454, i = 1, 6
       AA(i)=stresst(pos+9,i)
 454 continue

      BBtemp=matmul(TM2,TM1)
      BB=matmul(BBtemp,AA)
      do 455, i = 1 , 6
       stress(pos+9,i)=BB(i)
 455 continue


      pos=pos+9

      end if
c end van if


c     write (nw,*) phi

 800  continue
c end van for

      call time(Hour)
      write (nw,*) Hour, "    :Analysis Completed"
      write (nw,*)
      call time(Hour)
      write (nw,*) Hour, "    :Begining calculation of Factor of Safety"
      write (nw,*)

c ---------------------------------------------------------------
```

Stellenbosch University http://scholar.sun.ac.za/


```
c     Druk j en pos uit
c ---------------------------------------------------------------
c     write (nw,*)
c     write (nw,*)
c     write (nw,*)
c     write (nw,*)
c     write (nw ,*) j, pos

c ---------------------------------------------------------------
c     Bereken veiligheidsfaktor
c ---------------------------------------------------------------

c Insette van materiaal maks waardes
c Carbon/ T300
      sigma1p = 1500e6
      sigma1m = -1500e6
      sigma2p = 40e6
      sigma2m = -246e6
      sigma3p = 40e6
      sigma3m = -246e6
      toult   = 68e6
      touhars = 68e6

      do 850 j = 1 , upper

      if (stress(j,1) .GE. 0) then
        s1tmp=(stress(j,1)/sigma1p)
       else
        s1tmp=(stress(j,1)/sigma1m)
       end if


       if (stress(j,2) .GE. 0) then
        s2tmp=(stress(j,2)/sigma2p)
       else
        s2tmp=(stress(j,2)/sigma2m)
       end if

       s6tmp=(stress(j,6)/toult)

       if (stress(j,2) .GE. 0) then
        s4tmp=(stress(j,2)/sigma1p)
       else
        s4tmp=(stress(j,2)/sigma1m)
       end if

      vftemp(1)=1/((s1tmp**2+s2tmp**2+s6tmp**2-s1tmp*s4tmp)**0.5)

      if (stress(j,3) .GE. 0) then
       vftemp(2)=(touhars/stress(j,3))
      else
       vftemp(2)=(-touhars/stress(j,3))
      end if

      if (stress(j,4) .GE. 0) then
       vftemp(3)=(touhars/stress(j,4))
      else
       vftemp(3)=(-touhars/stress(j,4))
      end if

      if (stress(j,5) .GE. 0) then
       vftemp(4)=(touhars/stress(j,5))
      else
       vftemp(4)=(-touhars/stress(j,5))
      end if

      vf(j)=minval(vftemp)
```

Stellenbosch University http://scholar.sun.ac.za/


```
850  continue

     vfmin=vf(1)
     do 851 i=2,upper
      if (vf(i) .LT. vfmin) then
       vfmin=vf(i)
       vfplek=i
      end if
 851 continue

     call time(Hour)
     write (nw,*) Hour, "    :Factor of Safety calculations completed"
     write (nw,*)
     write (nw,*)

     call time(Hour)
     write (nw,*) "Die veiligheidsfaktor matriks is:"
     write (nw,*)
c     write (nw,*) vf(1:20)
     write (nw,*)
     write (nw,*)
     write (nw,*) "Die minimum veiligheidsfaktor is:" , vfmin
     write (nw,*)
     write (nw,*) "By posisie: " , vfplek

     call time(Hour)
     call time(endtime)
     write (nw,*) Hour, "    :Analysis complete"

     write (nw,*)
     write (nw,*)
     write (nw,*)
     write (nw,*)
     write (nw,*) "Analysis Started    =    ",begintime
     write (nw,*) "Analysis Ended    =    ",endtime


     stop
900  write (nw,*) 'input file read error'
1000 Format (T10,I10)
2000 Format (I10,E15.5,E15.5)
3000 Format (2I10,I7,I5,F7.2,F12.2,9I5)
4000 Format (I10, E15.5)
5000 Format (I10, E20.5,6E14.5)


     end
```

Stellenbosch University http://scholar.sun.ac.za/

APPENDIX E: SOURCE CODE FOR CALCULATING CROSS-SECTION WARPING

```
        Program    Warping

        use dfpo,t

---------------------------------------------------------------------
c       Die program is geskryf deur Johannes Steyn        (9308873)
c       Die datum is 06 Mei 1999
c
c       Dit is geskryf as deel van my MSCEng Tesis om die veiligheids faktor
c       uit te werk van spannings data verkry deur CROSEC
c

---------------------------------------------------------------------
        parameter  maxelem =20000
        common     /iotp/ nr,nw
        integer    idum
        Integer    nnode,nelem
        Integer    i, j, n, pos, mr, nw, n2, nvf
        double     precision elem(maxelem,9), elemm(maxelem,3)
        double     precision Warp(maxelem*10.3)
        double     precision Warpl(maxelem*10,3)
        double     precision Warp2(maxelem*10,3)
        double     precision Warp3(maxelem*10,3)
        double     precision Warp4(maxelem*10,3)
        double     precision Warp5(maxelem*10,3)
        double     precision Warp6(maxe1em*l0,3)
        double     precision Coord(maxelem*10,3)
        double     precision vfwaarde
        integer    Elemtype, upper
        character*8 Hour
        double     precision F1(3), max(3)
c---------------------------------------------------------------------
        nr        =10
        r1w       =11
        n2        =12
        nvf       =13
        open      (nr, file='warping.inp',status='old')
        open      (nw, file='warping.neu',status='new')
        open      (n2, file='cros.inp',status='old')
        open      (nvf,file='vfmatrix.out',status='old')

        write (*,*) 'Input F1(l),F1(2),F1(3),F1(4),F1(5),F1(6)'
        read (*,*)  F1(1),F1(2),F1(3),F1(4),F1(5),F1(6)

        read (n2,*) nnode,nelem
        read (n2,*)


c       call  time(Hour)
C        write (nw,*)    Hour,"      :Begining Analysis"
c
C-----    Kry aantal inskrywings
        read (nr,*)
        read (mr,*)
c       write(nw,*) nnode
c-----   Stel Warp = 0
        Warp=0
C
c-----   Lees in Warp matriks 1 en 2
```

Stellenbosch University http://scholar.sun.ac.za/


```
        Coord = 0
        do 50, j = 1, nnode
        read(n2,*)   idum,coord(j,2),coord(j,3),idum,idum,idum
 50       continue

        read(n2,*)

        do 60 i = 1, nelem
        read (n2,6000)   idum,idum,elemm(i,1),idum,elemm(i,2),elemm(i,3),
                      elem(i,1),elem(i,2),elem(i,3),
       2              elem(i,4),elem(i,5),elem(i,6),
       3              elem(i,7),elem(i,8),elem(i,9)
 60      continue


       do 200 , i = 1, 5, 2

       do 100, n = 1,  nnode
          read (nr,*)  idum,Warpl(n,1),Warpl(n,2),Warpl(n,3),
      2             idum,Warp2(n,l),Warp2(n,2),Warp2(n,3)
100       continue
c-----    Bereken Warp Matriks
       Warp = Warp + Warpl*Fl(i) + Warp2*Fl(i+l)
200       continue

       Coord=Coord+Warp
       write (nw,2OOO)
       write (nw,3000)
       write (nw,1000) (i,Coord(i,:),i=l,nnode)
       write (nw,*) "        -1"
       write (nw,4000)
       do 300 , i = 1, nelem
       if elem(i,4) .EQ. 0) then
       elemtype = 3
       else
       elemtype = 5
       end if
       write (nw,*) i,"124"," 1"," 19 ",elemtype,"     11","0"
       write (nw,7OOO) (elem(i,j),j=l,9)
       write (nw,*) "  0","  0","  0","  0","  0","  0","  0","  0","  0","  0"
       write (nw,*) "  0","  0","  0"
       write (nw,*) "  0","  0","  0"
       write (nw,*) "  0","  0","  0"
       write (nw,*) "  0","  0","  0","  0","  0","  0","  0","  0","  0","  0"

300       continue
       write (nw,*) "         -1"

c----     Writing vf to neutral file
c
       write (nw,7500)
       Write (nw,8000)
       read (nvf,*) upper
       read (nvf,*)
       do 400 i = 1 , upper
       read (nvf,9000) vfwaarde
       write (nw,*) i,vfwaarde
400       continue
       write (nw,*) "-1 0"
       write tnw,*) "     -1"

c       max = maxval(warp, dim=1)

c       write (nw,*)
c       write (nw,*) max
c
c
```

Stellenbosch University http://scholar.sun.ac.za/


```
c       call time(Hour)
c       write (nw,'*) Hour,"            "Analysis Complete"

1000     format (I8,"      0 ","0 ","1 ","46 "," 0","  0","  0","  0","  0"
       1                E23.16," ",E23.16," ",E23.16)
2000     format          (4X,"-1"/4X,"100"/"<NULL>"/"4.1"/4X,"-1")
3000     format          (4X,"-1"/"403")
4000     format          (4X,"-1"/"404")
5000     format          (4X,"-1"/"450")
6000     Format           (2I10,I7,I5,F7.2,F12.2,9I5)
7000     format          (9i10)
7500     format          (4X,"-1"/"450"/"1"/"Crosec Case   1"/"4     1"/"0."/"1"/
        2               "Done by JSteyn"/4X,"-I")
8000     format          (4X,"-1"/"451"/"1 7033 1"/"Factcr  of   Safety"/"1     0   0"/
       2                "100233 150233 200233 250233 0 0 0 0 0 0"/
       3                "0 0 0 0 0 0 0 0 0 0"/
       4                "0 0 4 8"/"1 0 1")
9000     format          (E20.14)
       end
```

Stellenbosch University http://scholar.sun.ac.za/

APPENDIX F: DYMORE PRE-PROCESSOR INPUT FILE

```
@@@@@@ PRF-1 : TITLE LINE
Rooivalk fully articulated rotor blade
@@@@@@ PRF-2 : CONTROL PARAMETERS
 97  27   1
  0   7   0   1
  0  17   0   1.0E+06
  7   0   0   0   0
  1   0   0   0   0   0   0   0
  0   0   0
  0   0
  0
 1.0e-15
@@@@@@ GEO-1 : TRIAD DEFINITION
 1 0  0.0        1.0        0.0        0.0        0.0        1.0
 2 0  0.0        1.0        0.0        0.0        0.0        1.0
 3 0  0.0        1.0        0.0        0.0        0.0        1.0
 4 0  0.0        1.0        0.0        0.0        0.0        1.0
 5 0  0.0        1.0        0.0        0.0        0.0        1.0
 6 0  0.0        1.0        0.0        0.0        0.0        1.0
 7 0  0.0        1.0        0.0        0.0        0.0        1.0
 8 0  0.0        1.0        0.0        0.0        0.0        1.0
 9 0  0.0        1.0        0.0        0.0        0.0        1.0
10 0  0.0        1.0        0.0        0.0        0.0        1.0
11 0  0.0        1.0        0.0        0.0        0.0        1.0
12 0  0.0        1.0        0.0        0.0        0.0        1.0
13 0  0.0        1.0        0.0        0.0        0.0        1.0
14 0  0.0        0.0        1.0        0.996194698  0.087155742  0.0
15 0  -0.087155742  0.996194698  0.0        0.0        0.0        1.0
16 0  -0.087155742  0.996194698  0.0        0.996194698  0.087155742  0.0
17 0  -0.087155742  0.996194698  0.0        0.0        0.0        -1.0
18 15  0.0       0.982169321  -0.187998466   0.0       0.187998466  0.982169321
19 15  0.0       0.985902742  -0.167319404   0.0       0.167319404  0.985902742
20 15  0.0       0.989200825  -0.14656646    0.0       0.14656646   0.989200825
21 15  0.0       0.992062114  -0.125748798   0.0       0.125748798  0.992062114
22 15  0.0       0.994485347  -0.10487561    0.0       0.10487561   0.994485347
23 15  0.0       0.996469453  -0.083956113   0.0       0.083956113  0.996469453
24 15  0.0       0.998013555  -0.062999544   0.0       0.062999544  0.998013555
25 15  0.0       0.999116973  -0.042015157   0.0       0.042015157  0.999116973
26 15  0.0       0.999779219  -0.021012217   0.0       0.021012217  0.999779219
27 0  0.996194698  0.087155742  0.0        -0.087155742  0.996194698  0.0
@@@@@@ GEO-2 : NODAL COORDINATES
 1   0  0  0.0        0.0        0.0        1  1  1  1  1  1
 2   0  0  0.0        0.0        0.0        1  1  1  1  1  1
 3   0  0  0.0        0.0        0.0        1  1  1  1  1  1
 4   0  0  0.0        0.0        0.0        1  1  1  1  1  1
 5   0  0  0.0        0.0        0.0        1  1  1  1  1  1
```

Stellenbosch University http://scholar.sun.ac.za/

6	0	0	0.0	0.0	0.0	1	1	1	1	1	1
7	0	0	0.0	0.0	0.0	1	1	1	1	1	1
8	0	0	0.0	0.0	0.0	1	1	1	1	1	1
9	0	0	0.0	0.0	0.0	1	1	1	1	1	1
10	0	0	0.0	0.0	0.0	1	1	1	1	1	1
11	0	0	0.0	0.0	0.0	1	1	1	1	1	1
12	0	0	0.0	0.0	0.0	1	1	1	1	1	1
13	0	0	0.0	0.0	0.0	1	1	1	1	1	1
14	0	0	0.0	0.0	0.0	1	1	1	1	1	1
15	0	0	0.0	0.0	0.0	1	1	1	1	1	1
16	0	0	0.0	0.0	0.0	1	1	1	1	1	1
17	0	0	0.0	0.0	0.0	1	1	1	1	1	1
18	0	0	0.0	0.0	0.0	1	1	1	1	1	1
19	0	0	0.0	0.0	0.0	1	1	1	1	1	1
20	0	0	0.0	0.0	0.0	1	1	1	1	1	1
21	0	0	0.0	0.0	0.0	1	1	1	1	1	1
22	0	0	0.0	0.0	0.0	1	1	1	1	1	1
23	0	0	0.0	0.0	0.0	1	1	1	1	1	1
24	0	0	0.0	0.0	0.0	1	1	1	1	1	1
25	0	0	0.0	0.0	0.0	1	1	1	1	1	1
26	0	0	0.0	0.0	0.0	1	1	1	1	1	1
27	0	0	0.0	0.0	0.0	1	1	1	1	1	1
28	0	0	0.0	0.0	0.0	1	1	1	1	1	1
29	0	0	0.0	0.0	0.0	1	1	1	1	1	1
30	0	0	0.0	0.0	0.0	1	1	1	1	1	1
31	0	0	0.0	0.0	0.0	1	1	1	1	1	1
32	0	0	0.0	0.0	0.0	1	1	1	1	1	1
33	0	0	0.0	0.0	0.0	1	1	1	1	1	1
34	0	0	0.0	0.0	0.0	1	1	1	1	1	1
35	0	0	0.0	0.0	0.0	1	1	1	1	1	1
36	0	0	0.0	0.0	0.0	1	1	1	1	1	1
37	0	0	0.0	0.0	0.0	1	1	1	1	1	1
38	0	0	0.0	0.0	0.0	1	1	1	1	1	1
39	0	0	0.0	0.0	0.0	1	1	1	1	1	1
30	0	0	0.0	0.0	0.0	1	1	1	1	1	1
41	0	0	0.0	0.0	0.0	1	1	1	1	1	1
42	0	0	0.0	0.0	0.0	1	1	1	1	1	1
43	0	0	0.0	0.0	0.0	1	1	1	1	1	1
44	0	0	0.0	0.0	0.0	1	1	1	1	1	1
45	0	0	0.0	0.0	0.0	1	1	1	1	1	1
46	0	0	0.0	0.0	0.0	1	1	1	1	1	1
47	0	0	0.0	0.0	0.0	1	1	1	1	1	1
48	0	0	0.0	0.0	0.0	1	1	1	1	1	1
49	0	0	0.0	0.0	0.0	1	1	1	1	1	1
50	0	0	0.0	0.0	0.0	1	1	1	1	1	1
51	0	0	0.0	0.0	0.0	1	1	1	1	1	1
52	0	0	0.0	0.0	0.0	1	1	1	1	1	1
53	0	0	0.0	0.0	0.0	1	1	1	1	1	1
54	0	0	0.0	0.0	0.0	1	1	1	1	1	1
55	0	0	0.0	0.0	0.0	1	1	1	1	1	1

Stellenbosch University http://scholar.sun.ac.za/


```
56  0  0  0.0          0.0          0.0          1  1  1  1  1  1
57  0  0  0.0          0.0          0.0          1  1  1  1  1  1
58  0  0  0.0          0.0          0.0          1  1  1  1  1  1
59  0  0  0.0          0.0          0.0          1  1  1  1  1  1
60  0  0  0.0          0.0          0.0          1  1  1  1  1  1
61  0  0  0.0          0.0          0.0          1  1  1  1  1  1
62  0  0  0.0          0.0          0.0          1  1  1  1  1  1
63  0  0  0.0          0.0          0.0          1  1  1  1  1  1
64  0  0  0.0          0.0          0.0          1  1  1  1  1  1
65  0  0  0.0          0.0          0.0          1  1  1  1  1  1
66  0  0  0.0          0.0          0.0          1  1  1  1  1  1
67  0  0  0.0          0.0          0.0          1  1  1  1  1  1
68  0  0  0.0          0.0          0.0          1  1  1  1  1  1
69  0  0  0.0          0.0          0.0          1  1  1  1  1  1
70  0  0  0.0          0.0          0.0          1  1  1  1  1  1
71  0  0  0.0          0.0          0.0          1  1  1  1  1  1
72  0  0  0.0          0.0          0.0          1  1  1  1  1  1
73  0  0  0.0          0.0          0.0          1  1  1  1  1  1
74  0  0  0.0          0.0          0.0          1  1  1  1  1  1
75  0  0  6.66976200E+00  5.226965000E+00  0.000000E+00  1  1  1  1  1  1
76      75      15      0.0133          0       0       0       0       0       0       0
        0
77      75      15      0.0267          0       0       0       0       0       0       0
        0
78      75      15      0.04            0       0       0       0       0       0       0
        0
79      78      15      0.054           0       0       0       0       0       0       0
        0
80      78      15      0.234           0       0       0       0       0       0       0
        0
81      78      15      0.302           0       0       0       0       0       0       0
        0
82      78      15      0.334           0       0       0       0       0       0       0
        0
83      78      15      0.803           0       0       0       0       0       0       0
        0
84      78      15      0.832           0       0       0       0       0       0       0
        0
85      78      15      0.873           0       0       0       0       0       0       0
        0
86      78      18      0.874           0       0       0       0       0       0       0
        0
87      78      18      0.875           0       0       0       1       1       1       1
        1
88      78      18      0.874           0       0       1       1       1       1       1
        1
89      88      19      0.18666672      0       0       0       0       0       0       0
        0
90      88      20      0.37333344      0       0       0       0       0       0       0
        0
```

Stellenbosch University http://scholar.sun.ac.za/


```
91      88      21      0.56000016      0       0       0       0       0       0       0
        0
92      88      22      0.74666664      0       0       0       0       0       0       0
        0
93      88      23      0.93333336      0       0       0       0       0       0       0
        0
94      88      24      1.12000008      0       0       0       0       0       0       0
        0
95      88      25      1.30666656      0       0       0       0       0       0       0
        0
96      88      26      1.49333328      0       0       0       0       0       0       0
        0
97      88      15      1.68000000      0       0       0       0       0       0       0
        0
@@@@@@ BLD-1 : BEAM ELEMENTS DEFINITION
 1  1  75  78  76  77  15  15  15  15   1   2   1   1
 2  1  78  81  79  80  15  15  15  15   2   5   3   4
 3  1  81  84  82  83  15  15  15  15   5  16   6  15
 4  1  84  86  85   0  15  15  15   0  16   7  17   0
 5  1  86  91  89  90  15  21  19  20   7  10   8   9
 6  1  91  94  92  93  21  24  22  23  10  13  11  12
 7  1  94  97  95  96  24  15  25  26  13  14  14  14
@@@@@@ PRD-1 : PRESCRIBED DISPLACEMENTS DEFINITION
  1  86  87  4   1
@@@@@@ TIM-1 : TIME STEPS DEFINITION
 0.0   0.2   0.001652893   5   0
 1.00E-05   1.25   1.0E-06   1.0e-02   0.06   5
@@@@@@ TIM-3 : USER DEFINED TIME FUNCTIONS
1   4
 0.0   0.0   0.04 0.184 0.2E+00  0.3490659 1  0.3490659
@@@@@@ GRV-1 : DEFINITION OF GRAVITY VECTOR
 0.0   0.0   0.0
@@@@@@ RIG-1 : RIGID BODY ROTATION DEFINITION
 1  75   0.00   -112.67845   0.0
@@@@@@ CRS-1 : CROSS-SECTION DEFINITION        1
0
@@@@@@ CRS-3 : SECTIONAL PROPERTY DEFINITION
----        RIGID      BEAMS
7.746E+10       3569194.3       3569194.3       0       456307717       2.483E+10
        2.483E+10       0
0.0373248       0.719998 0.359999 0.359999
0.0     0.0     0.0     0.0     0.0     0.0
@@@@@@ CRS-1 : CROSS-SECTION DEFINITION        3
  1
@@@@@@ CRS-2 : SECTIONAL PROPERTY DEFINITION
cross1.lcc
1
@@@@@@ CRS-1 : CROSS-SECTION DEFINITION        3
  1
@@@@@@ CRS-2 : SECTIONAL PROPERTY DEFINITION
```

Stellenbosch University http://scholar.sun.ac.za/


```
cross2.lcc
 1
@@@@@@ CRS-1 : CROSS-SECTION DEFINITION       3
   1
@@@@@@ CRS-2 : SECTIONAL PROPERTY DEFINITION
cross3.lcc
 1
@@@@@@ CRS-1 : CROSS-SECTION DEFINITION       3
   1
@@@@@@ CRS-2 : SECTIONAL PROPERTY DEFINITION
cross4.lcc
 1
@@@@@@ CRS-1 : CROSS-SECTION DEFINITION       3
   1
@@@@@@ CRS-2 : SECTIONAL PROPERTY DEFINITION
cross5.lcc
 1
@@@@@@ CRS-1 : CROSS-SECTION DEFINITION
0
@@@@@@ CRS-3 : SECTIONAL PROPERTY DEFINITION
----      JOINT   AT      NODE    84,85,86,87
13125049 2213.6456      102.66864       0       2637.7946       4206746.4       4206746.4
          0
0.9569347       0.3643052       0.3544957       0.0098096
0.0     0.0     0.0     0.0     0.0     0.0
@@@@@@ CRS-1 : CROSS-SECTION DEFINITION
0
@@@@@@ CRS-3 : SECTIONAL PROPERTY DEFINITION
----      BLADE   AT      NODE    88
12768653 6153.2395      71.87385 0      6415.4206       4092516.9       4092516.9       0

0.7452498       0.4444368       0.4383123       0.0061245
0.0     0.0     0.0     0.0     0.0     0.0
@@@@@@ CRS-1 : CROSS-SECTION DEFINITION
0
@@@@@@ CRS-3 : SECTIONAL PROPERTY DEFINITION
----      BLADE   AT      NODE    89
11945684 5309.8068      68.410744       0       6001.932 3828744.9      3828744.9       0

0.8884653       0.3309174       0.323895 0.0070224
0.0     0.0     0.0     0.0     0.0     0.0
@@@@@@ CRS-1 : CROSS-SECTION DEFINITION
0
@@@@@@ CRS-3 : SECTIONAL PROPERTY DEFINITION
----      BLADE   AT      NODE    90
10612915 4874.3653      62.156524       0       5332.3022       3401575.5       3401575.5
          0
0.6026792       0.2569655       0.2519365       0.005029
0.0     0.0     0.0     0.0     0.0     0.0
@@@@@@ CRS-1 : CROSS-SECTION DEFINITION
```

Stellenbosch University http://scholar.sun.ac.za/


```
0
@@@@@@ CRS-3 : SECTIONAL PROPERTY DEFINITION
----       BLADE   AT      NODE    91
9904582.3          4533.9644        57.885722        0        4976.4108        3174545.6
           3174545.6        0
0.5065351          0.240044 0.2357302        0.0043138
0.0        0.0     0.0     0.0     0.0     0.0
@@@@@@ CRS-1 : CROSS-SECTION DEFINITION
0
@@@@@@ CRS-3 : SECTIONAL PROPERTY DEFINITION
----       BLADE   AT      NODE    92
9161759.8          3693.5622        52.286903        0        4603.1906        2936461.5
           2936461.5        0
0.490253 0.229665 0.22571   0.003955
0.0        0.0     0.0     0.0     0.0     0.0
@@@@@@ CRS-1 : CROSS-SECTION DEFINITION
0
@@@@@@ CRS-3 : SECTIONAL PROPERTY DEFINITION
----       BLADE   AT      NODE    93
7988054.9          2905.3611        35.075141        0        4013.4799        2560274  2560274  0

0.4528504          0.2162937        0.2134724        0.0028213
0.0        0.0     0.0     0.0     0.0     0.0
@@@@@@ CRS-1 : CROSS-SECTION DEFINITION
0
@@@@@@ CRS-3 : SECTIONAL PROPERTY DEFINITION
----       BLADE   AT      NODE    94,95,96
7783175.2          2873.101 29.829545        0        3910.5411        2494607.4        2494607.4
           0
0.4347508          0.2020075        0.1996544        0.0023531
0.0        0.0     0.0     0.0     0.0     0.0
@@@@@@ CRS-1 : CROSS-SECTION DEFINITION        3
   1
@@@@@@ CRS-2 : SECTIONAL PROPERTY DEFINITION
cross6.lcc
 1
@@@@@@ CRS-1 : CROSS-SECTION DEFINITION        3
   1
@@@@@@ CRS-2 : SECTIONAL PROPERTY DEFINITION
cross7.lcc
 1
@@@@@@ CRS-1 : CROSS-SECTION DEFINITION        3
   1
@@@@@@ CRS-2 : SECTIONAL PROPERTY DEFINITION
cross8.lcc
 1
```

Stellenbosch University http://scholar.sun.ac.za/

APPENDIX G: ACCOMPANING CD

On this CD you can find

- The MSC/NASTRAN models of the final design
- The DYMORE files of the final design
- All technical drawings of the final design
- All technical drawings of the test bench
- All FORTRAN source code for both the factor of safety and warping programs
- DELPHI source code for the control program

All files are filed under unique and identifiable names on the CD.

Stellenbosch University http://scholar.sun.ac.za/

CD goes here